Title

Investigation of the structure and mechanism of a PQQ biosynthetic pathway component, PqqC, and a bioinformatics analysis of potential PQQ producing organisms.

Author

RoseFigura, Jordan M.

Publication Date

2010

Peer reviewed|Thesis/dissertation

Investigation of the structure and mechanism of a PQQ biosynthetic pathway component, PqqC, and a bioinformatics analysis of potential PQQ producing organisms.

Jordan M. RoseFigura

A dissertation submitted in partial satisfaction of the requirements for the degree of Doctor of Philosophy in Chemistry in the Graduate Division of the University of California, Berkeley

Committee in Charge:

Prof. Judith Klinman, Chair
Prof. Matthew Francis
Prof. Susan Marqusee

Fall 2010

Abstract

Investigation of the structure and mechanism of a PQQ biosynthetic pathway component, PqqC, and a bioinformatics analysis of potential PQQ producing organisms.

Jordan M. RoseFigura

Doctor of Philosophy in Chemistry
University of California, Berkeley
Professor Judith Klinman, Chair

PQQ is an exogenous, tricyclic, quino-cofactor for a number of bacterial dehydrogenase reaction. It has also been proposed to play a role as a bacterial vitamin. The following work has defined 144 bacteria species that contain the machinery to form PQQ. PQQ formation is based on a conserved operon, *pqqABCDEF*, in *Klebsiella pneumoniae*. The last enzymatic step in the PQQ biogenesis pathway is catalyzed by PqqC and involves a ring closure and eight electron oxidation of the substrate AHQQ (Figure 1). Wild type (WT) PqqC and various active site mutants have been studied. The asparagine and alanine mutations at the histidine 84 position have supported the published mechanism and shown a new role for H84 as an active site acid. This was shown by anaerobic reactions, where H84A was capable of proceeding to a quinol intermediate anaerobically, but the more conservative H84N mutation was not. Aerobically, both mutations were able to form PQQ. Recent X-ray investigations of PqqC variants Y175F (with PQQ bound), H154S (with PQQ bound) and a R179S/Y175S double mutant (with AHQQ bound) show that the enzyme is alternately in a closed, open and open conformation, respectively. Though R179S/Y175S does not form the characteristic closed conformation seen in the WT-PQQ structure, it is still able to inititate a ring closure with AHQQ. Using apo-glucose dehydrogenase to assay for PQQ production, none of the mutants are capable of product formation. Spectrophotometric assays give insight into the incomplete reactions being catalyzed by the mutants. Active site variants Y175F, H154N and R179S form a quinoid intermediate anaerobically. Y175S is capable of reaction further and forms a quinol intermediate anaerobically after forming a quinoid. Y175F, H154N and R179S require O_2 to proceed to the quinol intermediate. None of the mutants preclude substrate/product binding. Indicating that in all cases, oxidative chemistry is impeded because no mutants can react fully to form quinone even in the presence of O_2. The residues targeted are proposed to form a proteinaceous core O_2 binding structure that also contributes to O_2 activation.

Figure 1: The reaction catalyzed by PqqC, forming PQQ from AHQQ.

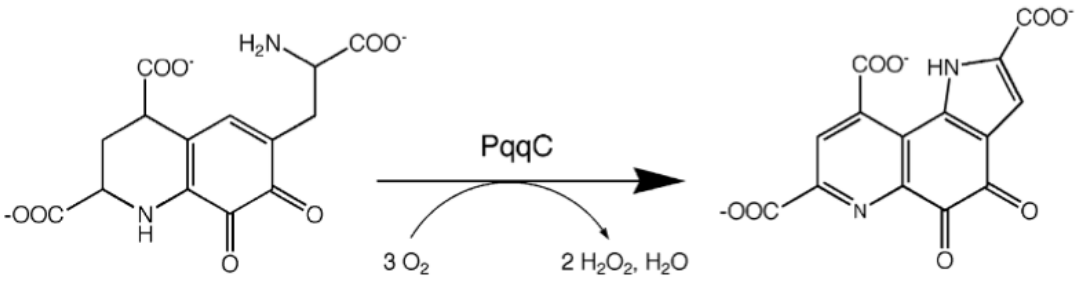

I would like to dedicate this thesis to my family- my parents, Elise Rose and Mark Figura, and my siblings, Leon, Max, and Rachel, who have always supported me, laughed with me and appreciate how my brain works.

I would also like to acknowledge my labmates; especially Dr. Oli Magnusson who started the work on PQQ in the Klinman lab, Dr. Kevin McCusker, Dr. Corinne Hess, Dr. Richard Welford, Dr. Kristi Humphreys, Dr. Zac Nagel, and Marcus Carr. I would also like to thank the undergraduates who helped me; Angel Lam, Chahyung Kim and Kun Zhang and our collaborators; Dr. Sandra Puehringer and Prof. Robert Schwarzenbacher at the University of Salzburg and Prof. Hirohide Toyama at the University of Ryukyus.

Abbreviation Lists:

PQQ: Pyrroloquinoline quinone, AHQQ: 3a- (2-amino-2- carboxyethyl) – 4,5- dioxo- 4,5,6,7,8,9 hexahydroquinoline-7,9- dicarboxylic acid , GDH: Glucose Dehydrogenase, PCR: Polymerase Chain Reaction, Ni-NTA: Nickle nitrilotriacetic acid, WT: Wild Type, KA: Kanamycin, SDS-PAGE: Sodium Dodecyl Sulfate – Polyacrylamide Gel Electrophoresis, IPTG: Isopropylthiogalactopyranosidase, PMS: Phenazine methosulfate, DNA: Deoxynucleic Acid, UV-vis: Ultra Violet-visible spectroscopy, K_D: Dissciation constant, HPLC: High Pressure Liquid Chromatography, EPR: Electron Paramagnetic Resonance, CPO: coproporphryinogen oxidase, MDH: Methanol Dehydrogenase, TPQ: Topaquinone, TTQ: Tryptophatryptophyl quinone, LTQ: Lysyltryptophyl quinone, CTQ: Cysteintryptophyl quinone, PMSF: Phenylmethanesulfonyl Fluoride, DCIP: Dichloroindolephenol, $PQQH_2$: The reduced form of PQQ, DTT: Dithiothreitol.SAM: S-Adenosyl Methionine, HAMAP: High-quality Automated and Manual Annotation of microbial Proteomes

Chapter 1

Quinone Cofactors

Quinone cofactors are the third family of cofactors, following pyridine nucleotides and flavin cofactors, and were first discovered in the 1960s when research into bacterial dehydrogenases indicated that these enzymes had a novel cofactor. Hauge et al. reported that a bacterial glucose dehydrogenase contained a dissociable cofactor that was neither a pyridine nucleotide nor a flavin[1]. It was not until the late 1970s that the structure of this cofactor, now known to be pyrroloquinoline quinone (PQQ), was solved by X-ray crystallography by Salisbury et al[2]. Over the following years, several PQQ-dependent enzymes were identified that catalyzed dehydrogenation of polyethylene glycol[3], alcohols[4, 5], hydroaromatics[6], lactate[7] and nitriles[8].

PQQ (4,5-dihydro-4,5-dioxo-1*H*-pyrrolo[2,3-*f*]quinoline-2,7,9-tricarboxylic acid) is an aromatic tricyclic ortho-quinone that was the first cofactor discovered in the quinone cofactor family. Other quinone cofactors in this family consist of topaquinone (TPQ), cysteine tryptophylquinone (CTQ), lysine tyrosylquinone (LTQ), and tryptophan tryptophylquinone (TTQ) (Figure 1). TPQ is ubiquitous, being found in prokaryotes, plants and eukaryotes. LTQ are eukaryotic quinone cofactors and TTQ is a bacterial cofactor. PQQ differs from all the other known members of the quinone cofactor family because they are covalently bound in the active site of the enzyme while PQQ is freely dissociable. The other members of the quinone cofactor family can be divided into two groups based on their biogenesis. In the first group, the quinone cofactors are generated via a self-catalyzing posttranslational modification in the enzyme active site. TPQ and LTQ are in this first group. In the second group, comprised of CTQ and TTQ, the quinone cofactors are still covalently bound in the enzyme active site, but other proteins are necessary their formation. While the biosynthesis of protein bound quinone cofactors, especially of TPQ and more recently TTQ, has been well studied, the mechanism of biosynthesis of the independent cofactor PQQ has continued to remain unknown.

PQQ is the only known cofactor in the quinone cofactor family that is dissociable from its cognate enzyme active site. All other members of this family represent a post-translational modification of amino acid side chains in the enzyme active site and remain covalently bound to the enzyme. However, in analogy to the other quinone cofactors, PQQ is derived from peptide bound glutamate (Glu) and tyrosine (Tyr). All the carbon and nitrogen atoms in PQQ originate from these two amino acids (Figure 2). This was demonstrated by labeling studies in the bacterium Methylobacterium extorquens AM1[9].

Figure 1: Quinone Cofactors: topaquinone (TPQ), cysteine tryptophylquinone (CTQ), lysyl tyrosylquinone (LTQ), and tryptophan tryptophylquinone (TTQ).

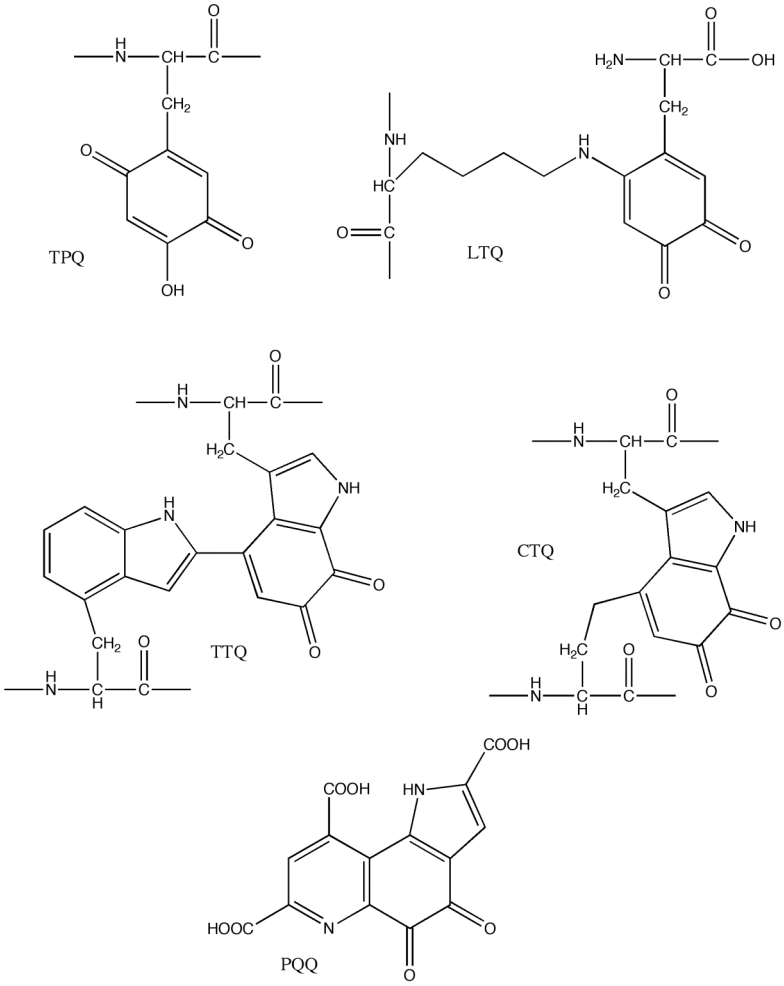

Figure 2: PQQ is shown originating from a tyrosine and a glutamate.

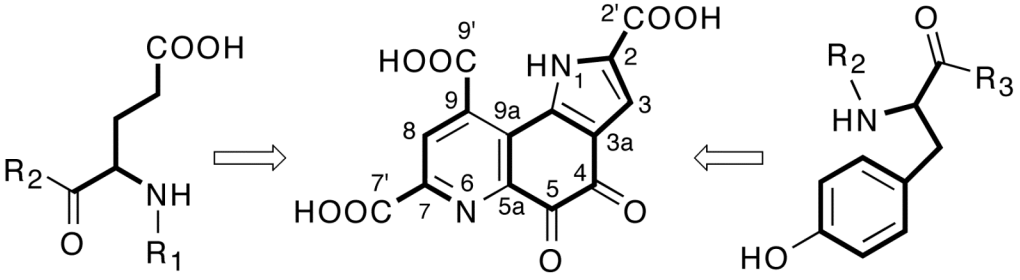

Topaquinone (2,4,5- trihydroxyphenylalanine quinone:TPQ) is derived from an active site tyrosine and was originally demonstrated in a bovine copper amine oxidase (BSAO). TPQ seems to exist in all levels of aerobic organisms. James et al. originally showed that the cofactor in BSAO was not PQQ, but a quinone derived from modification of a tyrosine residue[10]. TPQ is self catalyzing, with no other gene products necessary for cofactor biogenesis and has been best studied in bacterial and yeast copper dependent amine oxidases (CAOs). CAOs catalyse the oxygen dependent, two electron oxidation of amines to aldehydes[11], coupled to the production of H_2O_2, and have been found in plants, bacteria, fungal and mammalian sources[12].

Formation of TPQ involves oxidation of a specific active site tyrosine and insertion of two oxygens into the tyrosine ring. Biogenesis of TPQ has been shown to be oxygen- and copper-ion dependent[13] and it has been established that TPQ formation occurs at a conserved tyrosine contained in an active site motif with the consensus sequence N-Y-D/E[14, 15]. Biogenesis of TPQ and the catalytic ability of CAOs is abolished when any of the copper His ligands is removed by site specific mutagenesis[13].

Tryptophan tryptophylquinone (TTQ) is a cofactor that consists of two crosslinked tryptophan residues that has been best studied in methylamine dehydrogenase (MADH)[16]. PQQ was originally thought to be the cofactor of MADH because electron spin resonance and electron nuclear bond resonance studies by de Beer et al. described a quinone with two nitrogen atoms[17]. The structure of TTQ was eventually elucidated and its biosynthesis found to involve other gene products, making its biosynthesis different from both TPQ and PQQ[16]. The biogenesis of TTQ consists of crosslinking two tryptophans and the insertion of two oxygens to form the quinone moiety in the indole ring of one tryptophan. Mutations of MADH trap an intermediate in TTQ biogenesis where only one oxygen is inserted into the 7 position of tryptophan and the carbon-carbon bond between the tryptophans is not yet made[18, 19]. A recent structure of MADH in complex with the TTQ biosynthetic protein MauG, which finishes formation of TTQ from the monohydroxylated Trp, shows that numerous hemes are necessary for the final formation of TTQ[20]. This indicates that oxidation occurs before new carbon-carbon bond formation in TTQ biogenesis, which may have relevance for PQQ biogenesis.

Quinone cofactors may have had a role in early aerobic life on Earth. PQQ dependent methanol dehydrogenase has been found in many different types of bacteria including one archaea[21]. Recent results from the CIDA (Cometary and Interstellar Dust Analyzer) instrument on the Stardust spacecraft found numerous quinones, including ortho-quinones, in interstellar dust mainly from comet p/ Wild2[22]. In the positive ion spectra taken by the CIDA, pyridyl- and quinoline- quinones were the most likely compounds with the largest peak in the positive ion spectrum at *m/z* 331 which corresponds to PQQ[23]. This has given rise to speculation that PQQ from interstellar dust played a key catalytic role in the early Earth. It is interesting to note that PQQ is known to only be made bacterially on Earth and that all the evidence strongly indicates that it is peptide derived. As far as we know, there are no bacteria or proteins in space to form the PQQ found in interstellar dust. This raises many interesting questions about the presence of PQQ and the origin of its biosynthesis.

PQQ serves as cofactor for a number of prokaryotic dehydrogenases, largely, but not exclusively, from Gram-negative bacteria. PQQ plays a role in bacterial viability, leading to it being referred to as a bacterial vitamin. But many bacteria, including *Escherichia coli*, do not contain the *pqq* synthesis genes and so cannot biosynthesize PQQ themselves and must therefore acquire the PQQ necessary for their survival from their environment. PQQ is normally localized in the periplasm of Gram-negative bacteria. Recently, periplasm lacking, Gram-positive bacteria have been found to have the *pqq* biosynthetic genes and can presumedly form PQQ autonomously. *Streptomyces rochei* is one of the Gram-positive bacteria with the PQQ operon[24]. PQQ is formed in the cytosol of the cell and then transported into the periplasm, where the dehydrogenases that use it are located in Gram negative bacteria. The mechanism of translocation and enzyme insertion are also unknown.

The oxidative reactions catalyzed by PQQ-enzymes are involved in catabolic pathways and the best studied examples are methanol dehydrogenase (MDH) and glucose dehydrogenase (GDH)[25]. Plants and animals do not produce PQQ, but PQQ is found on plants

and in high concentration (~0.5 μM) in human breast milk. PQQ is also found in fetal tissue. Claims have been made that PQQ is involved in lysine degradation in mammals[26], but these have been refuted due to the belief that an erroneous sequence homology approach was used to relate known PQQ enzymes to the lysine degradation pathway[27, 28]. There has also been a lot of interest in PQQ as a previously unknown mammalian vitamin, but so far there has been no definite proof for this theory.

The possible mechanisms for PQQ dependent dehydrogenases are shown in Figure 3. These are an addition/elimination reaction where substrate covalently attaches to the PQQ cofactor (A) and a direct hydride transfer reaction (B). MDH is thought to proceed by a hydride transfer reaction[29]. A crystal structure of sGDH indicates that this enzyme also proceeds via a direct hydride transfer reaction (B) due to the presence of His144 of sGDH positioned directly above the C5 atom of PQQ and three positively charged residues that interact with the negatively charged C5 oxygen anion. The positioning of the glucose (substrate) molecule also supports the hydride mechanism, being orientated with the C1 atom of glucose pointing directly at the C5 atom of PQQ and at a distance of 1.2Å[21, 30].

Figure 3: Possible mechanisms of PQQ dependent dehydrogenases[30]. Substrate is shown as glucose, but can be a variety of other molecules. (A) is an addition/elimination reaction that involves a histidine acting as a general base followed by covalent addition of the substrate. (B) shows a mechanism of base catalyzed proton abstraction in concert with direct hydride transfer from substrate to PQQ.

A

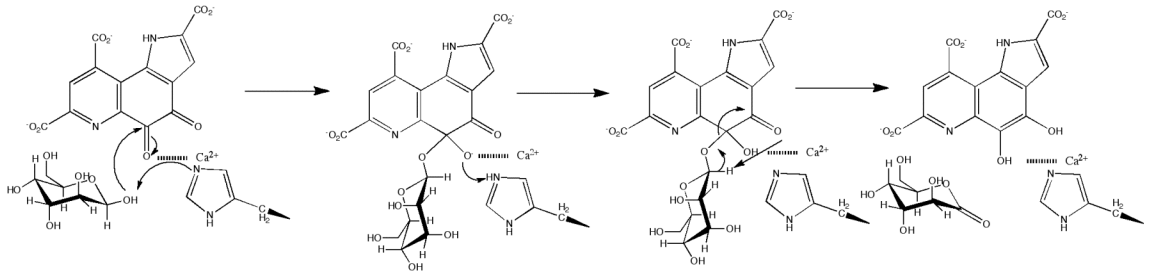

B

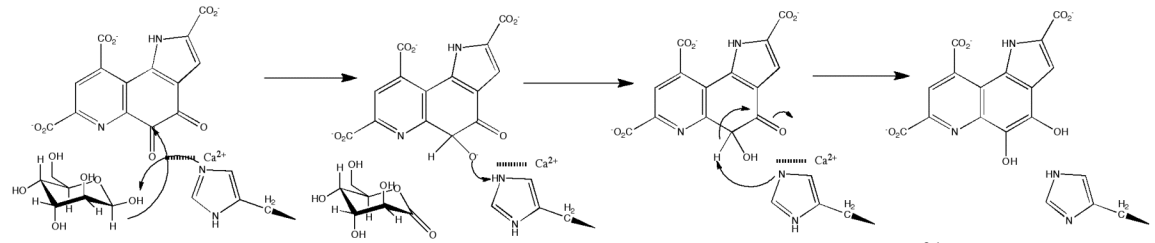

PQQ has also be prosed to act as a growth factor in animals [31], bacteria and plants[32]. Like vitamin C, glutathione, vitamin E and uric acid, PQQ ($PQQH_2$, the reduced form of PQQ) can act as an antioxidant[31]. PQQ has been found in all plant foods tested to date[33]. Approximately 3% of dietary PQQ is recovered in fecal matter. It is assumed that the remaining 97% is absorbed or derivatized. Normal mice chow contains 1-4ng PQQ per g. Adding 100-200 ug PQQ/kg weight to PQQ-free diets improves growth, development and reproduction in rodent models[31, 34]. Within two generations of mice fed a PQQ free diet, mice are no longer able to carry

pups to term. PQQ is seen to have a role in prenatal development in other species as well, with a large increase in PQQ concentration seen in quail eggs and rat embryos at the same time as rapid organogenesis. Mice fed with a PQQ-deficient diet tend to have delicate skin, smaller liter sizes and are lysine deficient, but no definite role or specific interaction with mammalian proteins for PQQ has been shown in mammals[27, 28].

No adverse effects of PQQ have been seen in standard clinical tests. Lethal dose oral toxicity tests in rats approximate a lethal dose of PQQ to be between 500 and 1000 mg/kg[35, 36]. The kidneys are suspected to be susceptible to PQQ because signs of renal tubular damage and inflammation are seen in post mortem examinations.[37]

PQQ has been found to have a significant role in plant life, being found on all plants tested and shown to encourage plant growth[38, 39]. This is at least partially to do with PQQ dependent bacteria that are symbiotic with plants. PQQ is thought to be involved in plant growth through solubilization of soil phosphorus and metals. PQQ acts a cofactor for GDH, which periplasmically oxidizes glucose to gluconic acid, which raises the pH of the surrounding environment and results in the solubilization of the aforementioned soil phosphoruses[40].

We are investigating PQQ biogenesis in *Klebsiella pneumoniae*, which requires 6 genes *pqqABCDEF*[41]. *Klebsiella pneumoniae* is a rod shaped gamma- proteobacteria that is mainly found in hospital acquired wound and urinary tract infection. PQQ has been called a bacterial vitamin, meaning bacterial survival is enhanced in its presence. Many pathogenic bacteria contain the *pqq* genes and so make the cofactor autonomously. PQQ is proposed to be a possible antibiotic target because pathogenic bacteria that make their own PQQ may lose their competitive edge when PQQ formation is inhibited. Development of antibiotics based on knocking out PQQ would be based on the biosynthetic machinery leading to PQQ, the mechanism of which is currently unknown.

The amino acid side chains that produce PQQ are proposed to come from a small peptide (23 amino acids in *Klebsiella pneumoniae*), PqqA, encoded for in the *pqq* operon[42]. PqqA has been identified as the original substrate of the PQQ pathway[9]. An absolutely conserved tyrosine and glutamate in PqqA have been implicated as the precursors of PQQ by labeling studies and mutagenesis. In PqqA there is a conserved sequence around the PQQ originating residues (in bold), consisting of GX**E**VTX**Y**. The other 5 genes (*pqqB-F*) in the *pqq* genome (Figure 4) are suspected biosynthetic genes and their proposed roles and function in PQQ biogenesis will be discussed here.

Figure 4: *pqqABCDEF*, the PQQ genome.

PqqE is proposed to be one of the initial steps of the PQQ biosynthetic reaction. PqqE is a 43 kDa, SAM-dependent Fe-S enzyme. PqqE contains two highly conserved cysteine motifs that are found at the N and C termini. PqqE is thought to catalyze the initial cross-linking between the conserved Tyr and Glu in PqqA by a radical mechanism. Results from the Klinman lab indicate that PqqD, a 10 kDa PQQ biosynthetic protein with unknown function, interacts with PqqE, possibly stabilizing the radical necessary for carbon-carbon bond formation (S. Wecksler and J. Klinman, in preparation). PqqA has not yet been shown to be modified by PqqE or in combination with PqqD. This indicates that other modifications are possibly necessary for PqqA to be a substrate for PqqE. Knockout studies found that removal of PqqD or PqqE results in no

PQQ being formed[43].

PqqB is a 33kDa protein. Originally proposed to be a dissociase for PqqC or a transport protein to get PQQ from the cytosol where it is formed to the periplasm, where it is used by numerous dehydrogenases[43]. This theory has fallen into disfavor because the amino acid sequence and crystal structure, solved through structural genomics, does not indicate any membrane spanning domains. Knockout studies with PqqB are interesting and worthy of discussion. Though the literature is unclear, there are two possibilities for *M. extorquens* cells lacking functional PqqB. These cells either form no PQQ or form the same red intermediate seen in PqqC knockout studies[43].

PqqF is a large protein with high sequence identity to the zinc-dependent hydrolase family. It is proposed to be a peptidase, which helps to free the cross-linked Tyr-Glu cofactor precursor from the PqqA peptide backbone. Efforts to express and purify PqqF have met with difficulties because PqqF kills the cells it is expressed in, even under no induction other than that which occurs under the notably leaky T7 promoter. It has been noted in previous studies that small amounts of PQQ are seen in cells without the presence of PqqF. This observation indicates that another endogenous protease could act on the substrate for PqqF. Excision of the cofactor precursor from the peptide backbone also poses an interesting conundrum because four peptide bonds must be cleaved to free the cofactor precursor. This consists of both N- and C-terminal cleavages. Needless to say, this is a lot for one enzyme to catalyze and it is very possible that other proteases not encoded for in the PQQ genome and endogenous to the cell play a role in PQQ biogenesis. Another protein encoded by the *pqq* operon in *M. extorquens* is PqqG. Not much is known about PqqG, but it also has sequence similarity of Zn-dependent proteases[44].

The only one of the *pqq* gene products with well defined function is PqqC. PqqC has been show to catalyze the final step of PQQ biogenesis[45-47]. PqqC takes AHQQ [3a(2-amino-2carboxyethyl-4,5-dioxo-4,5,6,7,8,9- hexahydroquinline-7,9-dicarboxylic acid] to PQQ, the final product of the pathway. The reaction (Figure 5) consists of a ring closure and an oxygen coupled eight electron oxidation. This is a novel reaction because PqqC does this without the presence of a metal or organic cofactor.

Figure 5: PqqC general reaction. PqqC catalyzes the formation of PQQ from AHQQ concomitant with the uptake of three equivalents of oxygen and the formation of two equivalents of hydrogen peroxide and two of water.

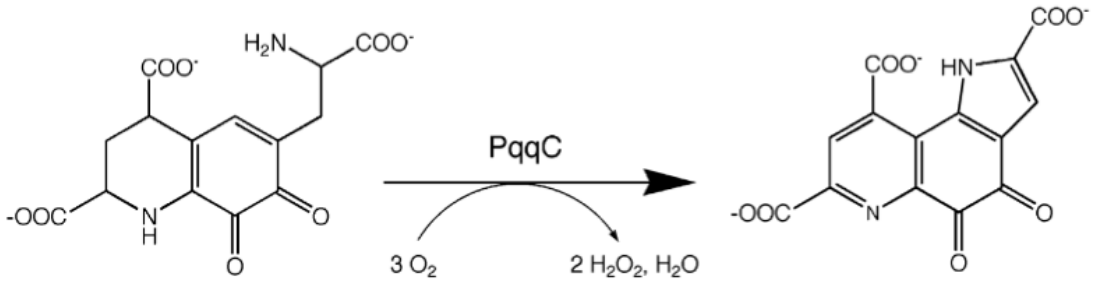

The X-ray structure of PqqC shows a perpendicular homodimer with a weight of 57.82 kDa[48]. Binding of PQQ in the PqqC active site induces a large conformational change in the protein. This conformational change is almost entirely confined to the α5a and α6b helices, which consist of residues 142-196. Helix α5b elongates to form helix α5' and helix α6a and α6b combine to form one long alpha helix. These changes effectively close off and fully form the active site and bind PQQ into the active site at the center of the protein[46].

There are many active site interactions identifiable in the crystal structure between PQQ and PqqC. There are 18 highly conserved residues in the PqqC active site (Y23, H24, R50, Y53, Q54, I57, K60, D61, R80, H84, Y128, T146, H154, R157, Y175, R179, K214, and L218) (Figure 6). The conservation of these residues and the alternative amino acids in the PqqC active site are found in Chapter 2. The only residues that are not strictly conserved are H24 which is some times found as glutamine, Q54 which is sometimes found as a histindine, I57 for which there are each one example of it being a valine or a leucine, H84 which is sometimes found as a glutamine and H154 which is sometimes found as a isoleucine, leucine or methionine. These residues form a coordination sphere around PQQ, interacting with the carboxylic acid moieties and the quinone oxygens[47].

Figure 6: PqqC Active site. PQQ is shown in gold with the putative oxygen density show in red above the quinone ring. Conserved active site residues (Y23, H24, R50, Y53, Q54, I57, K60, D61, R80, H84, Y128, T146, H154, R157, Y175, R179, K214, and L218) are shown in white[46].

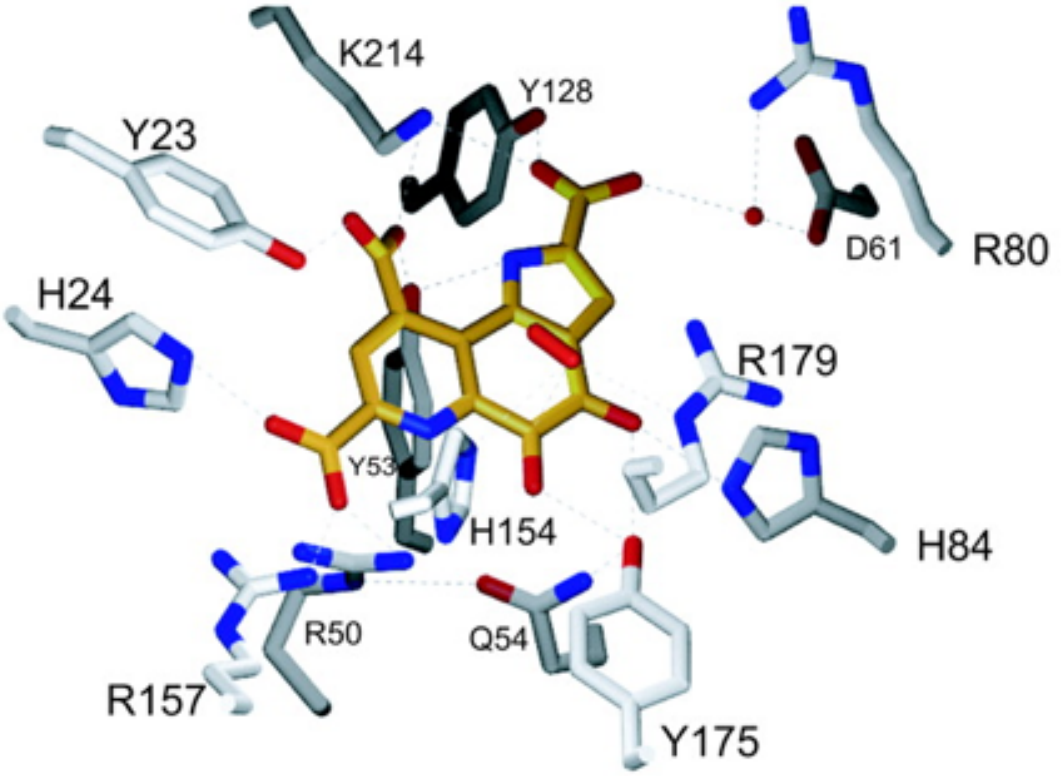

An interesting feature seen in the PqqC crystal structure is an electron density located less than 3Å above the C5 atom of PQQ. This density is elliptically shaped and cannot be fit to a water molecule or a small ion such as Na^+ or Cl^-, nor does it have the coordination site necessary for these ions. Modeling O_2 or H_2O_2 into the density does work well, but to differentiate between the two would require higher resolution data[46]. There are few crystal structures with trapped O_2 or H_2O_2 seen in a nonmetal site, though recent structures include urate oxidase, the other cofactorless oxidase[49]. There is also evidence for nonmetal oxygen binding site in other enzymes such as copper amine oxidases[11, 13].

The use of oxygen as a molecular oxidant is an interesting reaction. Enzymes that can do this "Janus-faced" chemistry, especially without the assistance of transition metal ions or

organic cofactors, must balance different factors. Dioxygen is kinetically unreactive in its ground state, but highly reactive when reduced. It is a very strong oxidant, with a reduction potential of +0.82V at pH 7 for the O_2/H_2O_2 coupling, indicating that, especially in the presence of reductants, O_2 is thermodynamically unstable. But, despite this potential, O_2 is kinetically inert due to a significant activation barrier to reaction. The ground state of dioxygen has two unpaired electrons, giving it a spin of S=1, meaning that it is a tripet biradical. The means that direct reaction between triplet oxygen and singlet organic molecules (S=0) violates the principle of conservation of angular momentum. The one electron reduction of O_2 to superoxide anion radical is unfavorable, having a potential of (-0.33V). In nature, a catalyst must overcome these barriers to react with O_2. This can be done by reaction with an organic radical, which is a spin allowed process, or by activation of O_2.

There are few other cofactorless oxidases. These are coproporphryinogen oxidase (CPO), urate oxidase and PqqC[50]. No structural motifs are shared between these cofactorless oxidases. CPO catalyzes the oxidative decarbozylation of two propionate substituents on coproporphyringoen III to vinyl substituents. There are two distinct families of CPOs, bacterial CPOs that are S-adenylmethionine enzymes and eukaryotic and prokaryotic CPOs that are cofactorless. Not much mechanistic evidence is available for CPOs, though the possible mechanisms are shown in Figure 7[51, 52].

Figure 7: CPO possible mechanisms

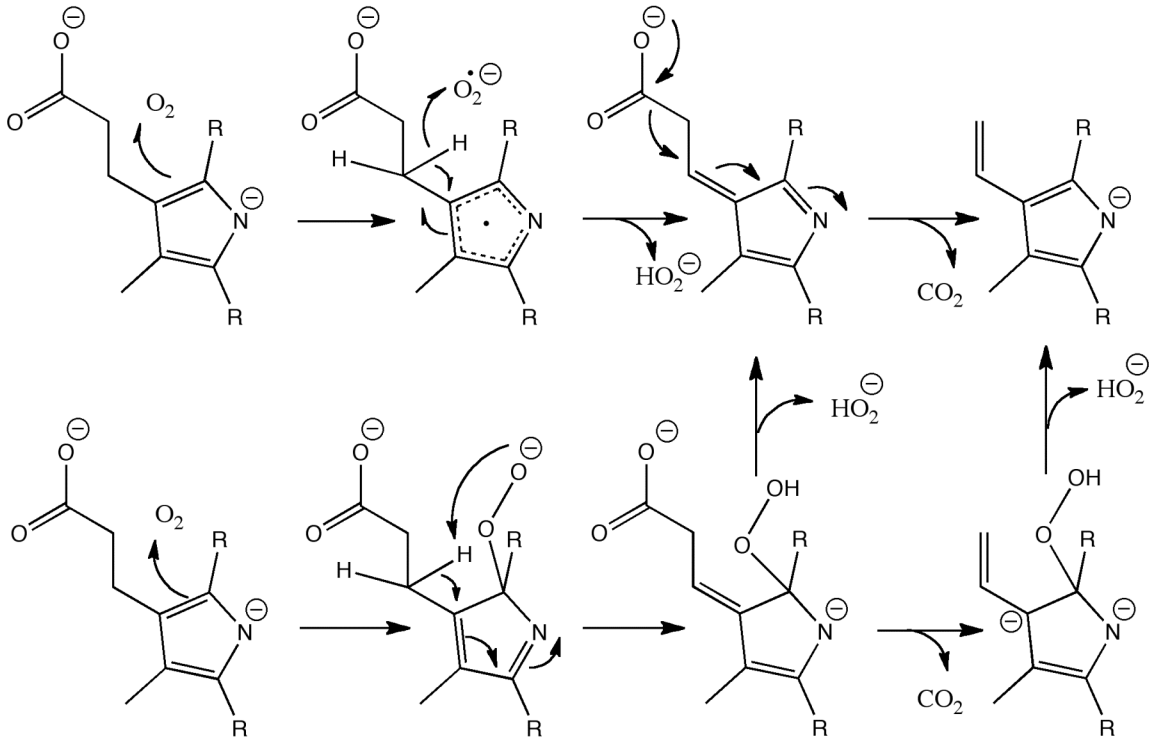

Another cofactorless oxidase currently known is urate oxidase. Urate oxidase is involved in purine degradation and catalyzes the oxidation of urate to 5-hydroxyisourate[53]. Urate oxidase is found in most organisms, including mammals, but it not found in humans and higher primates due to two mutations that cause premature termination of translation. Urate has been associated with good health due to its antioxidant properties, but is also associated with gout and renal stones at high concentrations. Urate oxidase has, at times, been classified as a copper

dependent enzyme but many urate oxidases have been shown to be catalytically active and free from copper, other metals and organic cofactors. Catalytically active cofactor-free urate oxidases have been found in bacteria, yeast, fungi, and bovine liver.

The mechanism of oxygen activation in enzymes has not been well studied, especially in nonmetal oxygen activation in protein[54]. Both urate oxidase and PqqC activate oxygen, forming hydrogen peroxide without the presence of a metal. The mechanism of conversion of molecular oxygen to hydrogen peroxide proceeds via numerous reactive oxygen species, namely superoxide and hydroperoxide radical. While the proposed mechanism of PqqC has been put forth by the Klinman lab to explain how PqqC catalyses this reaction[46], urate oxidase has been crystallized with several inhibitors and recently with its natural substrate, uric acid[54]. These indicate that the mechanism of urate oxidase proceeds by hydroxylation of uric acid to an intermediate, 5-hydroxyisourate, which then reacts further via a specific enzyme cascade to form S-allantoin (Figure 8).

Figure 8: Urate Oxidase reaction[53].

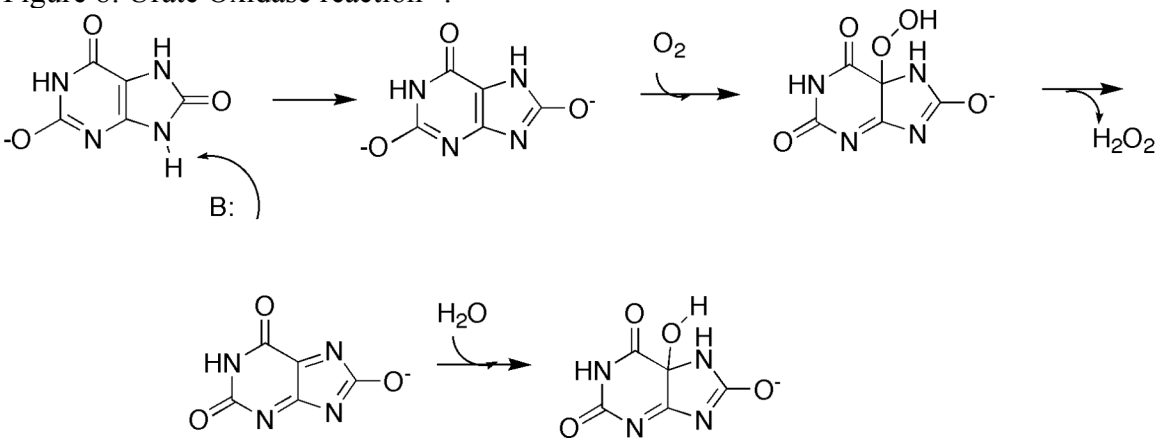

In the active site of urate oxidase there is a large hydrophobic pocket that is separated from the rest of the active site by a valine residue. Gases such as xenon and nitrous oxide specifically bind in this hydrophobic pocket[49]. Xenon is often used as a probe for O_2 binding, and these results indicate that this hydrophobic side pocket could be used as an oxygen binding/storage site for the active site of urate oxidase. PqqC does not have a similar hydrophobic pocket. In PqqC a putative oxygen/hydrogen peroxide molecule is seen in the active site. The residues in close proximity to this electronic density are histidine, tyrosine and arginine, which do not constitute a formal hydrophobic pocket[46], though portions of Try and Arg are capable of hydrophobic interactions with O_2. This leads to interesting questions, not only about the mechanism of PqqC, but also about the mechanism of metal-less oxygen activation and the forces necessary to accomplish it in cofactorless oxidases.

The are numerous cofactorless oxygenases which are all involved in catalysis of xenobiotic compounds or degradation of quinoline derivatives[55]. Quinone forming oxygenases, such as tetracenomycin F1 monooxygenase (TcmH) and the ElmH protein form antibiotic compounds in *Streptomyces* strains. TcmH is involved in formation of tetracenomycin C, where it catalyzes the oxidation of the naphthacenone tetracenomycin F1 at the C5 position[56]. ElmH parallels the reaction catalyzed by TcmH in the elloramycin A biosynthesis[57]. Enzymes in this family catalyze incorporation of one molecule of oxygen from molecular oxygen into their substrate along with formation of an equivalent of H_2O. A second family of cofactorless oxygenases is the carbon monoxide forming 2,4-dioxygenases which catalyze cleavage reactions

in N-heteroaromatic compounds. This is done by inserting molecular oxygen into the rings and releasing CO. Examples of this family are 1H-3-hydroxy-4-oxoquinoline 2,4 dioxygensase (Qdo)[58] and 1H-3-hydroxy-4-oxoquinaldine 2,4-dioxygenase (Hod)[59].

What ties all these reactions together is the ability of these enzymes to activate and react with oxygen without the presence of a metal or organic cofactor. Why this is impressive is that molecular oxygen exists in a triplet state while organic cofactors such as the substrate for PqqC, AHQQ, exists in the singlet state. This spin forbidden reaction, between a triplet and a singlet, is overcome by PqqC. The mechanism of, and the forces involved in this are the subject of some of the work in this thesis.

The structure of PQQ has been known for decades, but the full biogenesis pathway remains unknown. The work presented in this thesis investigates the mechanism of PqqC, the role and activity of PqqB in PQQ biogenesis and the distribution of the *pqq* biosynthetic genes among prokaryotic genomes.

Chapter 2

PqqC Position H84 and Indication of the Quinoid/Quinol Tautomerization

Introduction:

PQQ is a bacterial cofactor that is formed with the gene products of the *pqq* operon, *pqqABCDEF*. PQQ is derived from a tyrosine residue and glutamate residues in PqqA (Scheme 1).

Scheme 1. The carbon and nitrogen atoms of PQQ originate from a glutamate and a tyrosine residue.

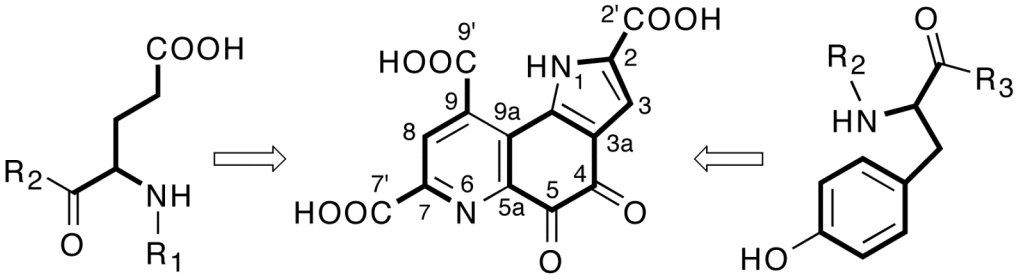

PqqC is the protein product of the third gene in the *pqq* operon, which catalyzes the final step of PQQ formation, is a 251 residue protein with a molecular mass of 28.8 kDa[1]. This enzyme takes 3a(2-amino-2carboxyethyl-4,5-dioxo-4,5,6,7,8,9- hexahydroquinline-7,9-dicarboxylic acid [AHQQ] to PQQ[2, 3] (Scheme 2).

Scheme 2. The PqqC reaction. This reaction involves an overall eight-electron oxidation, leading to a pyrrole and pyridine ring, and has previously been shown to consume three moles of O_2 per product formed.

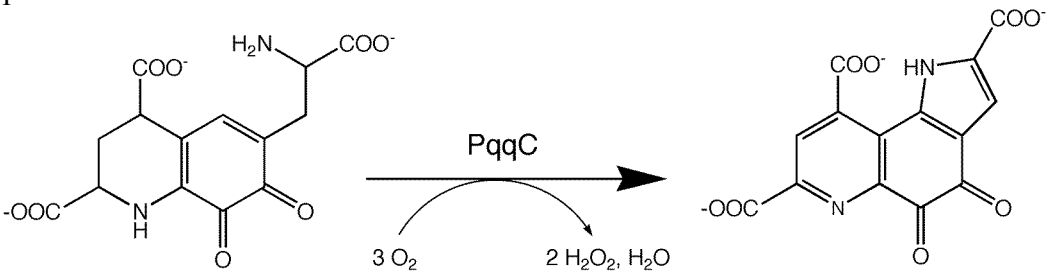

The structure of PqqC consists of a seven helix bundle (Figure 1, Figure 2). Upon binding of PQQ two coiled regions, between residues 151-158 and 170-187, fold to form helices, helix 5b' and 6' respectively, to effectively assemble and close off the active site of PqqC (Figure 2).

Figure 1: Alignments of PqqC from Klebsiella pneumoniae, Pseudomonas aeruginosa, Magnetospirillium magnetotactium, Desulfitobacterium hafniensis. The position of helices are shown by rectangles.

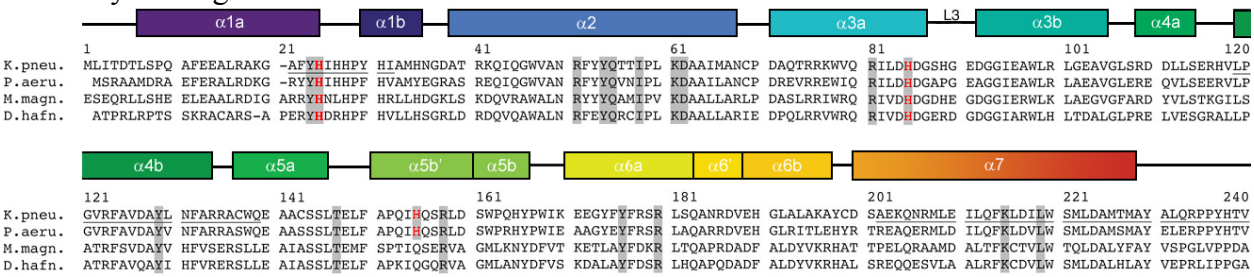

Figure 2: PqqC shown in the open (red) and closed (blue) forms. PQQ is show in the center of the molecule in gold sticks.

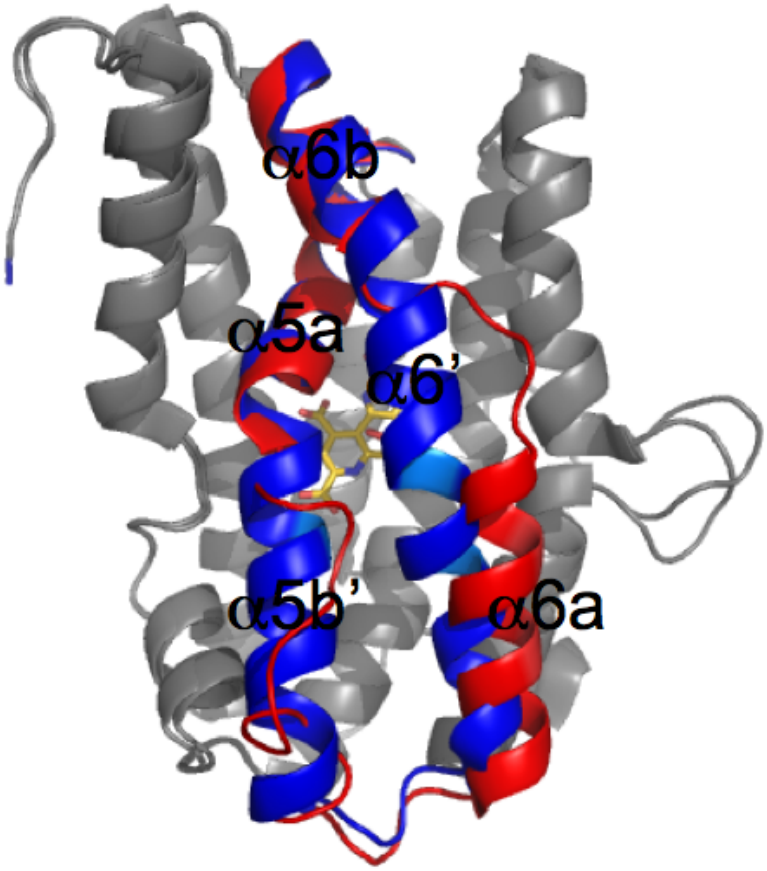

The active site of PqqC consists of 18 conserved residues (Y23, H24, R50, Y53, Q54, I57, K60, D61, R80, H84, Y128, T146, H154, R157, Y175, R179, K214 and l218: Figure 1, Figure 3, Table 1)[4].

Figure 3: The active site of PqqC. Conserved sidechains are shown in green and PQQ is shown in gold. The putative oxygen is shown in red above the quinone moiety of PQQ.

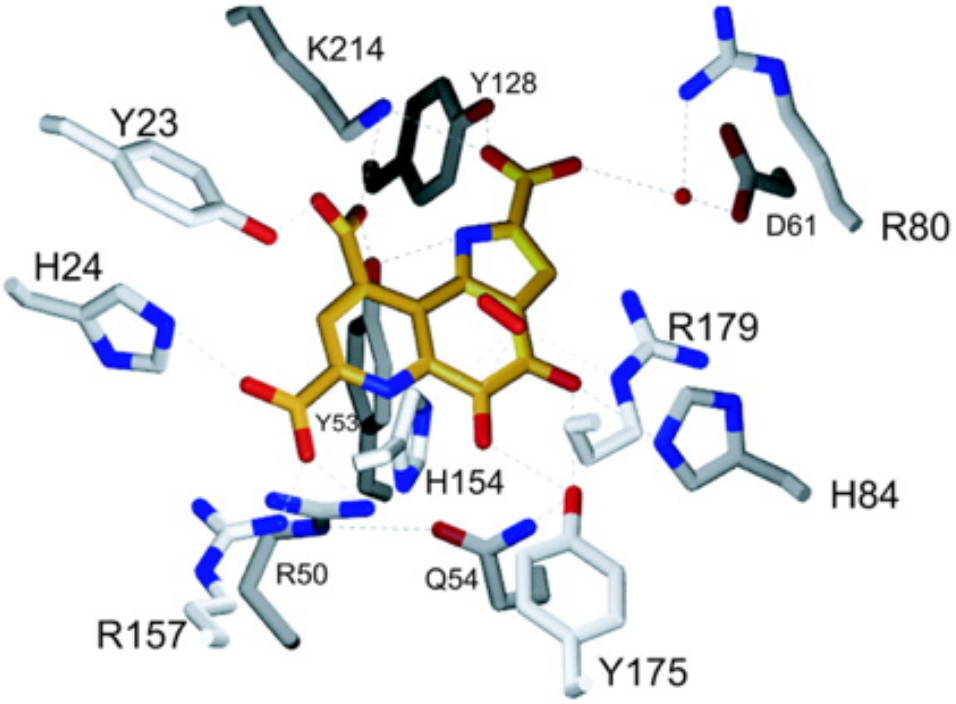

Table 1: Rates of conservation and possible replacements. Numbers are from an alignment of homologs created with Phylobuilder with a 30% identity cutoff. This process and the alignment itself will be discussed in Chapter 5.

Residue	Conservation? (X/149)	Alternates
Y23	100%	
H24	147/149 (98.6%)	2xW
R50	100%	
Y53	100%	
Q54	147/149 (98.6%)	2xH
I57	100%	
K60	100%	
D61	100%	
R80	100%	
H84	141/149 (94.6%)	8xQ
Y128	100%	
T146	100%	
H154	123/149 (82.5%)	6xM, 19xI. 1xL
R157	100%	
Y175	100%	
R179	100%	
K214	100%	

L218	100%	

Numerous active site residues move into the active site only upon PQQ binding. The active site residues moving into the active site in this way are R157 and H154 on helix 5 and Y175 and R179 on helix 6. In the crystal structure of PqqC with PQQ bound there is an electron density seen above the quinone ring of PQQ. This density cannot be fit to a metal or small ion, but fits very well to a molecule of molecular oxygen or hydrogen peroxide. Considering that there were reducing equivalents in the crystallization buffer combined with the redox active nature of the quinone moiety of PQQ, it is likely that this density is H_2O_2. During turnover the final equivalent of H_2O_2 formed by PqqC is tightly bound to the enzyme and PqqC must be denatured to detect this final H_2O_2.

There are a number of basic residues, which are postulated to stabilize the three negatively charged carboxylate ions of AHQQ/PQQ and to function in catalysis. These carboxylates are twisted out of alignment when PQQ is bound to PqqC. The overall reaction of PqqC is a ring closure along with an eight electron oxidation of AHQQ to form PQQ[4, 5]. The proposed mechanism of PqqC involves a series of base catalyzed proton abstractions followed by a quinoid/quinol tautomerization and oxidation of quinol back to a quinone (Scheme 3)[4].

Scheme 3. Proposed mechanism of PqqC. Note that steps I-III are shown in random order. B1, B2 and B3 denote residues proposed to act as base catalysts in the respective tautomerization reactions.

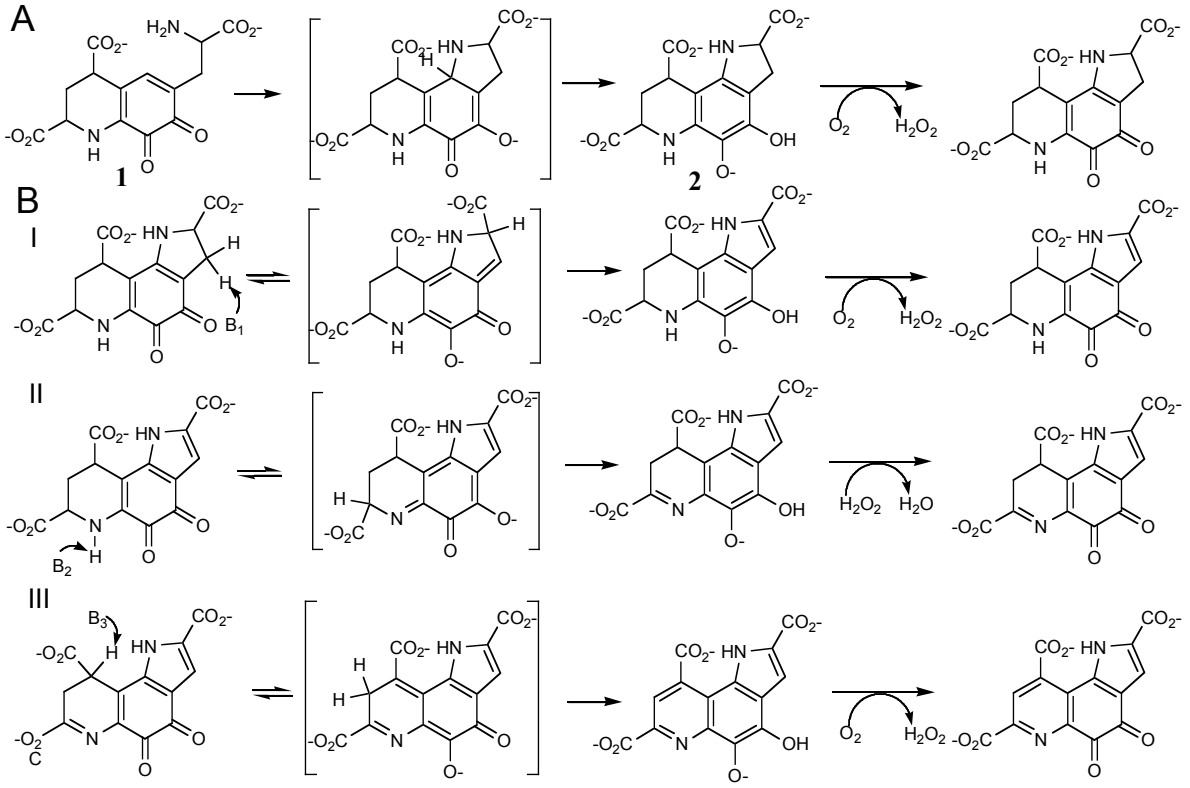

In particular, the proposed mechanism of the enzyme involves the action of three conserved basic residues (B1, B2 and B3 in Scheme 3), which have been tentatively assigned to the three

histidines in the active site, H24, H84 and H154. These three residues are all within 5Å of a site of proton abstraction in PQQ (Figure 4a, 4b).

Figure 4a: Structure and position of proposed catalytic histidine residues in the active site of the PqqC:PQQ complex with the putative oxygen/ hydrogen peroxide molecule. The dashed lines show distances in ångstrom, between the heavy atoms from which proton transfer reactions occur. These distances are based on the enzyme:product complex and will presumably be somewhat different in the enzyme:substrate complex. Proton transfer at C-9 could be facilitated by either H24 or the Y53/K214 diad (Figure 3). PQQ is shown in gold sticks and residues are shown in green sticks. The putative O_2 density is shown in red.

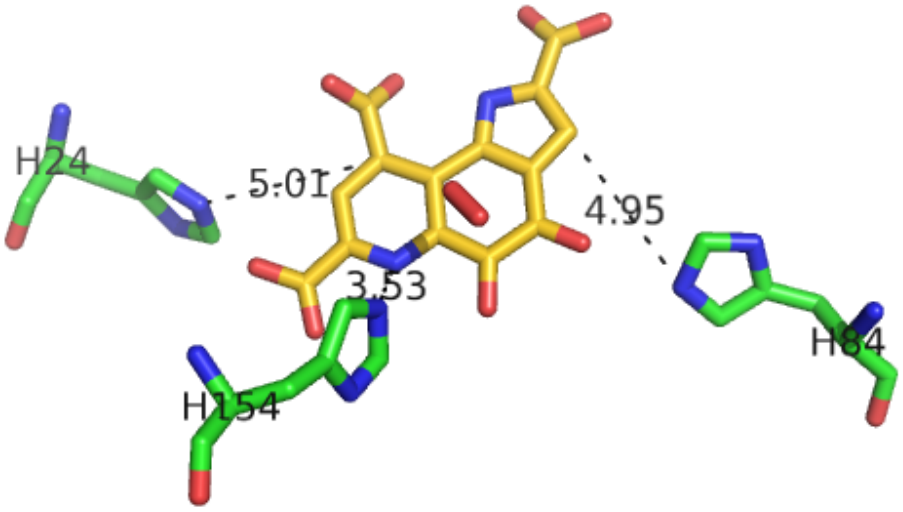

Figure 4b: An alternate view of the three proposed catalytic histidines along the plane of PQQ. Note that H24 and H84 are near to the plane of PQQ and H154 deviates greatly from the plane, occurring almost perpendicularly above the PQQ molecule.

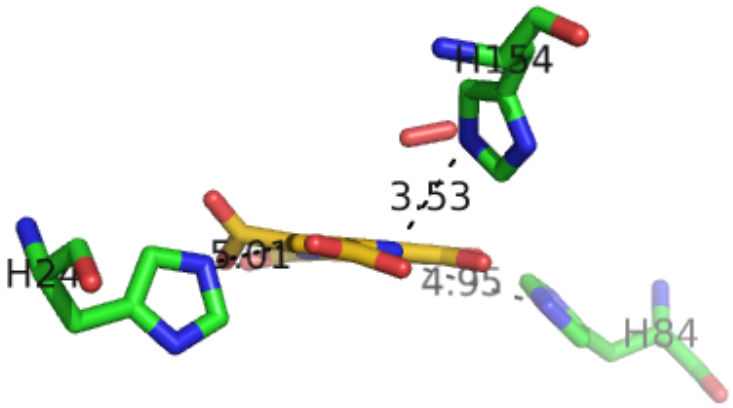

There is also a possible catalytic diad near H24 consisting of Y53 and K214. Both H84 and H24 lie in the plane of the PQQ molecule, though H154 is situated above PQQ and not in line with the N-H bond (Figure 4b). To test the role of one of these residues, H84, two mutations were made, H84A and H84N. The asparagine mutation maintains the bulk of the histidine, but does not have the proton accepting or donation capabilities of histidine. The alanine mutation removes bulk as well as capabilities for proton movement (Figure 5).

Figure 5: A view of the position of and spaces of the H84 position for WT-PqqC (green), H84N (cyan) and H84A (pink). Mutant residue positioning was developed with PyMol. The H84A structure overlays with the first carbon of the WT residue.

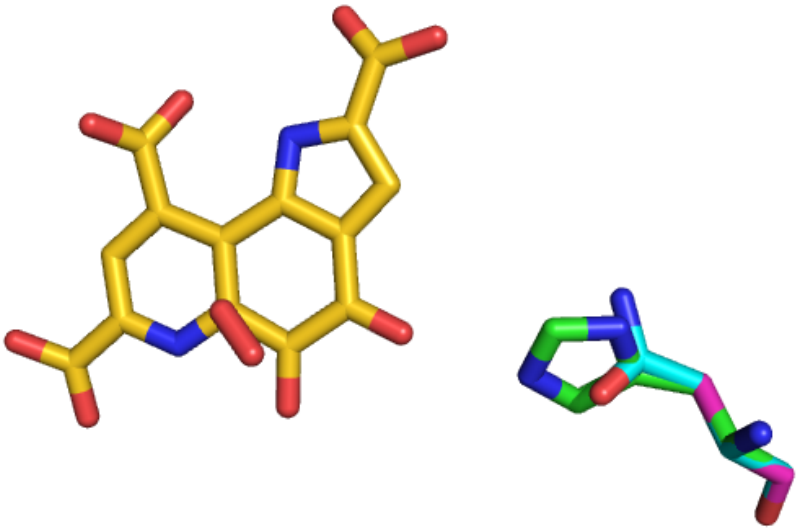

In this chapter the kinetic and binding properties of the wild-type (WT) PqqC enzyme and these two active site variants will be described. This includes the kinetics of the single turnover reaction of WT enzyme and two active site H84 mutants (H84N and H84A), and the spectroscopic detection of several intermediates; these data provide insight into the catalytic mechanism of PqqC, especially for the first step of reaction. Also, the binding of PQQ to WT enzyme and the H84 mutants will be discussed. Previous studies had shown that WT-PqqC only undergoes only a single turnover. Binding studies discussed here indicate that both WT-PqqC and mutant have a very low Kd. Work done previously by Dr. Olafur Magnusson has shown that multiple turnovers can be achieved with PqqC at sub-Kd concentrations of substrate so we can consider PqqC an enzyme. Thus, while severe product inhibition affects the biochemical experiments possible with PqqC, the spectroscopic experiments discussed allow the properties of early steps in the reaction to be interrogated.

Materials and Methods:

Chemicals, Reagents and Molecular Biology Products:

Buffers, salts, general reagents and culture media were obtained from Sigma and Fisher and were of the highest available purity. Dichloroindole phenol (DCIP), phenazine methosulfate (PMS), Q-Sepharose, SP-Sepharose and Phenyl-Sepharose resins were from Sigma. PQQ (> 99 %) was from Fluka. The concentration of PQQ in aqueous solution was determined spectrophotometrically as described elsewhere[6]. Ni-Nitriloacetic acid (NTA) resin, DNA purification kits and PCR primers were purchased from Qiagen. Enzymes and reagents for PCR reactions were from Roche, including Expand™ High Fidelity DNA polymerase. Restriction

enzymes and appropriate reaction buffers were purchased from New England Biolabs. Bugbuster™ reagent, benzonase, T4 DNA ligase, cell lines, vectors for cloning and expression and sequencing primers were obtained from Novagen. AHQQ was purified from the *pqqC* mutant strain EMS12 of *M. extorquens*[2] as described elsewhere[5]. Concentration of AHQQ was determined spectrophotometrically at pH 7 by averaging the concentrations determined at three wavelengths with the following extinction coefficients[4]: ε_{222}=15.7 $mM^{-1}cm^{-1}$, ε_{274}=8.26 $mM^{-1}cm^{-1}$, ε_{532}=2.01 $mM^{-1}cm^{-1}$. Plasmid (pBCP-165) containing all the genes in the PQQ operon of *K. pneumoniae* was a generous gift from Professor Robert Rucker, University of California, Davis. This plasmid was originally made in the laboratory of Professor Peter W. Postma, University of Amsterdam, The Netherlands[3, 7]. An *E. coli* recombinant strain pGP492, harboring the gene for soluble glucose dehydrogenase (sGDH) from *Acinetobacter calcoaceticus* is from the laboratory of Professor Hirohide Toyama, Yamaguchi University, Japan.

Cloning and Expression:

To investigate the mechanism of PqqC, the wild-type gene was cloned out of the operon, histidine tagged and expressed in E. coli (Dr. O. Magnusson). PCR cloning was performed using the following primers:

pqqC/D-1, 5'-GGCATTACATATGCTGATCACTGACACGCTGTCGCCGC-3';

pqqC/D-2, 5'-GACCGCTCGAGTTACTCTGGCTCACGGCAGGTGATCCACTT-3'.

Underlined sequences are restriction sites for *NdeI* and *XhoI*, respectively that were designed for subsequent cloning. Reaction mixture contained 10 mM Tris buffer, pH 8.3, 50 mM KCl, 2.5 mM $MgCl_2$, 200 µM dNTPs, 2 µM primers, 70 ng/µl pBCP-165 and 3.5 U/µl DNA polymerase. Reaction conditions: melting, 95 °C; annealing, 55 °C; elongation, 72 °C. Each step was 1 min for a total of 35 cycles. The purified PCR product was digested with *Nde*I and *Bam*HI, followed by ligation into pET-24b for generation of wild-type PqqC. After transformation into NovaBlue cells, screening for positive colonies was done by plasmid purification and restriction analysis of clones. The isolated plasmid named pET-24b-pqqC/D was sequenced from both directions using the T7 promoter and terminator primers, respectively. The H84N mutation was made in the Schwarzenbacher lab. The H84N mutant gene is on pET-21d plasmid (EcoRI/XhoI), contains a C-terminal His-tag and confers resistance to ampicillin. The following primers were used for Quickchange PCR mutagenesis:

H84Nf, 5'-GCATCCTCGACAACGACGGCAGCCAC-3';

H84Nr, 5'-GTGGCTGCCGTCGTTGTCCAGGATCC-3'.

The H84A mutation is on a pET-24b pqqC plasmid that contains a C-terminal His-tag and confers resistance to kanamycin. Mutagenesis of H84A was performed using a commercial kit (Stratagene) and the following primers were used:

H84Af, 5'-CGGATCCTCGACGCCGACGGCAGCCAC-3';

H84Ar, 5'-GTGGCTGCCGTCGGCGTCGAGATCCG-3'.

Expression of plasmids was done using BL21(DE3) cells in LB medium supplemented with 50 µg/mL kanamycin (WT and H84A) or 100 µg/ml ampicillin (H84N). Cultures were grown at 37 ˚C to an optical density at 600 nm of ~0.8, at which time IPTG (1 mM) was added and the cells harvested ~4 h later. Both pET-24b-pqqC/D and pET-28b-pqqC/D produced high quantities of WT-protein as judged by SDS-PAGE analysis. Solubility tests using Bugbuster reagent in the presence of 0.2 M potassium phosphate, pH 8 showed that ~ 50 % of the protein was soluble with the remainder presumably as insoluble inclusion bodies. Considerably lower expression of the H84 mutants was observed; however most of the protein remained soluble after cell lysis with the addition of ~0.9M KCl in the lysis buffer. The PqqC in the pET-21d vector

varied from the PqqC previously tested. This gene is from a different species of *K. pneumoniae, K. pneumoniae MGH 78578*, that was cloned from genomic DNA by the Schwarzenbacher lab. These gene varied at three positions from the sequence deposited by Postma (Pubmed accession number: X58778): A21D, D37N and K41E. WT-PqqC from both sources were shown to exhibit the same behavior.

Purification of Wild Type PqqC:

Cells harboring pET-24b-pqqC/D (~30 g) were resuspended in 0.2 M potassium phosphate buffer, pH 8, containing 1 mM DTT, 1 mM PMSF and 1 mM EDTA. Cell lysis was performed by sonication using a Branson sonifier with output setting at #8, duty cycle at 30% (3 x 5 min). Lysed cells were centrifuged and the clear supernatant diluted 5-fold with 20 mM Tris, pH 8, 1 mM DTT (Buffer A). The diluted sample was applied to a Q-Sepharose column (2.5 x 30 cm, flow rate = 1.7 mL/min), equilibrated in Buffer A, followed by a buffer wash (~150 mL). PqqC was eluted with a gradient of 0-300 mM KCl in Buffer A (2 L total volume) and the collected fractions were analyzed by SDS-PAGE, followed by concentration of PqqC containing fractions (Amicon YM10). The protein was further purified by size-exclusion chromatography using Ultrogel AcA54 column (2.5 x 110 cm, flow rate = 0.3 mL/min) in 100 mM potassium phosphate buffer, pH 8 (Buffer B). PqqC containing fractions were pooled based on SDS-PAGE analysis, and the protein subsequently concentrated using an Amicon YM10 ultrafiltration device followed by freezing in liquid nitrogen and storage at –80 ˚C. Sample of purified protein was sent to the AAA Service Laboratory, Boring, OR for quantitative amino acid analysis. Triplicate analysis of the protein in conjunction with UV-Vis absorption of the same sample yielded an extinction coefficient of $\varepsilon_{280} = 2.06\ (mg/mL)^{-1}$, or 59.6 $mM^{-1}cm^{-1}$. WT protein with N-terminal His-tag (pET-28b-pqqC/D) was not purified.

Purification of H84N and H84A.

Cells (~25 g) were resuspened in Buffer C (0.2 M potassium phosphate, pH 8, 300 mM NaCl, 10 mM imidazole, 10 mM ß-mercaptoethanol) augmented with 1 mM EDTA, 0.5 mM PMSF and 0.9 M KCl. After sonication and centrifugation as described for WT the clear supernatant was applied to a 10 mL Ni-NTA column that had been equilibrated in Buffer C. After a buffer wash the His-tag bound protein was eluted with Buffer C supplemented with 300 mM imidazole. Fractions containing mutant enzyme were analyzed by SDS-PAGE, pooled, concentrated and further purified by size-exclusion chromatography as described above for the WT protein. Due to precipitation at higher concentrations, H84A could only be concentrated to approximately 55 μM.

Single-Turnover Kinetics:

100 μM enzyme (WT or H84N) or 50 μM (H84A) was mixed with substrate, AHQQ (40 μM or 20 μM respectively) in 100 mM potassium phosphate buffer, pH 8.0 in a total volume of 100 μL. The mixture was transferred to a microcuvette and UV-Vis spectra recorded within 20 seconds of mixing. Spectra were obtained on a HP-8452A diode-array spectrophotometer and the temperature of the reaction was maintained at 20 ˚C using a circulating water bath. Spectra were acquired at predetermined timepoints and the data exported to Specfit/32 for analysis. A control sample, containing enzyme only was also measured under identical conditions. The spectra obtained in this manner were subtracted from spectra at same timepoints during the enzymatic reaction. The control run was necessary to correct for absorption due to light scatter resulting from some protein precipitation during the course of the reaction.

Anaerobic reactions were done under the same conditions as described above. Enzyme and substrate were made anaerobic by repeated cycles of Argon purging and high-

vacuum evacuation on a Schlenk line. The sealed samples were brought into an anaerobic chamber, the protein was transferred into a microcuvette fitted with a rubber stopper and the substrate was loaded into a syringe and the needle inserted through the stopper and into the top of the cuvette. The cuvette with the syringe attached was brought out to the spectrophotometer and the substrate was mixed thoroughly with enzyme before spectra were recorded. After some time, when no further changes were observed in the UV-Vis spectrum of the samples, the stopper was removed and air was blown over the surface of the sample for a few seconds, demonstrating product formation in all cases.

Fluorescence Binding Assay for PQQ.

Binding of PQQ to PqqC (WT, H84N and H84A) was measured fluorimetrically. Assays were done in 100 mM potassium phosphate buffer, pH 8.0 at 25 ˚C. A fixed concentration of PQQ (ligand) was employed (50 nM for WT and 20 nM for H84N) and the concentration of enzyme varied. Samples were incubated for 30 min and fluorescence emission spectra recorded (slit width 10 nm) with excitation wavelength at 365 nm (slitwidth 5 nm) and 0.2 s integration time. Data were fitted to a quadratic binding isotherm (equation 1), where ΔF equals the change in fluorescence in a given sample compared to free ligand, ΔF_M equals the change in fluorescence at saturation, $[E]_T$ equals the total concentration of enzyme in each sample, $[L]_T$ equals the concentration of total ligand and K_D is the dissociation constant of the enzyme-ligand complex. Data fitting was done using Kaleidagraph (Synergy Software).

$$\Delta F = \Delta F_M \cdot [([E]_T + [L]_T + K_D) - (([E]_T + [L]_T + K_D)^2 - 4 \cdot [E]_T \cdot [L]_T)^{0.5} / (2 \cdot [L]_T) \quad] \qquad (1)$$

Results:

PqqC from *K. pneumoniae* has been successfully cloned and expressed in *E. coli*. Purification of the wild type enzyme involves a two-step chromatographic procedure involving anion-exchange chromatography followed by size-exclusion. The purity of the isolated protein was judged to be ≥ 95% based on SDS-PAGE analysis. The overall yield of protein for this procedure was ~ 25 mg/L culture. In single turnover studies PqqC behaved identically to PqqC carrying a His-tag, which has been previously prepared and used in published structural studies[1, 4]. The decision was therefore made to construct all subsequent mutants with His-tags for the purpose of rapid purification. In addition, the His-tag form of the enzyme appears to be somewhat more soluble than the native enzyme. The H84N and H84A mutants were purified by affinity chromatography on a nickel column followed by size-exclusion chromatography. The expression for these mutants was lower than WT and yielded ~ 3 mg/L culture.

Single-Turnover Kinetics of WT, H84N and H84A:

The rate of the reaction catalyzed by PqqC is slow, displaying a first-order rate constant of ~0.4 min^{-1} under single-turnover conditions using an assay based on quantitation of PQQ by HPLC[4]. The substrate, AHQQ, has a wine-red color due to a distinct quinonoid transition with λ_{max} at 532 nm and the product, PQQ, also has multiple transitions in the UV-Vis range, including a band at 331 nm[5]. These properties make this system ideal to probe for spectral changes during the course of the reaction. Reactions were done with excess enzyme over substrate (2.5 equivalents) to simplify the kinetics by ensuring that all substrate was in the E-S complex. Spectra at various timepoints during the WT-PqqC reaction are shown in Figure 6A.

Figure 6. Spectral changes during the WT-PqqC reaction under single-turnover conditions at 20 ˚C. (A) Nine representative spectra at the indicated timepoints (0.33, 0.65, 1.1, 2.3, 4.0, 5.6, 7.9, 12.5 and 29.5 min, respectively). A total of 59 scans were acquired in the experiment. (B) Spectral traces at four single wavelengths, representative of different species or processes during the reaction. Closed diamonds (◆) show changes at 536 nm, representing disappearance of substrate. Open circles (○) show changes at 316 nm, representing formation and dissipation of an intermediate (WT-I). Closed circles (●) show changes at 332 nm, which is the isosbestic point between WT-I and product. Open diamonds (◊) show changes at 346 nm, which represents the final enzyme-PQQ complex.

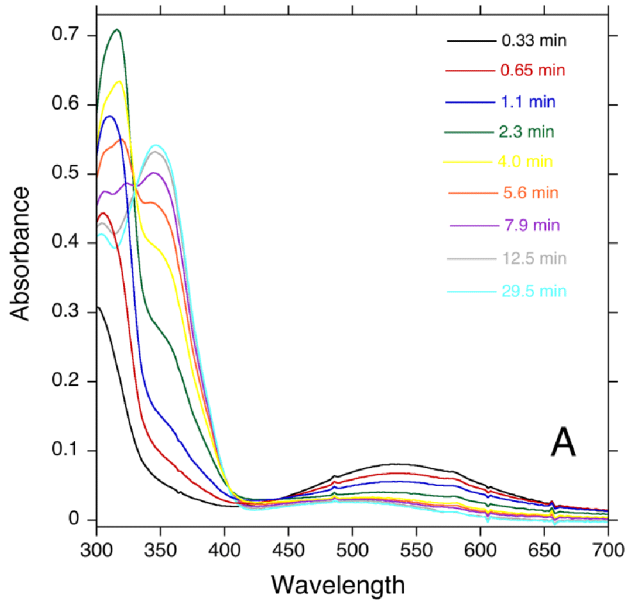

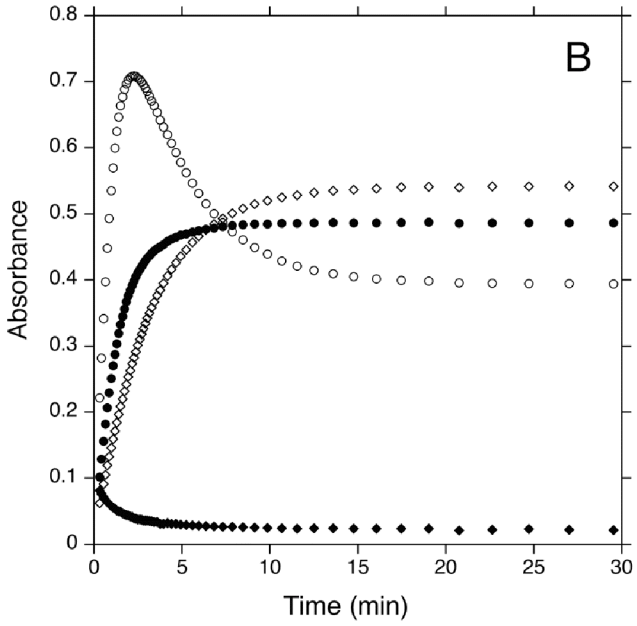

Qualitative assessment of the data shows the rapid decay of substrate at 532 nm, concomitant with the appearance of a chromophore with λ_{max} at 316 nm (WT-I). This species subsequently decays and a direct precursor-product relationship with a new chromophore with λ_{max} at 346 nm can be seen by the isosbestic point at 332 nm. The final chromophore represents enzyme bound PQQ (WT-PQQ) as determined by comparison to the spectrum of a sample of PqqC with enzyme after the addition of authentic PQQ (data not shown). The spectrum of enzyme bound PQQ is red-shifted by about 15 nm compared to the free cofactor (Table 2). Data at single wavelengths (Figure 6B) can be fit directly to a process involving three enzyme bound species; however a more accurate analysis was obtained by global fitting of the data using the program SPECFIT/32. Singular-value decomposition analysis yielded each individual spectral component and the data were fit to an irreversible, two consecutive exponential model, which yielded first-order rate constants k_1 = 0.960 (± 0.013) min^{-1} and k_2 = 0.340 (± 0.005). Compilation of the results obtained from the global fitting procedure are shown in Table 2.

Table 2. Results from global fitting (SPECFIT/32) of spectral changes during the aerobic WT-PqqC reaction.

Species[a]	λ_{max} (nm)	ε ($mM^{-1}cm^{-1}$)	Rate constants (min^{-1})
WT-AHQQ	536	2.0	
WT-I	316	22.8	k_1 = 0.960 (± 0.013)
WT-PQQ	346, 498	11.5, 0.6	k_2 = 0.340 (± 0.005)
PQQ[b]	331, 475	10.0, 0.7	

[a] The WT prefix refers to enzyme bound species.
[b] From reference 22.

Single-turnover studies were also performed with the active-site variants, H84N and H84A under identical conditions as described for the WT enzyme. Representative spectra during the course of the reaction are shown in Figure 7A (H84N) and Figure 8A (H84A). The overall reaction is slower than for WT enzyme and the spectral changes during the H84N reaction can be described involving either four or five different species. The global fit is slightly better using five species, as determined by the residuals of the fit and by visual assessment of the quality of fits at single wavelengths. Summary of global fitting using an irreversible, four consecutive exponential model is shown in Table 3 for H84N and the concentration profile

obtained by the fit is shown in Figure 7B. The final enzyme bound product (λ_{max} = 366 nm, 329 nm) appears very different from that observed for WT enzyme; however incubation of enzyme with authentic PQQ displays the same spectrum, arguing that this chromophore represents enzyme bound PQQ (see Discussion). The rate of PQQ formation in H84N (0.0562 min^{-1}) is 6-fold slower than for WT, consistent with a proposed role of H84 in the enzymatic reaction[4]. All three intermediates observed in the reaction have different spectral properties than WT-I. H84N-I_A has a single absorption maximum at 344 nm, whereas H84N-I_B has two maxima at 330 nm and 448 nm, and H84N-I_C has two maxima at 320 nm and 445 nm, respectively.

Figure 7. Single-turnover reaction of the active site variant H84N. (A) Representative spectra during the reaction at the following timepoints: 0.32, 0.54, 1.1, 2.5, 4.2, 8.5, 29.5 and 91.5 min, respectively. A total of 251 spectra were recorded for the reaction (see Supplementary Material). (B) Percentage concentration profile as determined by global fitting of the five enzyme bound species observed in the reaction. S is substrate; I_A is first intermediate; I_B is second intermediate; I_C is third intermediate and P is product.

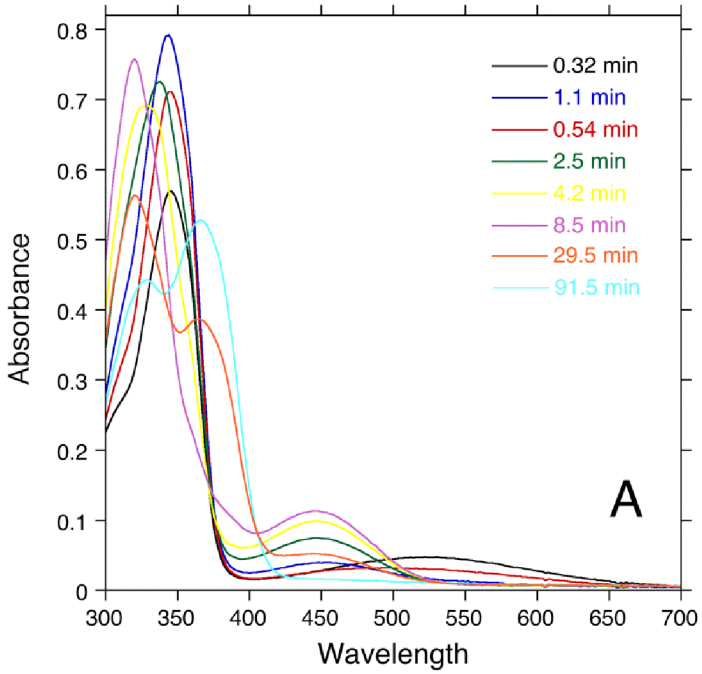
Absorbance
Wavelength
0.32 min
1.1 min
0.54 min
2.5 min
4.2 min
8.5 min
29.5 min
91.5 min
A

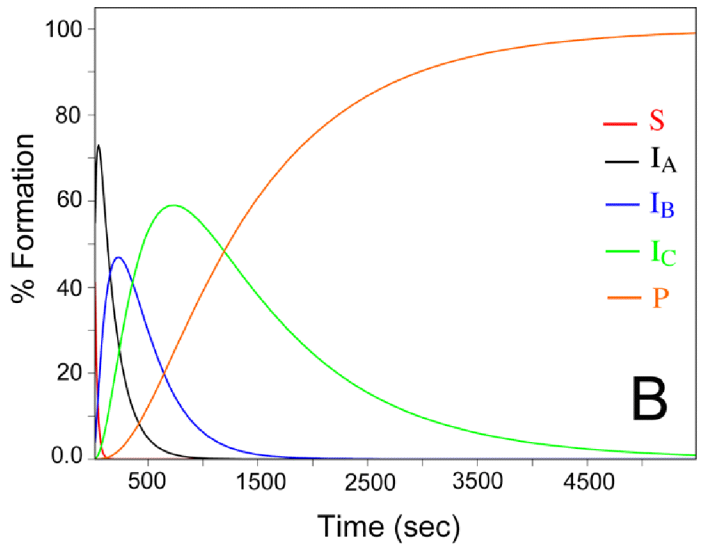
% Formation
Time (sec)
S
I_A
I_B
I_C
P
B

Table 3. Results from global fitting (SPECFIT/32) of spectral changes in the aerobic reaction of H84N.

Species[a]	λ_{max} (nm)	ε ($mM^{-1}cm^{-1}$)	Rate constant for formation of species (min^{-1})
H84N-AHQQ	532	2.1	
H84N-I_A	344	20.1	k_1 = 2.75 (± 0.04)
H84N-I_B	330, 448	15.1, 2.7	k_2 = 0.378 (± 0.022)
H84N-I_C	320, 445	19.7, 3.0	k_3 = 0.218 (± 0.006)
H84N-PQQ	366, 329	11.2, 9.2	k_4 = 0.0562 (± 0.0005)
PQQ[b]	331, 475	10.0, 0.7	

[a] H84N prefix refers to enzyme bound species.
[b] From reference 22.

Figure 8. Single-turnover reaction of the active site variant H84A. (A) Representative spectra during the reaction at the following timepoints: 0, 0.5, 1, 1.5, 2, 2.5, 3, 5, 7, 10.5, 11, 13, 16, 18 and 22 min, respectively. A total of 251 spectra were recorded for the reaction. (B) Percentage concentration profile as determined by global fitting of the four enzyme bound species observed in the reaction. S is substrate; I_A is first intermediate; I_B is second intermediate and P is product.

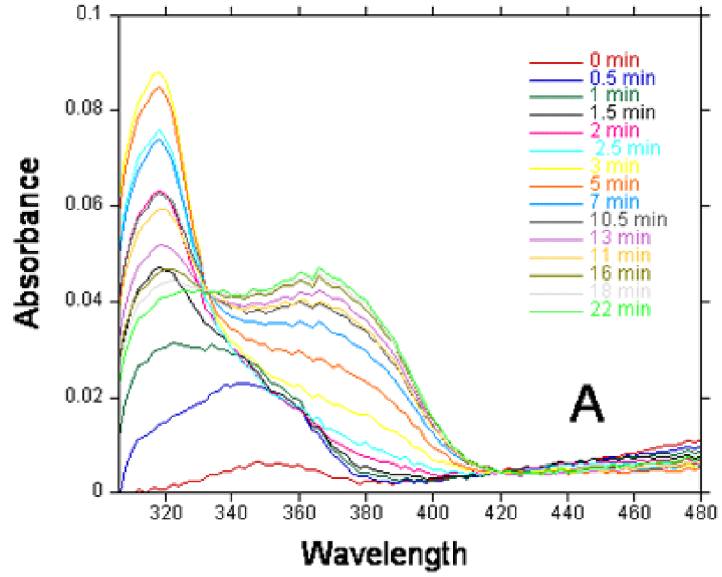

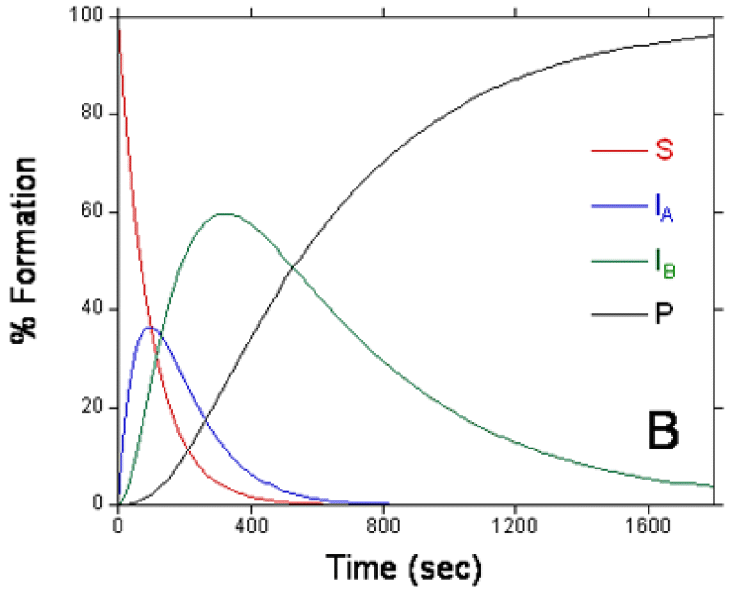

Table 4. Results I_A from global fitting (SPECFIT/32) of spectral changes during the aerobic H84A reaction.

Species[a]	λ_{max} (nm)	ε ($mM^{-1}cm^{-1}$)	Rate constant for formation of species (min^{-1})
H84A-AHQQ	532	2.1	
H84A-I_A	344	5.9	k_1 = 0.90 (± 0.19)
H84A-I_B	318	37.2	k_2 = 0.57 (± 0.08)
H84A-PQQ	366, 329	9.5, 0.7	k_3 = 0.09 (±0.00)
PQQ[b]	331, 475	10.0, 0.7	

[a] H84A prefix refers to enzyme bound species.
[b] From reference 22.

The single turnover analysis of H84A is simpler than for H84N with the appearance of only two intermediates at 340 and 318 nm. The absence of the third intermediate seen at 330 nm for H84N could have indicated that a three-exponential model is the more appropriate one for H84N. However, as discussed below the anaerobic behavior of the two H84 mutants is quite different. We note that the rate of formation of enzyme bound PQQ is *ca*. 2-fold faster for the less conservative mutation, H84A, (k = 0.09 min^{-1}) in relation to H84N (k = 0.056 min^{-1}).

Reactions under Anaerobic Conditions

By excluding oxygen from the samples, one can study the initial phases of the PqqC reaction and Figure 9A, B and C shows the spectral changes that occur in the reactions with WT, H84N and H84A, respectively. The WT reaction displays a time-dependent formation of two independent chromophores with λ_{max} at 318 nm and 356 nm, Figure 9A, that appear with rate constants of 2.42 ± 0.07 min^{-1} and 1.22 ± 0.06 min^{-1}, respectively (see Table 5). Exposure of the sample to air yields similar results as when oxygen was present during initiation of the reaction by AHQQ (Figure 6A), indicating that although two species are formed in the absence of oxygen, both can go on to form PQQ.

Figure 9. Spectra obtained in the PqqC reaction under anaerobic conditions with WT (A), H84N (B) and H84A (C). Representative spectra for the WT reaction are shown at the following timepoints: 0.5, 0.8, 1.1, 1.4, 2.4, 3.4, and 5.4 min. The WT data (A) shows the appearance of two intermediates at 318 and 356 nm. The H84N data (B) shows the timecourse for the anaerobic reaction and the buildup of a single intermediate at 344 nm. The H84A representative spectra are shown at 0.3, 1.3, 3., 4.3, 8.3, 15, 21.6, 28.3, 36.3, 44.3, 52.3, and 61.3 min. The H84A data (C) shows the appearance of a 344 nm intermediate and a 318 nm intermediate.

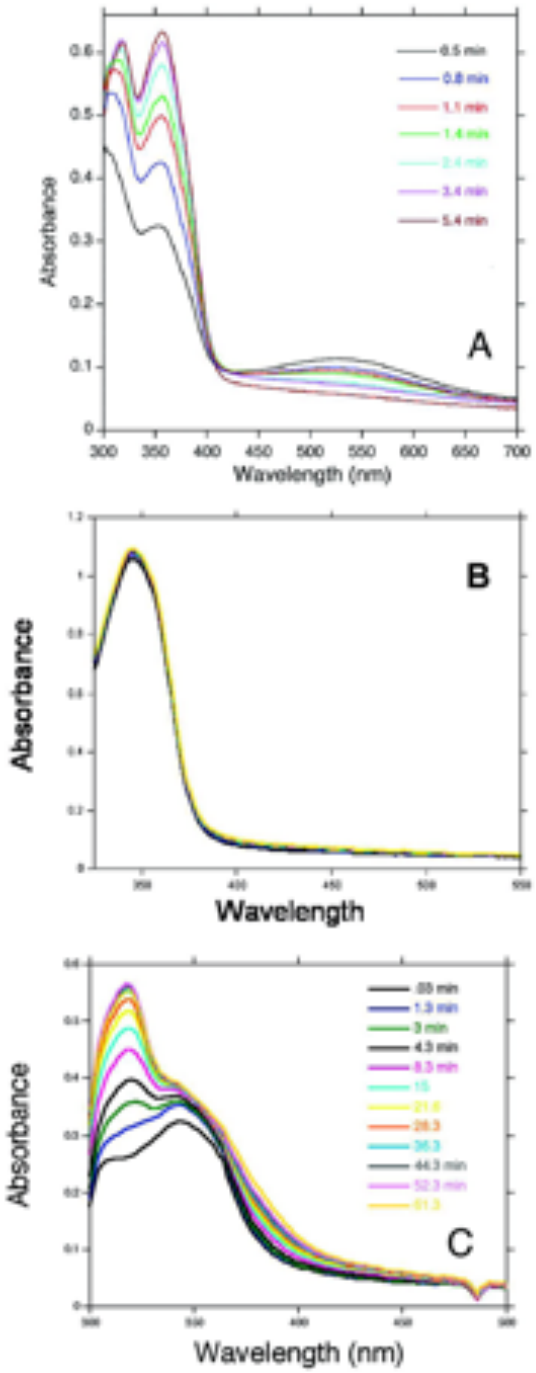

Table 5. Results from global fitting (SPECFIT/32) of spectral changes in the anaerobic reaction of PqqC.

Species[a]	λ_{max} (nm)	ε ($mM^{-1}cm^{-1}$)	Rate constant for formation of species (min^{-1})
WT-AHQQ	536	2.1	
WT-I_A	318	21.8	k_1 = 2.42 (±0.07)
WT-I_B	356	12.3	k_2 = 1.22 (±0.06)
H84N-AHQQ	532	2.1	
H84N-I_A	344	21	k_2 = 0.80 (±0.02)
H84A-AHQQ	532	2.1	
H84A-I_A	344	5.6	k_1 = 1.57 ((±0.06)
H84A-I_B	318	31	k_2 = 0.12 (±0.02)

The H84N reaction performed under anaerobic conditions produces a single chromophore, which persists for hours if oxygen is excluded from the sample, Figure 9B and Table 5. The absorption maximum (344 nm) and extinction coefficient (21 mM^{-1} cm^{-1}) of the chromophore show that it is H84N-I_A, which is the first species formed in the H84N reaction in the presence of air (Figure 7, Table 3). Exposure to air leads to the formation of the other two intermediates (H84N-$I_{B/C}$) followed by PQQ (data not shown).

The H84A reaction under anaerobic conditions produces spectra similar to that of the first two intermediates in the H84A aerobic reaction, Figure 8C and Table 5. However, while the first intermediate (344 nm) has an extinction coefficient similar to the aerobic reaction (Table 4), the 318 nm species has a much lower extinction coefficient. The anaerobic H84A reactions show characteristics of both the H84N and WT-reactions: Analogous to H84N, H84A shows an intermediate at 344 nm; however, similar to WT, a species is also observed at 318 nm (Table 5). We note that the extinction coefficients differ among the WT, H84N and H84A species, with the largest difference seen in the 318 nm peak, observed both aerobically or anaerobically. This could be due to the formation of different quinol species (cf. Scheme 3), to the fact that the SPECFIT analysis is of many overlapping peaks, or a combination of these factors.

Binding of PQQ to WT-PqqC, H84N and H84A

PqqC from *K. pneumoniae* and *M. extorquens* are reported to undergo only a single-turnover *in vitro*. The addition of an uncharacterized, proteinaceous activating factor and

NADPH is reported to result in increased activity of the enzyme, presumably due to multiple turnovers. In order to study factors leading to the apparent "inactivation" of the enzyme, we have measured the binding affinity of PqqC for PQQ. A sensitive fluorescent assay was developed for the binding process, which takes advantage of a bathochromic shift in the emission spectrum between free PQQ (F_{max} = 488 nm) and enzyme bound PQQ (F_{max} = 442 nm) and a large increase in fluorescence for the PQQ:PqqC complex compared to free PQQ (Figure 10A).

Figure 10. Binding of PQQ to WT and H84N form(s) of PqqC as determined by fluorescence spectroscopy. (A) Fluorescence emission spectra of buffer (dotted line), free PQQ (50 nM) (dashed line) and of PQQ (50 nM) plus various concentrations of PqqC (solid lines). (B) Binding curve for PQQ (50 nM) binding to WT PqqC. Data were fitted to Eq.1 and yielded a K_D of 2.0 (± 0.1) nM. (C) Binding curve for PQQ (20 nM) binding to H84A. Data were fitted to Eq.1 and yielded a K_D of 1.7 (± 0.2) nM. (D) Binding curve for PQQ (20 nM) binding to H84N. Data were fitted to Eq.1 and yielded a K_D of 0.55 (± 0.07) nM.

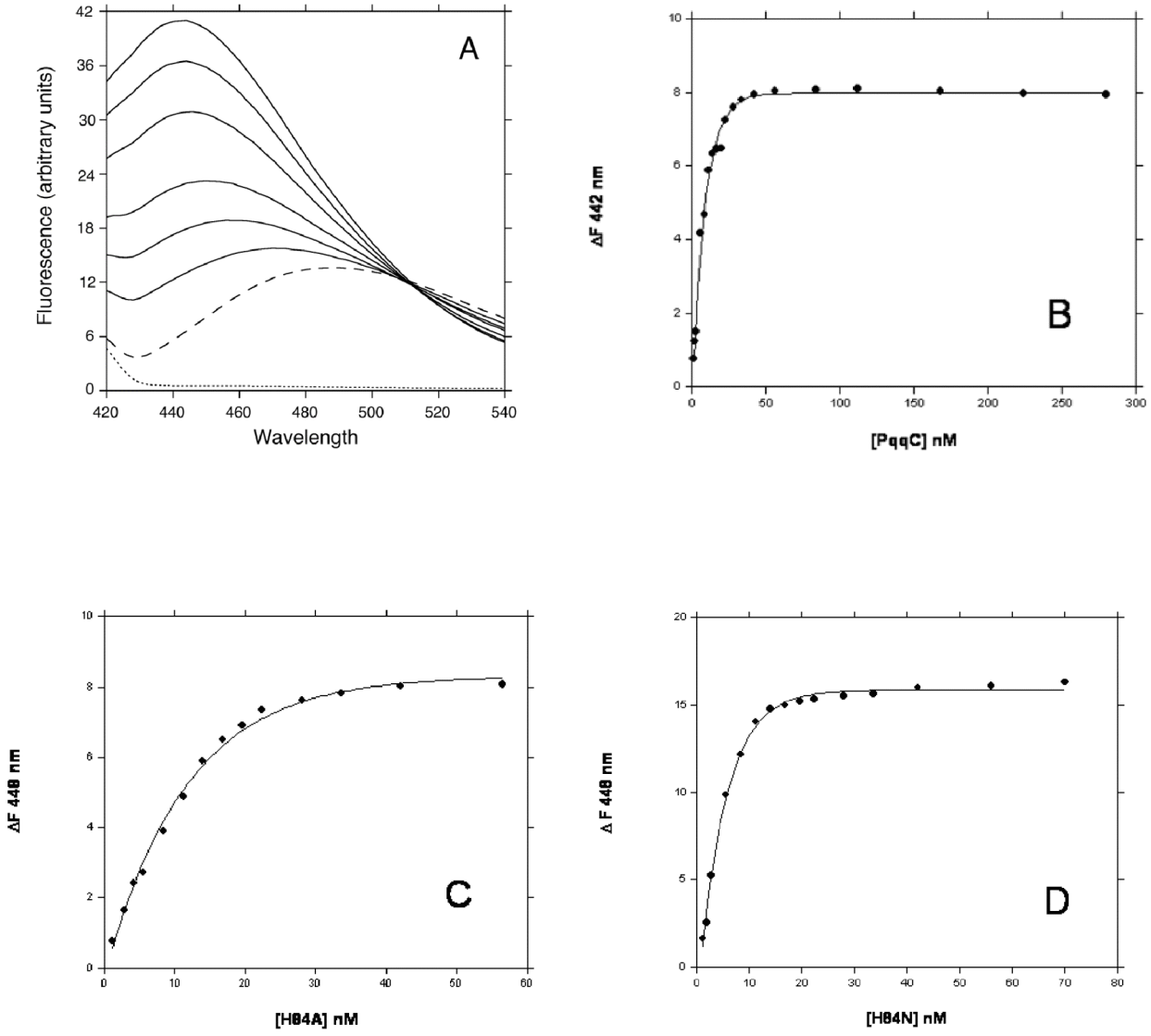

In these experiments, the concentration of PQQ was kept constant at a concentration similar in magnitude to K_D and the concentration of the enzyme was varied. The data were fitted to a quadratic binding isotherm to derive binding constants (Eq. 1). Results with both WT, H84A and H84N are shown in Figure 10B, C and D, respectively. A small hypsochromic shift is observed in the H84N:PQQ or H84A:PQQ complexes (F_{max}= 448 nm) compared to WT:PQQ (F_{max} = 442 nm). The apparent K_D values derived from the data were 2.0 (± 0.1) nM for WT, 1.7 (± 0.2) for H84A and 0.55 (± 0.07) nM for H84N, which show that product binding is extremely tight in all cases. These results are perhaps not surprising given the number of interactions in the PqqC:PQQ complex seen in the X-ray crystal structure[4].

O_2 Consumption in H84A

To test the equivalents of oxygen used in by H84A during turnover a Clark type electrode was used. It was found that H84A consumed 2.8 equivalents of O_2 for every equivalent of PQQ formed. This is the same result as seen with WT, so it can be assumed that H84 mutations are not affecting the O_2/H_2O_2 ratio in the products of the PqqC reaction.

Discussion:

PqqC catalyzes a complex reaction that involves ring closure via a C-N bond formation followed by an eight-electron oxidation reaction, all in the absence of a metal or organic cofactor[4]. Under single turnover conditions, this reaction consumes three equivalents of O_2, with the remaining two electrons needed to complete the oxidation cycle being used to reduce an intermediate H_2O_2 molecule produced in the enzyme active site. The net reaction is thus the consumption of 3 moles of O_2 and the production of 2 moles of H_2O_2 and one mole of H_2O[4]. The proposed mechanism of PqqC (Scheme 3) shows how the enzyme may facilitate this reaction, by utilizing the inherent chemical reactivity of the substrate to bring about the oxidative chemistry. The first step is illustrated as the ring closure process, followed by O_2-mediated oxidation of the resulting quinol. Although not explicitly shown in Scheme 3, oxidation presumably occurs in two steps in which an outer sphere electron transfer to O_2 forms as a transient superoxide:semiquinone intermediate prior to quinone and hydroperoxide formation. The subsequent steps are proposed to involve three successive tautomerisation reactions (I-III), which serve to activate each of the intermediates for oxidation in the absence of a cofactor. This property of PqqC puts the protein in a small class of enzymes, which carry out oxidative chemistry without the aid of metals or organic cofactors. What these enzymes have in common is that their respective substrates are already predisposed to react directly with molecular oxygen. Members of this family[8] include urate oxidase[9], 1H-3-hydroxy-4-oxoquinoline 2,4-dioxygenase[10-12] and ActVA-Orf6 monooxygenase[13].

Single Turnover Studies in the Presence and Absence of O_2

This study describes the formation and decay of various spectroscopic intermediates on the reaction pathway (Scheme 3). In particular, the function of H84, which is proposed to serve as a general-base catalyst and a possible proton donor, has been probed by studying the H84N and H84A variants. The mechanism in Scheme 3 predicts the use of catalytically important basic residues to facilitate the keto-enol tautomerisations required to activate the substrate for subsequent oxidations. Intermediates shown in brackets in Scheme 3 are believed to be unstable under wild type conditions and to partition subsequently towards the quinol due to the large driving force of aromatization. The X-ray crystal structure of the PqqC:PQQ complex supports this mechanism[4] and presents many interactions that could support the proposed mechanism. Three conserved histidine residues (H84, H154 and H24) are

strategically placed to abstract protons at positions C-3, N-6 and C-9, respectively (Scheme 3, Figure 4A). H84 is also in a position to interact with the C4 oxygen of bound PQQ, while H154 is within 4 angstroms of the putative oxygen molecule and could possibly have a role in oxygen binding and reactivity.

Kinetic studies of the WT enzyme under single-turnover conditions show the formation of a single spectroscopic intermediate (WT-I) with λ_{max} at 316 nm. The position and intensity of this band, along with the absence of bands at higher wavelengths, suggests that this intermediate is one of the quinol species on the reaction pathway. The intermediate is formed in a kinetically competent manner (0.96 min^{-1}), i.e., approximately 3-fold faster than PQQ. The rate of formation of PQQ (0.34 min^{-1}) is similar to what has been observed by a different method based on detection of PQQ by HPLC after quenching in acid (0.38 min^{-1})[4]. Kinetically, the k_{obs} found by PQQ formation in the HPLC does not take into consideration that there are numerous steps of reaction. These intermediate steps are seen in by the spectroscopic methods. Interestingly, enzyme bound PQQ displays a bathochromic shift for absorbance of about 15 nm compared to the free cofactor. This shift is likely to result from the electrostatic environment in the enzyme active site, which apparently decreases the energy separation of a π to π^* transition in PQQ.

When the reaction is done anaerobically two different chromophoric species are observed, with λ_{max} at 318 nm (2.42 min^{-1}) and 356 nm (1.22 min^{-1}), respectively (Figure 9A). Although these chromophores appear at different rates, they are both precursors to cofactor as exposure to air leads to formation of WT-I followed by PQQ (data not shown). Scheme 4 depicts the relationship among the species, with the central reaction occurring aerobically and the two side branches representing the anaerobic process.

Scheme 4: Proposed pathway and accompanying rate constants for the generation of PQQ with WT-PqqC. The center line represents the aerobic reaction and the outer processes are intermediates detected anaerobically.

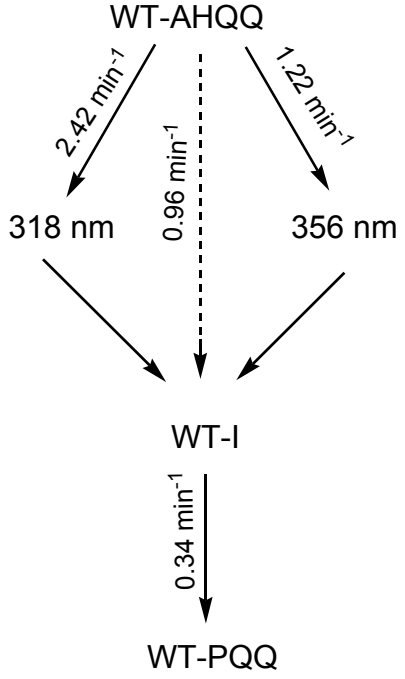

As illustrated, all species are suggested to funnel through WT-I. While the chemical identity of the spectroscopic intermediates remains unproven, the proposed mechanism of the reaction (Scheme 3) allows plausible predictions. The anaerobic reaction prevents oxidation from occurring, such that only an initial quinol species (tentatively assigned to 2 in Scheme 3) would be expected to form. Notice that 2 is drawn in an ionized form, which will undergo reaction with O_2 more rapidly than a fully protonated intermediate. However, the pK_a of the quinol in the active site could be such that under the present experimental conditions this group is only partially deprotonated - hence the two different chromophores for WT-PqqC. The 318 nm species is likely to be the fully protonated quinol, whereas the species at 356 nm is tentatively assigned to monoanionic quinol, Scheme 5. Quinol absorbance is known to red shift at higher pHs supporting the proposal of the higher wavelength being a monoanionic quinol. Changing the pH from 6 to 10 results in an approximate 10nm red shift (J. RoseFigura, data not shown) indicating that the monoprotonated quinol would be at a higher wavelength than the diprotonated quinol.

The reaction of the H84N mutant shows greatly different spectroscopic and kinetic properties than observed for WT. In the presence of O_2, three intermediates (H84N-I_{A-C}) are observed based on global fitting of the data (Figure 7, Table 3). Importantly, under anaerobic conditions, a sole species is formed, H84N-I_A, with a λ_{max} at 344 nm (Figure 8B, Table 5). The likely identity of the 344 nm species is discussed in greater detail below.

H84N-I_B and I_C have very similar spectral properties, with both chromophores displaying two transitions above 300 nm, and a signature peak at ~ 450 nm (Figure 7, Table 3). The position of the ~ 450 nm transitions suggests that these could originate from an n to π^* transition of quinone intermediates. The other possibility is that these could represent a semiquinone:superoxide radical pair. Though X-band EPR experiments were unable to detect any signal due to a radical (data not shown), the possibility of strong magnetic coupling between the two radicals rendering the system EPR-silent cannot be ruled out.

Turning to the H84A mutant in the presence of O_2, this shows two intermediates (H84A-I_A and H84A-I_B) before product formation (Figure 8, Table 4). The H84A reaction has properties similar to both the wild type and H84N reactions. Like H84N, H84A forms PQQ with a blue-shifted absorbance (λ_{max} = 330 nm, 366 nm). The intermediate seen before PQQ formation (λ_{max} = 318 nm) in the H84A reaction is absent in the H84N reaction, but similar to an intermediate in the wild type reaction. Under anaerobic conditions, two species are seen in the H84A reaction (Figure 9C). These are quite analogous to what is seen in the aerobic reaction, but do not proceed to product. We note that the first intermediate of both the aerobic and anaerobic H84A reactions (Figure 9C) is similar to that single anaerobic species formed from H84N (λ_{max} = 344 nm) (Figure 9B) and that no such species is seen in the wild type reaction. The second intermediate (λ_{max} = 318 nm) is comparable to the anaerobic intermediate found in the wild type reaction, but is absent from the H84N reaction.

In the anaerobic reaction the final species should be the first quinol species (2 in Scheme 3), but H84N is only able to form an intermediate at 344 nm. The wild type reaction forms a species, which we believe to be the quinol species at 318 nm. This species is also seen in the H84A reaction, but following a species at 340 nm. It is believed that the mutations cause the formation of the quinol species to be rate-limiting, leading to build up of a species at approximately 340 nm.

The aggregate spectral data under anaerobic conditions are particularly valuable as they simplify the observed processes and allow us to address the initial series of chemical

steps. The band at 318 nm is easily assigned to the fully protonated, first quinol intermediate (Scheme 5) while the band at 344 nm is compatible with a quinoid intermediate[14].

Scheme 5. Possible steps of the PqqC reaction in the absence of oxygen. The present analysis assumes that ring closure is the first step. In the wild type reaction, H84 is proposed to act as a proton donor to the C4 oxygen of the intermediate, allowing the subsequent tautomerization to the quinol to occur. In H84N, there is no proton donor and so, under anaerobic conditions, protonation and therefore tautomerization cannot occur. In the case of the H84A mutation, space in the active site is proposed to facilitate access of a water molecule that can function as an alternate proton source to bind and act as a proton donor.

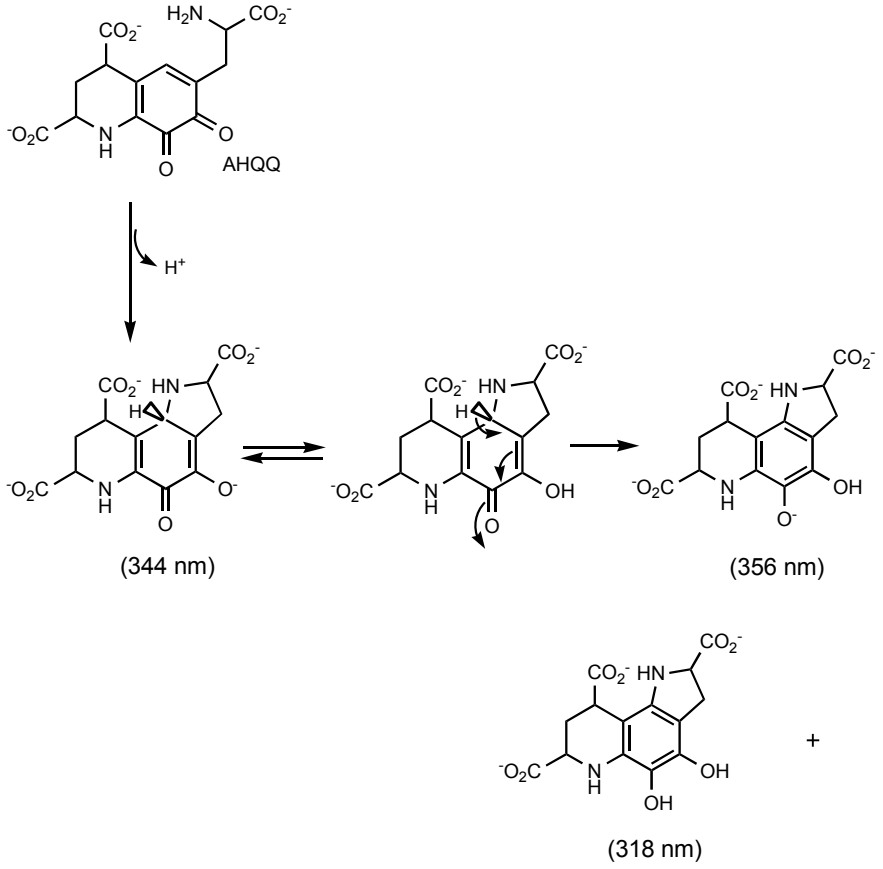

Figure 11: Possible bases and distances in the active site of PqqC

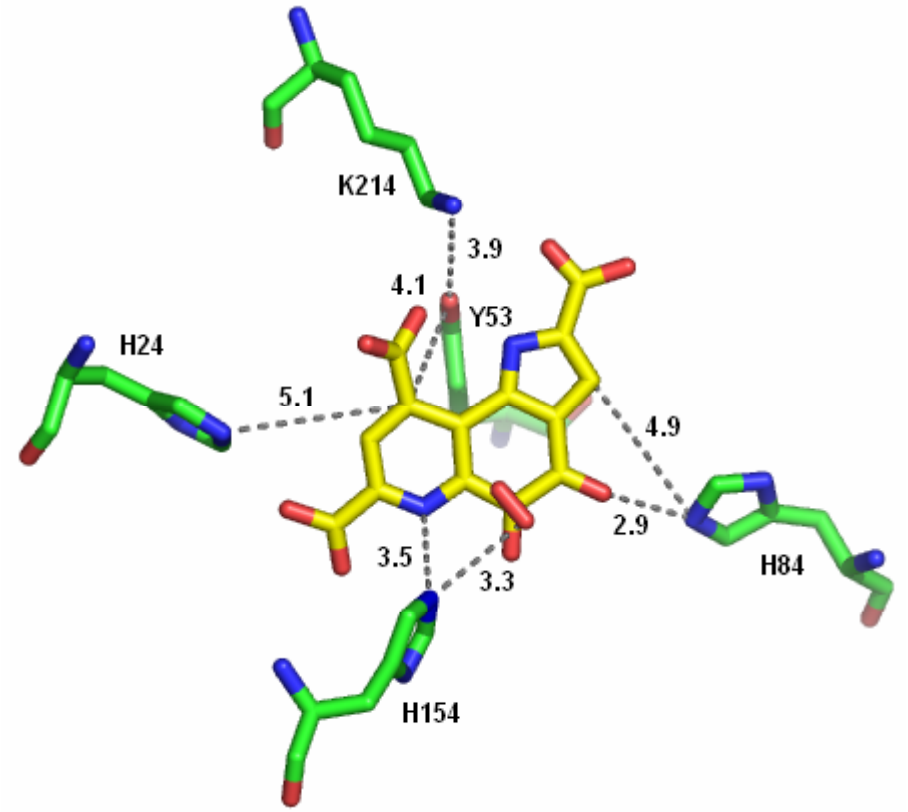

The fact that H84 is very close (< 3Å) to the C4 oxygen of product (Figure 11) leads us to propose that this histidine acts as a proton donor in the course of the isomerization of the quinoid to quinol intermediates. The finding that H84A can proceed to the first quinol product while H84N cannot, requires some structural rationalization. The most likely explanation is that H84A generates a cavity with enough room for a water molecule to act as a proton donor[15], while Asn, which is approximately the same size as His prevents access of water as an alternative proton donor. The kinetic properties of the anaerobic reaction are summarized in eq (2):

$$\text{E-AHQQ} \xrightarrow{k_1} \underset{\text{E-(Quinoid)}}{344\text{ nm}} \xrightarrow{k_2} \underset{\text{E-(Quinol)}}{318\text{ nm}} \qquad (2)$$

WT: 2.42 min^{-1}	WT: very fast
H84N: 0.80 min^{-1}	H84N: NR
H84A: 1.57 min^{-1}	H84A: 0.12 min^{-1}

As illustrated, the observed rate constant for WT is assigned to k_2, since no 344 nm accumulates, indicating that $k_2 >> k_1$. The similarity among the k_1 values for WT, H84Q and H84A indicates that quinoid formation can occur independent of the nature of position 84, while the quinoid to quinol transformation is critically dependent on H84. One notable feature is that H84N turns over to product in the presence of O_2. This suggests structural changes upon O_2 binding that permit proton donation to take place for H84N as well as H84A. We emphasize that while H84N may act as an active site base in PQQ formation, Scheme 3, the anaerobic reaction implicates a key role for this residue as a proton donor.

One feature of the aerobic spectra of PQQ in the H84 mutants is a different UV-vis spectrum for the PQQ complexes (Tables 2- 4). Although it was possible that the observed

complexes were not PQQ, control experiments in which authentic PQQ was added to mutant enzyme yielded the same spectra as observed in the reactions with AHQQ (data not shown). The origin of large perturbation in the UV-Vis spectrum may be explained by the possible presence of a hydrated form of PQQ. In fact, partial hydration occurs in aqueous solution of PQQ at neutral pH[10]. PQQ-H_2O does not display the weak and broad signature n to π^* transition at ~480-500 nm and this transition is also lacking in the mutant-PQQ complexes. Moreover, π to π^* transitions of PQQ-H_2O in solution are observed at ~ 330 nm and 360 nm[16], which is similar to what is seen for the mutant-PQQ product complexes. We, therefore, propose that H84 mutations shift the population of bound product towards the hydrated form of PQQ.

Fluorescence titration experiments show that PQQ binds its product very tightly. The binding constant is only 2.0 nM, and, perhaps somewhat surprisingly, the binding affinity is not compromised in the H84N mutant (0.55 nM) or the H84A mutant (1.7 nM). The tight binding of PQQ can explain why enzymatic assays of PqqC had been unable to detect more than a single turnover. In these assays the concentration of PqqC was typically in the high nM or low μM range such that PQQ formed in the reaction remained tightly bound at the active site (Figure 10). By lowering the concentration of enzyme below the K_D a different result is obtained, where approximately 6 enzyme turnovers can be detected[17]. Further analysis to measure kinetic parameters (k_{cat}/K_M) is currently underway; however these experiments are complicated due to the low reactivity of PqqC and sensitivity of the enzymatic assay (sGDH), which is employed to detect PQQ.

The data described herein provide important information regarding the mechanism of PqqC, including the spectral detection of several intermediates in the catalytic cycle. The role of one putative catalytic residue (H84) has been probed, leading to its proposed role as a general acid catalyst in the conversion of quinoid to quinone species. The anaerobic reactions provide evidence of the mechanism of the first step of reaction. Though we can still not speak to the order of the proposed steps (A, B1, B2 and B3 in Figure3), the different species seen in the anaerobic reactions indicate that the mechanism of oxidation for PqqC involves a quinoid species (λmax approximately 344nm), which proceeds onto a quinol species (λmax approximately 318nm) that will persist in an anaerobic environment. This supports the proposed mechanism. The demonstrated tight binding of PQQ at the active site of PqqC raises the question of how this enzyme can catalyze multiple turnovers *in vivo*. Additionally, although PQQ is formed in the cytosol gram negative bacteria, it must be delivered to the periplasm before it can function. So far no factor has been identified that causes PqqC to have a significantly lower Kd for PQQ. Binding of the reduced (quinol) form of PQQ is not as tight as it is for the oxidized for, but it is still in the nM range. While PQQ is necessary for bacterial growth, it is not thought that large amounts are needed for survival. It is possible that a combination of a low turnover number, along with export from the cytosol to the periplasm cause the concentration of PQQ to be sub-nanomolar in the cytosol, neatly avoiding the problematic severe product inhibition seen in the biochemical assays.

Chapter 3

PQQ Formation in O_2 Core Mutants of PqqC

Introduction:

Pyrroloquinoline quinone (4,5-dihydro-4,5-dioxo-1*H*-pyrrolo-[2,3-*f*]quinoline- 2,7,9-tricarboxylic acid: PQQ (Figure 1)) is an aromatic, tricyclic *ortho*-quinone that serves as cofactor for a number of prokaryotic dehydrogenases, largely but not exclusively from Gram-negative bacteria.

Figure 1: The structure and origin of PQQ. PQQ is shown originating from a glutamate and a tyrosine.

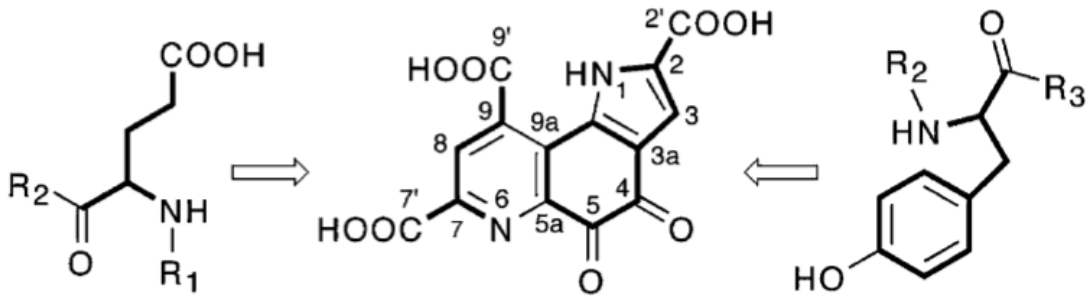

These dehydrogenases are found in the periplasm of Gram-negative bacteria. The oxidative reactions catalyzed by PQQ dependent enzymes are involved in catabolic pathways, where the best studied examples are methanol dehydrogenase (MDH) and glucose dehydrogenase (GDH)[1, 2]. GDH has long been the standard for chemically sensing PQQ. PQQ is part of the quinone family of cofactors and has remarkable antioxidant properties[3]. Like all known quinone cofactors, PQQ is peptide derived. But unlike the other quinone cofactors, such as TPQ, TTQ, LTQ and CTQ, it is freely dissociable from the enzyme and biogenesis is independent of the site of catalysis. The biosynthesis of PQQ is a complex process and, in *Klebsiella pneumoniae*, is catalyzed by the gene products of *pqqABCDEF*. All the carbon and nitrogen atoms in PQQ come from a conserved tyrosine and glutamate in the gene encoded peptide PqqA (Figure 1). The final step of PQQ formation is the best studied part of the pathway. This step is catalyzed by PqqC and involves a ring closure and the eight electron oxidation of AHQQ (3a- (2-amino-2-carboxyethyl) – 4,5- dioxo- 4,5,6,7,8,9 hexahydroquinoline-7,9- dicarboxylic acid)[4, 5]. The reaction has been well characterized and occurs using molecular oxygen as an oxidant and proceeds without the use of an external cofactor or metal[5].

Recent studies of PqqC focused on the conserved active site residue histidine 84, where asparagine and alanine mutations at the 84 position were analyzed[6]. H84 had been hypothesized to act as an active site base due to its position close to a site in PQQ where proton abstraction is necessitated in the reaction from substrate (AHQQ) to product (PQQ). A mechanism has been proposed for the PqqC reaction (Figure 2)[5], where the reaction proceeds via a series of reactions where the first intermediate formed in each step is a quinoid intermediate that tautomerizes to a quinol intermediate.

Figure 2: The proposed mechanism of PqqC. There is ring cycization (A) followed by a series of base catalyzed tautomerizations and an overall six electron H2O2/O2 mediated oxidation of the tricyclic intermediate formed in (A). The order of the steps BI-III is not known and written arbitrarily.

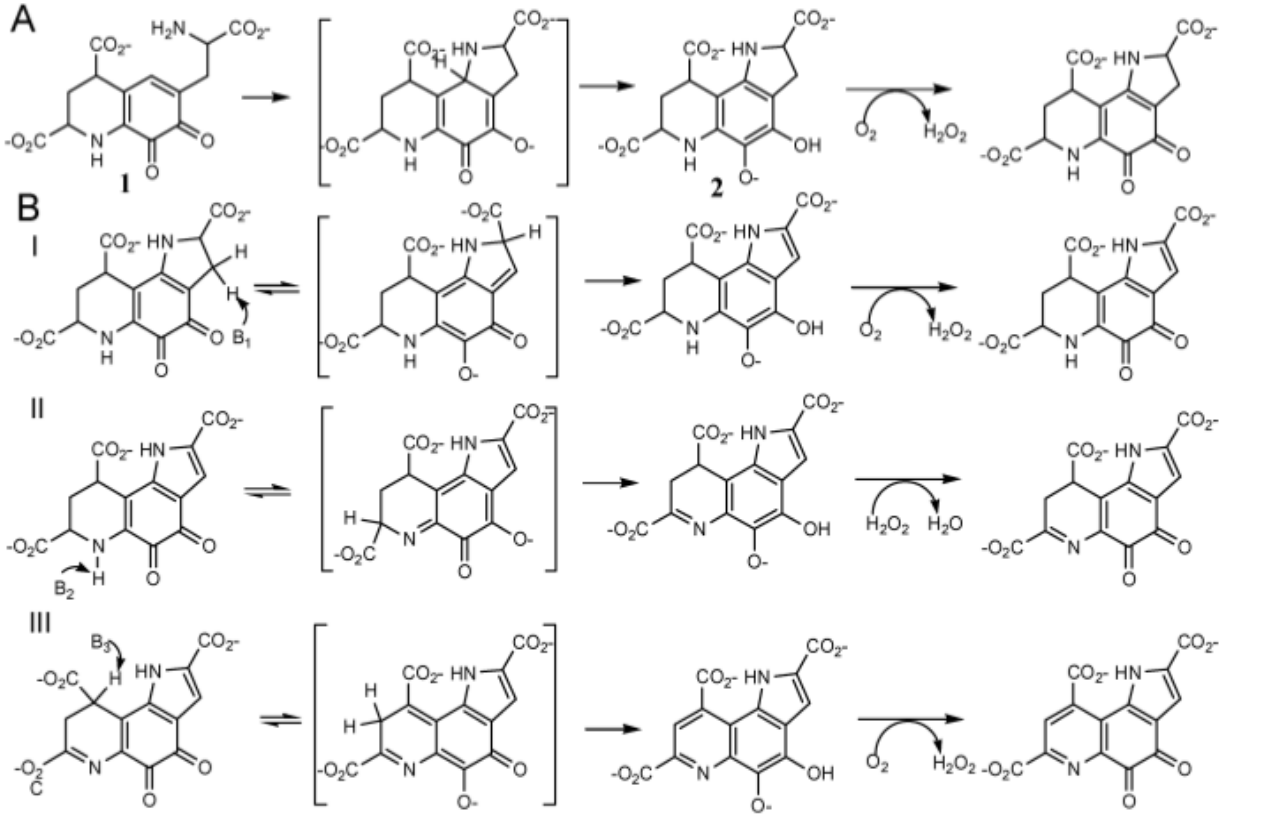

These quinol intermediates are then oxidized using molecular oxygen or hydrogen peroxide to a quinone, which is then capable of proceeding onto another step of the reaction. In the H84 study it was seen that the H84N variant was not capable of proceeding to quinol anaerobically, while wildtype (WT) and H84A were able to form quinol anaerobically. All these enzymes were capable of forming PQQ aerobically[6]. This dependence of a quinoid to quinol conversion, a non-oxidative process, on the presence of molecular oxygen warranted further investigation into the interactions between oxygen and the active site of PqqC. PqqC is one of three known cofactorless oxidases. The other is urate oxidase, where oxygen is seen to bind in a hydrophobic pocket outside of the active site before presumedly being used in the urate oxidase reaction[7, 8]. PqqC does not have such a hydrophobic pocket. In the WT structure of PqqC (1OTW) there is a density seen above the quinone ring of PQQ that fits only to oxygen or hydrogen peroxide[5, 9]. The residues within 5 Å of this density are H154, Y175 and R179 (Figure 3).

Figure 3: O_2 core residues in the active site of PqqC. PQQ is shown in gold and the putative oxygen density is shown in red above the quinone ring. Shown are residues H154, Y175 and R179 along with H84[6].

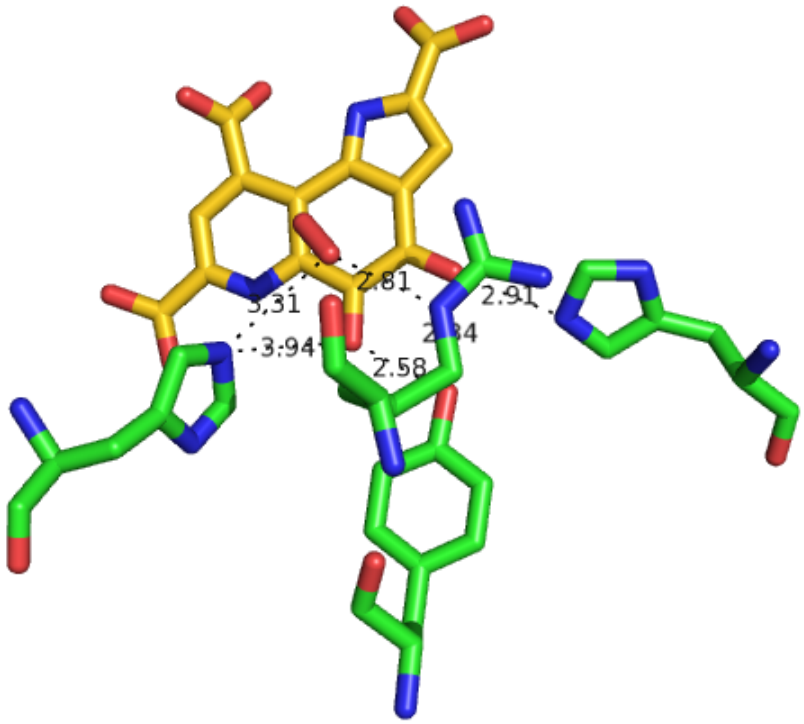

These residues are all polar residues, though the aromatic ring of Y175 and the side chain of R179 are hydrophobic. Y175 and R179 are conserved while in two instances a glutamine is found at position H154. Four mutations were made in the PqqC protein of *Klebsiella subspecies pneumoniae MGH 78578*. These variants (H154N, Y175F, Y175S and R179S) are investigated further in this chapter.

Crystal structures involving some of these PqqC mutants have previously been described. Y175F is overlay-able with WT, with all the active site residues in the appropriate position. A mutation not studied here, H154S, is seen with PQQ bound, but in an open conformation similar to the structure of WT without PQQ bound. A double mutant, R179S/Y175S, was co-crystallized with AHQQ and gives a structure which appears to be the first AHQQ-derived intermediate detected structurally. This intermediate is a nonplanar tricyclic species, implicating the cyclization of AHQQ as the first step in the overall eight electron oxidation to form PQQ (Figure 2).

Methods:

Chemicals, Reagents and Molecular Biology products:

Buffers, salts, general reagents, and culture media were obtained from Sigma and Fisher and were of the highest available purity. Ni-nitriloacetic acid (NTA) resin, DNA purification kits, and PCR primers were purchased from Qiagen. Enzymes and reagents for mutagenesis reactions were from Strategene. PQQ was purchased from Fluka. Restriction

enzymes and appropriate reaction buffers were purchased from New England Biolabs. Cell lines were obtained from Invitrogen. Plasmids were made from genomic DNA from *Klebsiella pneumonia subspecies pneumoniae MGH 78578*.

PCR cloning and Expression of Plasmids:

Expression and Purification of PqqC mutants: PCR cloning was performed by Sandra Puhringer of the Schwarzenbacher group. Plasmids were constructed in pET29 with kanamycin resistance and a C-terminal His tag. The isolated plasmids were sequenced from both directions using the T7 promoter and terminator primers. *Klebsiella subspecies pneumoniae MGH 78578* wildtype PqqC varies from the previously described *Klebsiella pneumoniae* wildtype PqqC at the base of the 3rd alpha helix. There are three differences between the two sequences: A21D, D37N and K41E. A21D were detected in the original crystal structure, while the changes at positions 37 and 41 can be shown to be in agreement with the sequence deposited by Postma (Pubmed accession number: X58778).

Expression and Purification of PqqC Variants:

Expression of plasmids was done using BL21(DE3) cells in LB medium supplemented with 50 μg/mL kanamycin. Cultures were grown at 37 C to an optical density at 600 nm of ~0.8, at which time IPTG (1 mM) was added, and the cells were harvested ~4 h later. All pET-29b-pqqC/D plasmids produced high quantities of protein as judged by SDS-PAGE analysis. Cells were resuspended in lysis buffer containing 50 mM KH_2PO_4, 300 mM NaCl, 1 mM PMSF and 5 mM $MgCl_2$. After sonication and centrifugation as described previously the clear supernatant was applied to a 10 mL Ni-NTA column that had been equilibrated in 20 mM tris buffer supplemented with 300 mM NaCl and 5 mM imidazole. After two buffer washes with increasing amounts of imidazole (5mM and 10mM) the His-tagged bound protein was eluted with 25 mM tris buffer supplemented with 300 mM NaCl and 250 mM imidazole. Fractions containing mutant enzyme were analyzed by SDS-PAGE, pooled, concentrated and buffer exchanged into 100mM monobasic potassium phosphate pH 8.0 before being aliquoted and snap frozen. Further column chromatography only provided inactive enzyme unlike what was seen in wildtype PqqC and H84 varients which were further purified by size-exclusion chromatography. A single band was seen on an SDS-PAGE gel, and the Ni-NTA column chromatography provided enzyme with greater than 90% purity. The expression for these mutants was lower than WT and yielded ~3 mg/L of culture.

Expression and Purification of sGDH:

The apo-form of sGDH was expressed and purified with a simplified modification of literature procedures[10]. Instead of using a fermentor, overnight cultures (18 L) in shaker flasks were employed. Cells (~ 80 g) were disrupted by sonication in 250 mL of 0.1 M Tris, pH 7.5, 0.2 M NaCl, 3 mM $CaCl_2$, 0.5 mM PMSF, and 1000 U benzonase. After centrifugation, the clear supernatant was dialyzed overnight against 20 mM Tris, pH 7.5, 3 mM $CaCl_2$ (GDH Buffer). The dialysate was passed through an SP-Sepharose column (2.5 x 30 cm) and after a buffer wash, sGDH was eluted with a NaCl gradient (0-450 mM) in GDH Buffer. Fractions containing sGDH were assayed as described elsewhere[10], pooled based on enzyme activity and concentrated to ~ 20 mL. Tris buffer, pH 7.5 was added to a final concentration of 0.1 M and solid $(NH_4)_2SO_4$ to a final concentration of 1M and the protein solution was passed over a Phenyl-Sepharose column (1.5 x 20 cm). The protein was eluted by a gradient (500 mL) of decreasing concentration of $(NH_4)_2SO_4$ (1 M to 0). Enzyme containing fractions based on activity assays were combined and dialyzed against GDH Buffer overnight. The purified protein was concentrated by ultrafiltration (Amicon YM10), frozen in liquid nitrogen and stored at –80 ˚C.

This procedure yielded a single band on a gel and gave ~ 20 mg of protein with specific activity of ~7000 U/mg, which is comparable to that reported in the literature[10].

GDH Assay:

This was carried out to quantify product PQQ production from AHQQ. In order to prevent non-enzymatic formation of a quinone from reaction intermediates, after aerobic reaction of PqqC (25 μM) and AHQQ (20 μM) for one hour, the assay mixture were taken into an anaerobic chamber, where enzymes samples were denatured with acid. After centrifugation and adjustment of the pH back to pH8, the resulting supernatants were incubated with GDH anaerobically. Following this incubation, the GDH bound PqqC products were removed from the anaerobic chamber and assayed for glucose oxidation as previously published[10]. This end point assay looks at the amount of PQQ formed after one hour of reaction with PqqC enzymes. All enzymes were shown to come to an end point spectroscopically within one hour. Amount of PQQ formed can be inferred from the rate of DCIP reduction catalyzed by GDH, which corresponds to a decrease in the absorbance at 600nm. Reactions were run between 10 and 30 minutes or until no further change was observed; the initial point of each reaction was normalized to one.

Quinol Assays:

To directly test and compare the ability of the WT and mutant enzymes to do oxidative chemistry 20 μM PQQ was anaerobically reduced using 1.25 equivalents of dithiothreitol (25μM). This reduced quinol was then bound to 25 μM PqqC enzyme anaerobically and sealed in a cuvette. This anaerobic cuvette was taken out of the anaerobic chamber and exposed to oxygen approximately 10 seconds before starting spectroscopic scans. Free reduced PQQ has an absorbance at 308nm which shifts to 315-318nm when the chromophore is bound to PqqC. The spectral traces were analyzed with the program SpecFit. The data were baseline corrected at 800nm and then fit to a single exponential to find the rate of oxidation of quinol to quinone.

When H_2O_2 was tested as an oxidant instead of O_2, the sealed cuvette remained sealed and a gastight syringe was preloaded with H_2O_2 in an anaerobic chamber. H_2O_2 was added to the quinol sample directly before spectra were collected. Spectral traces were analyzed by the same method as the O_2 reoxidized spectral traces.

Results:

GDH Assay Results:

A PQQ standard, WT product and H84A product all give similar amounts of reaction indicating that they are forming the same amount of PQQ (Figure 4). Previous work has indicated that WT and H84A form PQQ at very different rates[6], but since the experiments run here are endpoint assays, it is not surprising that the final concentration of PQQ is similar.

Figure 4: Results of the GDH Assay. PqqC reactions were run aerobically, followed by an anaerobic acid denaturation and incubation with GDH. GDH assays were run aerobically, looking at the decrease of absorbance at 600nm, which corresponds with quenching of DCIP which relates to turnover of GDH. Assays with the products of a PQQ standard, WT, H84A, H154N, Y175F, Y175S and R179S reactions are shown. The product of AHQQ when subjected to the same reaction conditions as the enzyme reactions was capable of acting as a cofactor of GDH, as seen by the decrease in A_{600} in the green line.

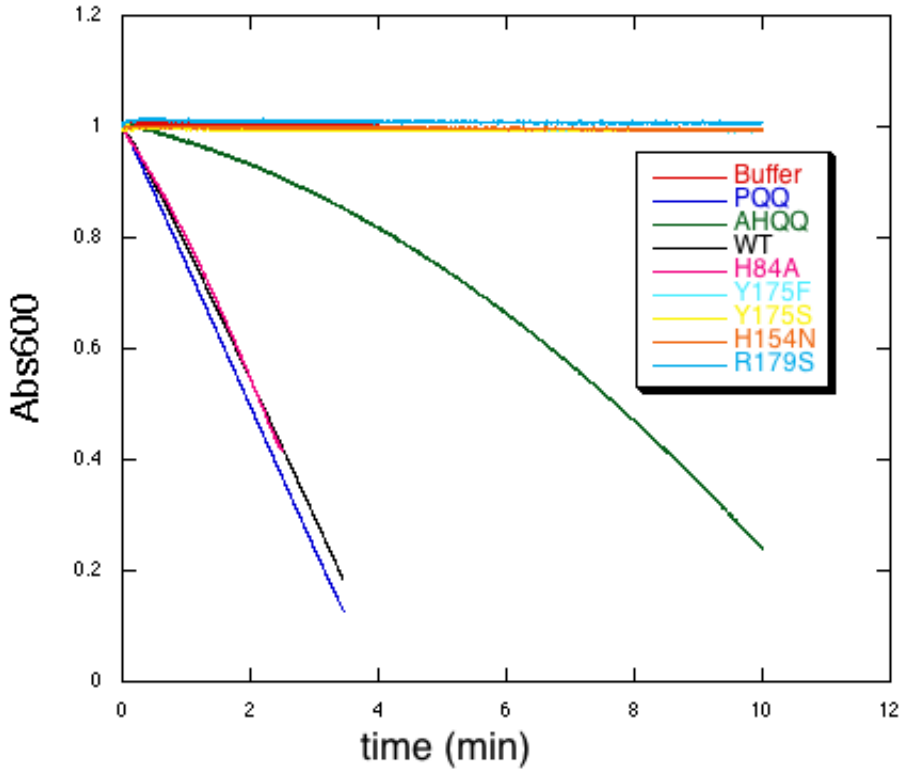

A surprising result from this study is that the product of the reactions between the substrate of the PqqC reaction, AHQQ, and different O_2 core variants of PqqC cannot act as a cofactor for GDH. When AHQQ alone is subjected to the same protocol as the enzymatic reactions, it can act as a cofactor for GDH. $PQQH_2$ was also shown to give turnover of GDH, though at a slower rate than PQQ (data not shown). This indicates that the products of the O_2 core mutants cannot function as a substrate for GDH, meaning that they are reacting partially, but not fully, to form either PQQ or a close homolog.

PQQ reoxidation:

To test the ability of these PqqC variants to do any oxidative chemistry the reaction needed to be simplified. To look only at the oxidative step (from quinol to quinone), authentic PQQ was reduced to $PQQH_2$ and the resulting quinol first incubated with enzyme anaerobically and then exposed to air (Figure 5).

Figure 5: $PQQH_2$ reoxidation to PQQ.

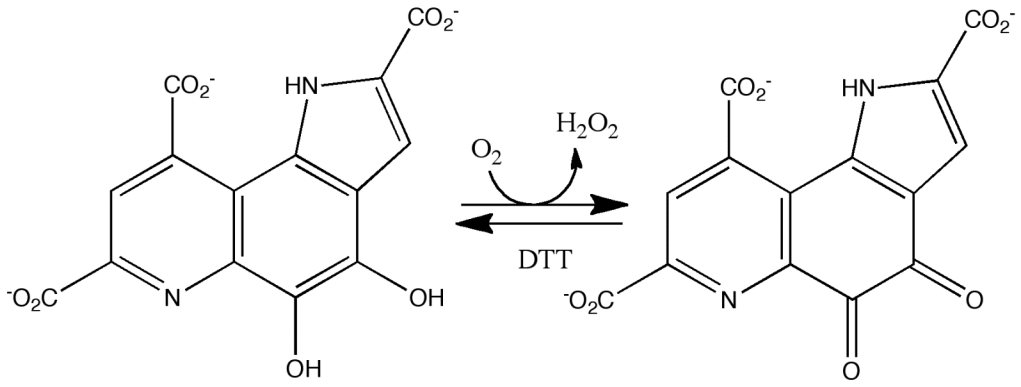

Quinols are known to reoxidize to quinones in buffer in the presence of air. As shown in Figure 7, the reoxidation of $PQQH_2$ to PQQ does not show a clear precursor-product relationship in buffer, it is concluded that $PQQH_2$ in contrast to the reactions in the presence of PqqC (Figure 6A-D), reoxidation occurs in solution via a different mechanism from reoxidation on the enzyme.

Figure 6: The spectra of reoxidation in the O2 core mutants with O_2. The quinol species can be seen at approximately 318nm, where, upon exposure to oxygen it decreases and an increase is seen at wavelengths above 300nm. (A) WT-quinol (B) Y175F-quinol (C) Y175S-quinol (D) H154N-quinol.

Figure 6A:WT-quinol reoxidation

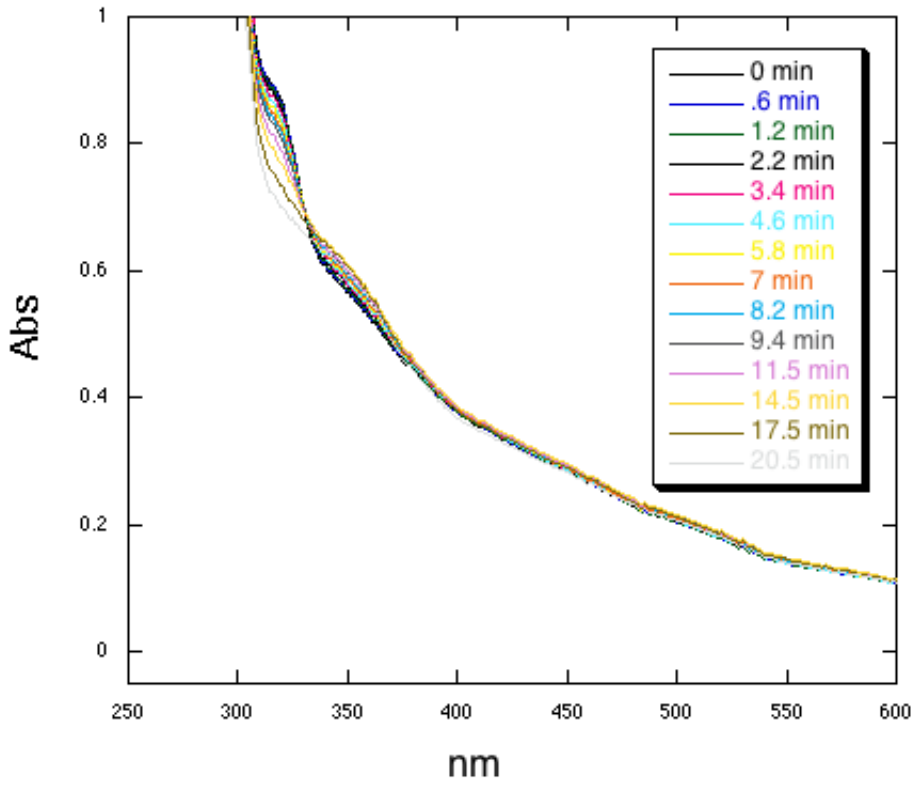

Figure 6B:Y175F quinol reoxidation

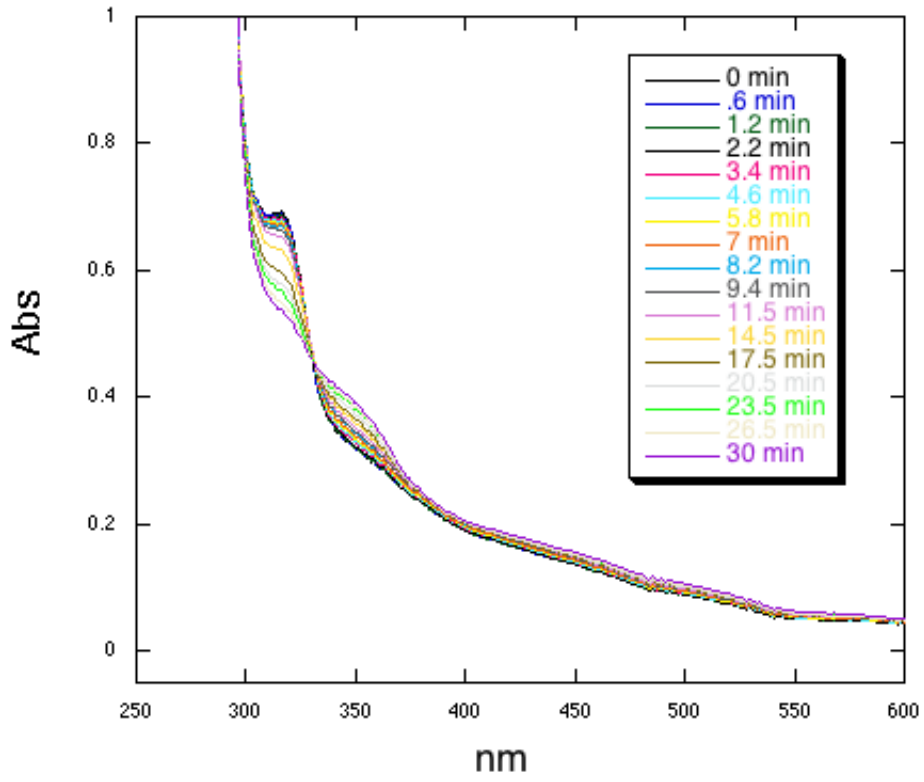

Figure 6C: Y175S Quinol reoxidation

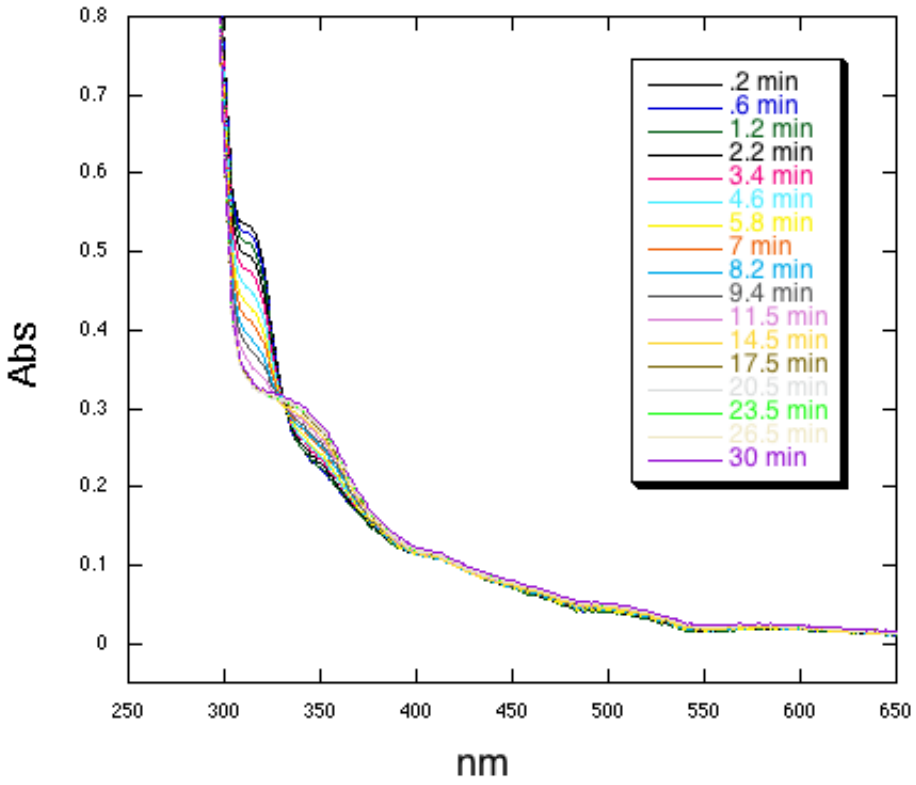

Figure 6D: H154N Quinol reoxidation

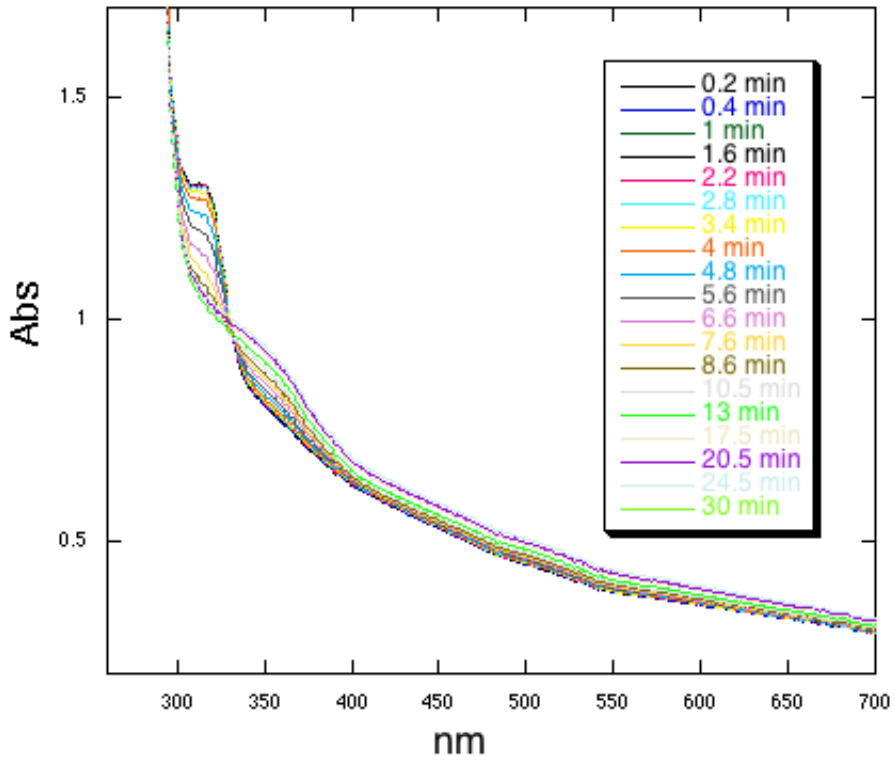

To test the ability of the O_2 core mutants to do oxidative chemistry, the rate at which they reoxidize $PQQH_2$ to PQQ is compared to that of WT. Interestingly, though the GDH assays strongly suggest that PQQ is not being formed, these mutants are capable of doing some oxidative chemistry. WT reoxidizes $PQQH_2$ with a rate of 2.12 min^{-1}. The O_2 core mutants also reoxidize PQQ, but at significantly lower rates (Table 1). The rates for reoxidation with H_2O_2 (Table 2) did not significantly change with Y175F and Y175S, but the rate was approximately 3-fold slower in WT compared to O_2 reoxidation. Interestingly the rate for quinol reoxidation with H_2O_2 in H154N is approximately 3-fold higher than that for O_2 reoxidation.

Table 1: Rates of $PQQH_2$ reoxidation to PQQ in the presence of O_2

	k1 (min^{-1})
WT	2.12 (±0.97)
Y175F	0.115 (±0.099)
Y175S	0.097 (±0.076)
H154N	0.120 (±0.089)
Buffer	0.071(±0.005)

Table 2: Rates of $PQQH_2$ reoxidations to PQQ in the presence of H_2O_2

	k1 (min^{-1})
WT	0.646(±0.387)
Y175F	0.095(±0.015)
Y175S	0.010(±0.006)
H154N	0.308(±0.009)

Figure 7: The spectra of reoxidation of $PQQH_2$ in buffer. The quinol species disappears before the quinone species appears, not giving the precursor-product relationship seen in the enzymatic reactions. This indicates that the oxidation reaction from $PQQH_2$ to PQQ occurs via different mechanism in buffer and on the enzyme.

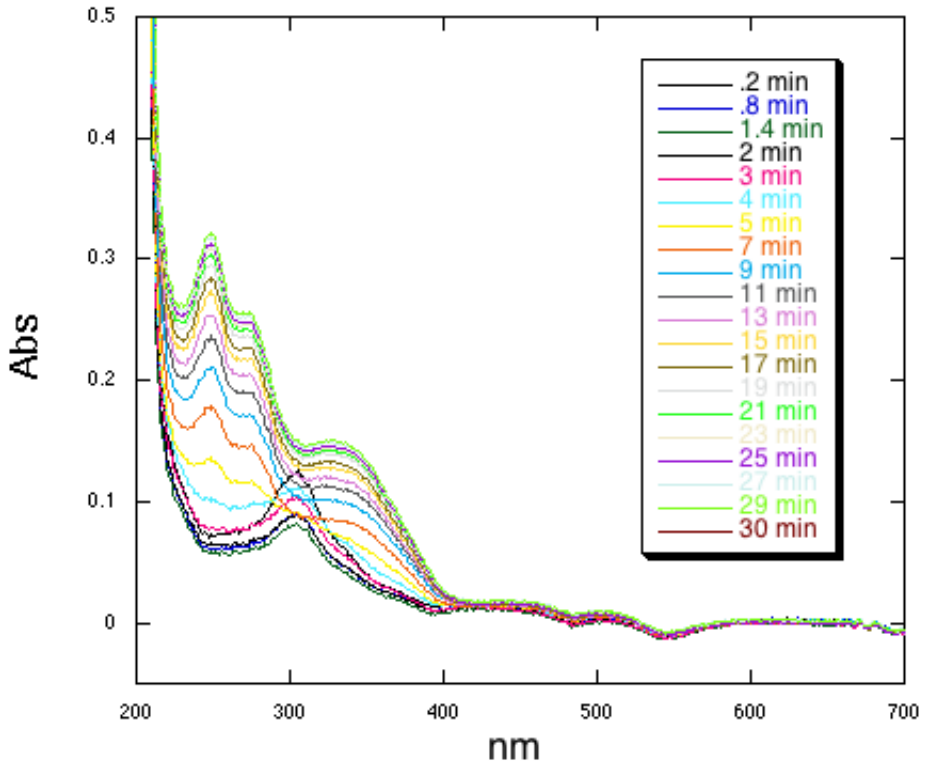

Since WT has a measured K_d of 114nM for $PQQH_2$ (Figure 8) and reoxidation assays were run at 20 μM PQQ/$PQQH_2$ with an excess of enzyme all the PQQ/ $PQQH_2$ should be bound so the enzymatic assays are not complicated by any reaction occuring in buffer.

Figure 8: WT-Quinol K_d. Binding of $PQQH_2$ to WT enzyme as determined by fluorescence spectroscopy. PQQH2 was kept in the reduced form with an excess of DTT and the binding cure of PQQ (20 nM) binding to WT. Data yielded a K_D of 114.3 nM.

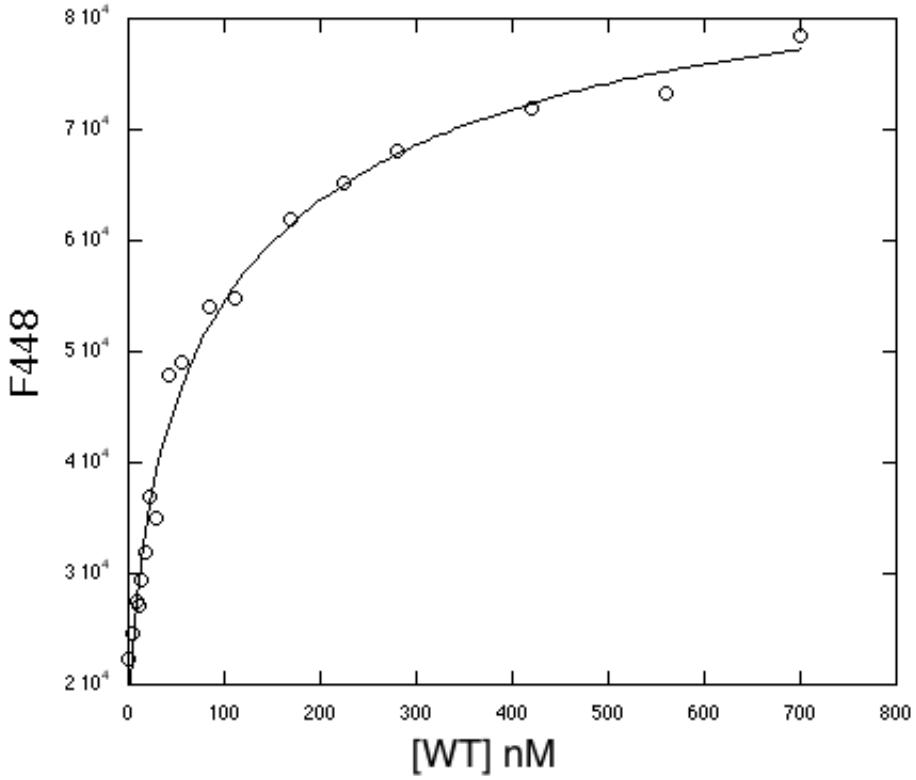

Discussion:

The PqqC reaction has been well characterized, but questions still remain as to the mechanism it follows and how an enzyme without a metal or cofactor activates and reacts with oxygen. The evidence presented here strongly suggests that mutations of PqqC in the O_2 core stop the enzyme from being able to form PQQ. Since all these residues are either proton donating or positively charged residues, they probably have a role in activation of oxygen rather than binding of oxygen. The fact that a different behavior is seen between the substrate, AHQQ, with no enzyme and substrate with mutant enzyme indicates that these mutants are catalyzing a reaction with substrate. The product of this reaction cannot be used as a cofactor by GDH, which is why we see no reaction in the GDH assay.

In the GDH assays the PqqC reaction was allowed to proceed aerobically due to the requirement of molecular oxygen for PQQ formation, while acid denaturation to free the product of this reaction was conducted anaerobically to protect any products from nonenzymatic oxidation. Since the mutations investigated here had changes in the putative oxygen pocket, this method was necessary to be sure that the direct products of the reaction were being observed.

The activity of GDH is dependent on the concentration to PQQ. A PQQ standard of 20 μM authentic PQQ, WT reaction and H84A (which has previously been shown to make PQQ spectroscopically) all had similar rates of reduction to DCIP, which is the final electron acceptor in the GDH assay. This indicates that similar amounts of PQQ (~20 μM) were made in these assays. WT and H84A are practically overlayable and so gave the same amount of PQQ. The PQQ standard has slightly more activity, but this is not surprising because some of the enzymatically produced PQQ may have been lost during enzyme denaturation. Addition of buffer and the products of the O_2 core mutant reactions (H154N, Y175F, Y175S and R179S) gave no reaction indicating that they did not form PQQ or anything that could act as a cofactor for GDH. The substrate for the reaction, AHQQ, was able to work as a cofactor for GDH, though at a rate much lower than that of PQQ. AHQQ is an unstable compound having a half life of approximately two hours at pH 6 and room temperature which means that it probably degraded to a molecule that was capable of acting as a cofactor for GDH. Denaturation of the mutants aerobically did give reaction with GDH (results not shown), though not on the same level as PQQ indicating that the resulting molecule, which acted as a cofactor for GDH, was not PQQ.

Since the mutations were in the O_2 core pocket, the ability of the mutant enzymes to do oxidative chemistry needed to be tested directly. To do this we decided to look at the final step of the PqqC reaction, oxidation to form PQQ. Taking genuine PQQ, we chemically formed the reduced form of PQQ, $PQQH_2$, with DTT (Figure 5). All mutations were able to do oxidative chemistry, but when compared to the WT enzyme, the rates of the O_2 core mutants are significantly reduced. WT proceeds at a rate of approximately 2 min^{-1}. The O_2 core mutants have rates between 0.09 and 0.12 min^{-1} (Table 1). While it was unexpected that these mutations could be able to do oxidative chemistry after seeing that they did not form PQQ, there is a significant decrease in the rate of oxidative chemistry, i.e. oxidizing $PQQH_2$ to PQQ. The nonenzymatic rate of quinol reoxidation in buffer occurs at a similar rate to reoxidation in the O_2 core mutants, though appears to happen via a different mechanism due to the loss of the precursor-product relationship seen in in the presence of enzyme. Because of this the oxidation seen with the O_2 core mutants may be a baseline oxidation due to the reactivity of the quinol species.

Using hydrogen peroxide as an oxidant instead of molecular oxygen gave unexpected results (Table 2). It was expected that WT-$PQQH_2$ reoxidation would be slower because the oxidation of $PQQH_2$ to PQQ in WT uses O_2 as an oxidant, not H_2O_2 inferred from the equivalent of bound H_2O_2 at the completion of the PqqC reaction. This loss in rate with the non-natural oxidant was seen and gives the first direct experimental evidence to the oxidant in a specific step of the PqqC reaction. Interestingly, quinol reoxidation in H154N was approximately 3-fold faster with H_2O_2 than with O_2 leading us to propose that H154 has a role in O_2 to H_2O_2 reaction. The rates of reoxidation in all other mutations were not affected by the identity of the oxidant, indicating again that the oxidation rates seen may be baseline and not mechanistically important.

The loss of rate in the O_2 core mutants indicates that while we may not be completely stopping oxidative chemistry, it is significantly inhibited in the O_2 core mutants. This is probably the reason that the products of the O_2 core mutant reactions are not capable of acting as a cofactor for GDH. These mutants form a product that is not fully oxidized and therefore cannot act as a cofactor for GDH. These results further suggest that binding of the PqqC derived products to GDH prevents further oxidation.

There are two possible reasons why the product of the O_2 core mutants cannot act as a cofactor for GDH. The first is that these products bind incorrectly to GDH. The second is that whatever these products are, they do not lie on the GDH reaction path and cannot be cycled into the reaction with DCIP. Either way, the O_2 core mutants are not forming PQQ but are reacting with substrate to form a currently uncharacterized intermediate. The reason that these variants cannot form PQQ is most likely due to inhibition of their ability to do oxidative chemistry.

In conclusion we have found that the O_2 core in PqqC is highly specific. Any changes in this pocket cause PqqC to be unable to form PQQ because of loss of ability to do oxidative chemistry. Interestingly, one mutation tested, H154N, was capable of doing more oxidative chemistry with H_2O_2 as an oxidant than O_2.

Chapter 4

Reactions in the O_2 core Mutants of PqqC

Introduction:

Pyrroloquinoline quinone (4,5-dihydro-4,5-dioxo-1*H*-pyrrolo-[2,3-*f*]quinoline- 2,7,9-tricarboxylic acid: PQQ[1] [Figure 1]) is an aromatic, tricyclic *ortho*-quinone that serves as cofactor for a number of prokaryotic dehydrogenases, largely but not exclusively from Gram-negative bacteria. The oxidative reactions catalyzed by PQQ-enzymes are involved in catabolic pathways, where the best studied examples are methanol dehydrogenase and glucose dehydrogenase[1, 2]. PQQ is part of the quinone family of cofactors and has remarkable antioxidant properties[3]. Like all known quinone cofactors, PQQ is peptide derived. But unlike the other quinone cofactors, such as TPQ, TTQ, LTQ and CTQ, it is freely dissociable from the enzyme and biogenesis is independent of the site of catalysis. The biosynthesis of PQQ is a complex process and in *Klebsiella pneumoniae* is catalyzed by the gene products of *pqqABCDEF*[4]. All the carbon and nitrogen atoms in PQQ come from a conserved tyrosine and glutamate in PqqA (Fig. 1)[5, 6].

Figure 1: The carbons and nitrogen in PQQ originate from a glutamate and a tyrosine.

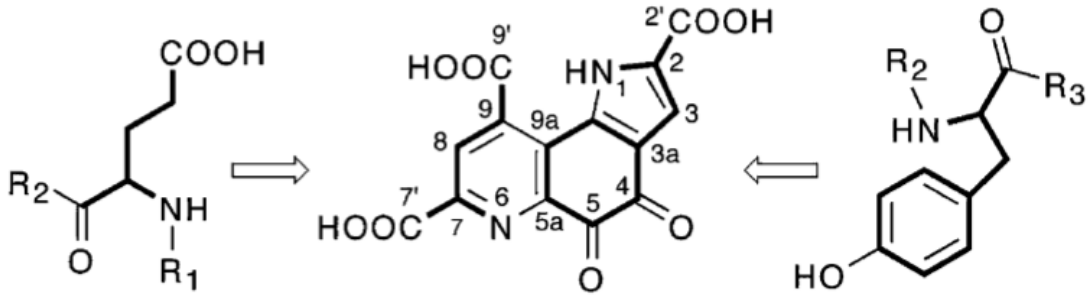

The final step of PQQ formation is the best studied part of the pathway. This step is catalyzed by PqqC and involves a ring closure and the eight electron oxidation of AHQQ (3a- (2-amino-2-carboxyethyl) – 4,5- dioxo- 4,5,6,7,8,9 hexahydroquinoline-7,9- dicarboxylic acid)[7]. The reaction has been well characterized and occurs using molecular oxygen as an oxidant and proceeds without the use of an external cofactor or metal[8]. This has raised some very interesting questions as to the mechanism of the reaction and how oxygen is activated in a metal and cofactor free active site.

Previous studies were focused on the H84 active site residue in PqqC. The proposed mechanism of the enzyme involves the action of three conserved histidine residues (H24, H84 and H154) as general acid/base catalysts, and H84 has been shown to act as a proton donor in the quinoid to quinol tautomerization in the PqqC reaction (Fig. 2)[8, 9].

Figure 2: The proposed mechanism of PqqC.

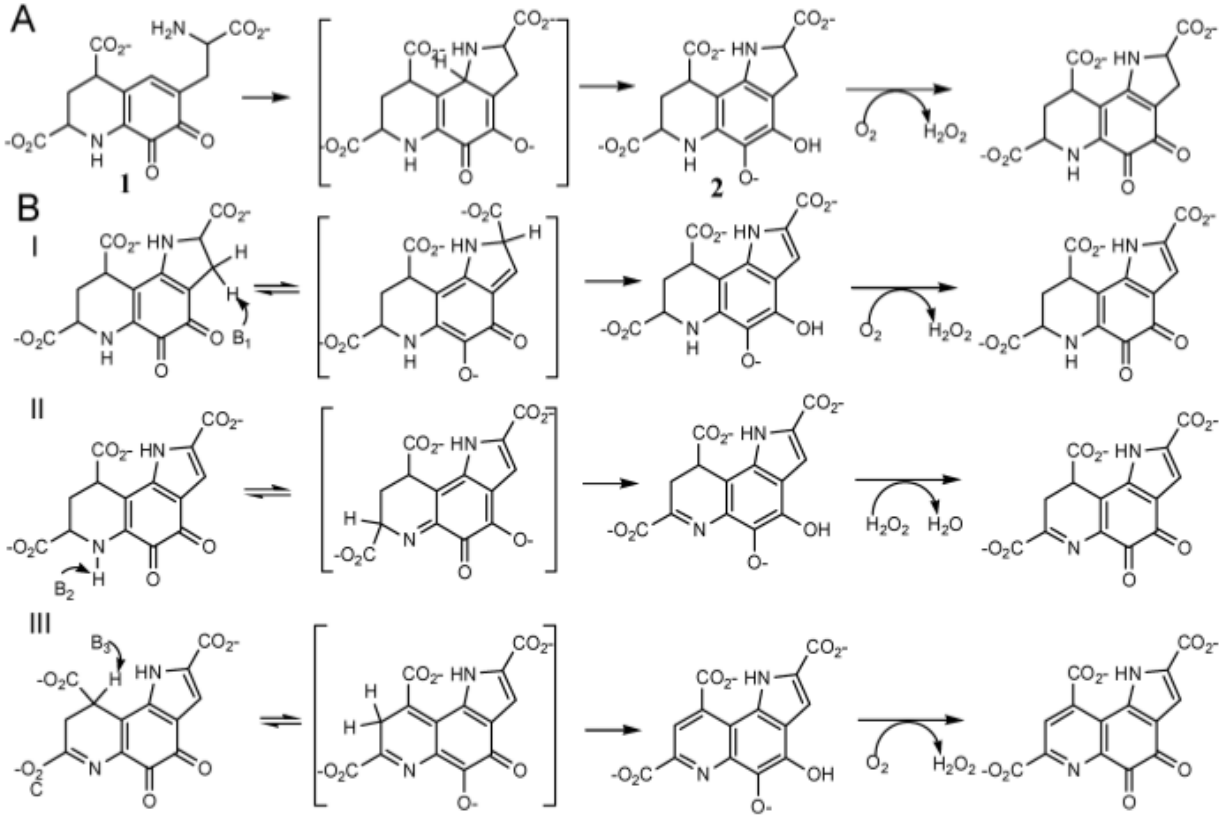

H24 and H84 are fully conserved, H154 is partially conserved with a glutamine occurring at the 154 position in proteobacterium *Magnetospirillum magnetotacticum* (protein ID ZP_00052131), and the Gram-positive bacterium *Desulfitobacterium hafniense* (protein ID ZP_00101389)[8], for example. It is possible that this is a misassignment due to the fact that the codon for histidine is one base pair away from glutamine (CAC/U vs. CAA/G). As stated before, H84 was proposed to be a active site base, but mutagenic studies showed that H84 acts as an active site acid and gave no evidence that H84 acted as an active site base. It was found that the H84N variant reacted differently from H84A or WT, with the quinoid/quinol tautomerization in the former case being dependent on the presence of O_2. X-ray crystallography has shown that there are three residues, H154, Y175 and R179, positioned near the quinone moiety of bound PQQ and within 5 angstroms (Å) of the putative oxygen in the active site (Fig. 15)[10]. These residues from here on out will be referred to as the O_2 core. Unlike H84, these three residues all move into the active site upon PQQ binding, i.e. PQQ binding must occur to form the O_2 core. H154 is found in the α5 helix and Y175 and R179 are the only residues from the α6 helix that are found in the PqqC active site. These residues, Y175 and R179, move from a extremely solvent exposed position into the active site upon PQQ binding. Herein we describe the kinetics of the reaction of four active-site mutants (H154N, Y175F, Y175S, R179S) under single-turnover conditions that permit the detection of spectroscopic intermediates and then comparison to the wild-type enzyme.

PqqC involves multiple turnovers with respect to oxygen and, in one step, uses an equivalent of hydrogen peroxide as the oxidant[8]. As illustrated (Figure 2), the ability of substrate to undergo oxidation in the absence of an organic or metal cofactor is directly linked to the structure of the substrate, which is capable of a series of quinol/quinone interconverstion. The

stoichiometry of the reaction requires that three of the four illustrated steps utilize O_2 as an oxidant, while the remaining step utilizes H_2O_2[8]. X-ray structure analysis indicates that mutants at positions H154S and Y175F have different effects on the structure of the enzyme/product complexes. H154S/PQQ is unable to form the closed complex whereas Y175F/PQQ structure closely resembles WT. In the present work we demonstrate the aberrant kinetic courses found with H154N, two Y175 variants and R179S. In the previous chapter we showed that these mutants do not form PQQ while this chapter addresses the reactions catalyzed by these mutations. These findings implicate H154, Y175 and R179 in roles directly related to the binding of O_2 and its subsequent activation as electron acceptor from AHQQ and its partially oxidized intermediates.

Materials and Methods:

Chemicals, Reagents and Molecular Biology products:

Buffers, salts, general reagents, and culture media were obtained from Sigma and Fisher and were of the highest available purity. Ni-nitriloacetic acid (NTA) resin, DNA purification kits, and PCR primers were purchased from Qiagen. Enzymes and reagents for mutagenesis reactions were from Strategene. PQQ was purchased from Fluka. Restriction enzymes and appropriate reaction buffers were purchased from New England Biolabs. Cell lines were obtained from Invitrogen. AHQQ was purified from a *ppqC* mutant strain EMS12 of *Methylobacterium extorquens* as described[8]. Concentration of AHQQ was determined spectrophotometrically at pH 7 by averaging the concentrations determined at three wavelengths with the following extinction coefficients: 222 nm = 15.7 mM^{-1} cm^{-1}, 274 nm = 8.26 mM^{-1} cm^{-1}, and 532 nm = 2.01 mM^{-1} cm^{-1}. Plasmids were made at the University of Salzburg (see below) from genomic DNA from *Klebsiella pneumoniae MGH 78578*. *Klebsiella pneumoniae MGH 78578* varies from the previously described wild-type PqqC at the base of the 3rd alpha helix. There are three differences between the two sequences: A21D, D37N and K41E. A21D is present in the original crystal structure[10], but the changes at positions 37 and 41 are shown in agreement with the sequence deposited by Postma (Pubmed accession number: X58778). Since *Klebsiella subspecies MGH 78578* forms PQQ we assume that the two WT PqqCs from these *K. pneumoniae* subspecies, which are 98.8% identical, are comparable. The reactions of both WT enzymes give the same intermediates and similar rates.

PCR cloning and Expression of Plasmids and Purification of PqqC mutants:

PCR cloning was performed by Sandra Puhringer of the Schwarzenbacher group (Univ. of Salzburg). Plasmids were constructed in pET29 with kanamycin resistance and a C-terminal His tag. The isolated plasmids were sequenced from both directions using the T7 promoter and terminator primers.

Expression of plasmids was done using BL21(DE3) cells in LB medium supplemented with 50 μg/mL kanamycin. Cultures were grown at 37 C to an optical density at 600 nm of ~0.8, at which time Isopropyl β–D-1-thiogalactopyranoside(IPTG) (1 mM) was added, and the cells were harvested ~4 h later. All pET-29b-pqqC/D plasmids produced high quantities of protein as judged by SDS-PAGE analysis. Cells were resuspended in lysis buffer containing 50 mM KH_2PO_4, 300 mM NaCl, 1 mM PMSF and 5 mM $MgCl_2$. After sonication and centrifugation as described previously the clear supernatant was applied to a 10 mL Ni-NTA column that had been equilibrated in 20 mM tris buffer supplemented with 300 mM NaCl and 5 mM imidazole. After two buffer washes with increasing amounts of imidazole (5mM and 10mM) the His-tagged bound protein was eluted with 25 mM tris buffer supplemented with 300

mM NaCl and 250 mM imidazole. Fractions containing mutant enzyme were analyzed by SDS-PAGE, pooled, concentrated and buffer exchanged into 100mM monobasic potassium phosphate pH 8.0 before being aliquoted and snap frozen. Further column chromatography only provided inactive enzyme, unlike what was seen in wild-type PqqC and H84 varients which were further purified by size-exclusion chromatography. A single band was seen on an SDS-PAGE gel, and the Ni-NTA column chromatography provided enzyme with greater than 90% purity. The expression for these mutants was lower than WT and yielded ~3 mg/L of culture.

Single Turnover Kinetics:

The enzyme in the highest concentration possible without precipitation (Y175F: 27μM, Y175S: 55μM, H154N: 25μM, R179S: 30μM) was mixed with substrate, AHQQ (12μM final concentration), in 100 mM potassium phosphate buffer, pH 8.0, in a total volume of 100 μL. The enzyme mixture was transferred to a microcuvette, and UV-vis spectra were recorded within 10 s of addition of AHQQ. Spectra were obtained on a Cary spectrophotometer, and the temperature of the reaction was maintained at 25 C using a circulating water bath. Spectra were acquired at predetermined time points and the data exported to SPECFIT/32 for analysis. Because of protein precipitation during the course of the reaction, all spectra were corrected via a baseline correction in SpecFit.

Anaerobic reactions were done under the same conditions as described above. Enzyme and substrate were made anaerobic by repeated cycles of argon purging and high-vacuum evacuation on a Schlenk line. The sealed samples were brought into an anaerobic chamber, the protein was transferred into a microcuvette fitted with a rubber stopper, and the substrate was loaded into a syringe and the needle inserted through the stopper and into the top of the cuvette. The cuvette with the syringe attached was brought out to the spectrophotometer, and the substrate was mixed thoroughly with enzyme before spectra were recorded. After some time, when no further changes were observed in the UV-vis spectrum of the samples, the stopper was removed, and air was blown over the surface of the sample for a few seconds, demonstrating further reaction in some cases.

PQQ Binding:

PQQ binding was investigated spectroscopically. One equivalent of genuine PQQ was added to enzyme in 100 mM potassium phosphate at pH 8. Then the spectra recorded and analysed. All mutants showed absorbance of one species with UV/vis spectroscopy. K_Ds were acquired fluorometrically as previously described[8]. Data were fit using Kaleidagraph (Synergy Software). Data were fit to a quadratic binding iostherm (equation 1), where ΔF equals the change in fluorescence in a given sample compared to free ligand, ΔF_M is the change in fluorescence at saturation, $[E]_T$ equals the total concentration of enzyme in each sample, $[L]_T$ equals the concentration of total ligand and K_D is the dissociation constant of the enzyme-ligand complex (equation 1). Some mutants, namely Y175F and R179S, did not result in a fluorometric change in the presence of PQQ. Due to published crystal structures and a spectroscopic shift seen on binding of PQQ to Y175F we assume that binding is occurring and that the interaction necessary for the bathochrometric shift and fluorescence increase normally seen upon PQQ binding to PqqC is not present in the Y175F-PQQ or R179S-PQQ complexes.

$$\Delta F=\Delta F_M[([E]_T+[L]_T+K_D)-(([E]_T+[L]_T+K_D)^2-4[E]_T[L]_T)^{0.5}/2[L]_T)] \quad (1)$$

Results:

Single Turnover Kinetics of H154N, Y175F, Y175S and R179S

Aerobic results:

PqqC requires oxygen for PQQ formation. Previous work done on WT PqqC shows that anaerobic reactions form quinol intermediates that proceed to PQQ upon the addition of oxygen. Upon addition of the substrate for the reaction, AHQQ, the PqqC active site variant Y175F forms spectra very similar to that of WT PqqC reacted anaerobically (Figure 3).

Figure 3: Single-Turnover reaction of active site variant Y175F under aerobic conditions. Representative spectra at time points: 0.2, 0.8, 1.6, 2.4, 3.2, 4, 6.4, 8, 9.6, 12, 14.4, 19.5, 25.5, 33.5, 41.5, 47.5, 55.5 and 59.5 minutes.

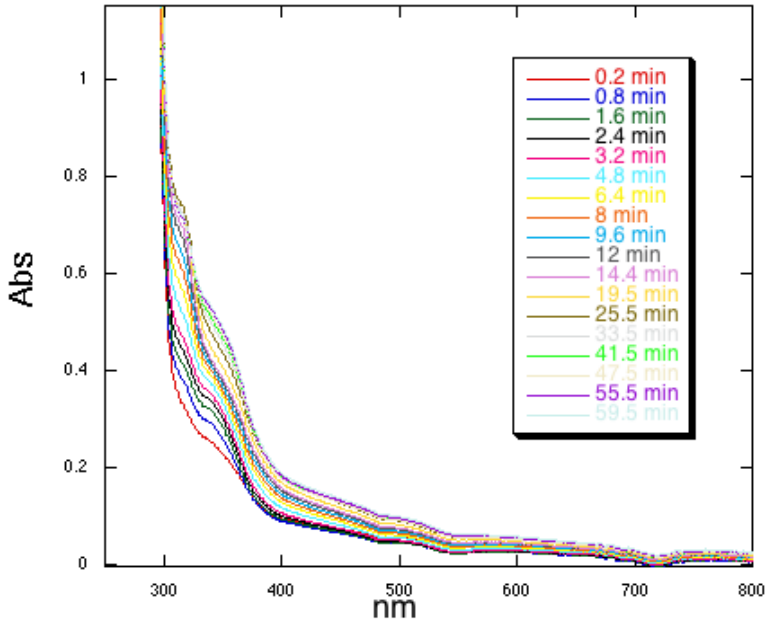

Two species form independently, one at 318 and the other at 356. Unlike WT enzyme, the species with Y175F persist in an aerobic environment (reactions run up to 3 hours). These intermediates are thought to both be quinols, with one intermediate being the monoprotonated quinol and the other corresponding to the diprotonated quinol[8]. R179S forms the same species at 318nm and 356nm aerobically (Figure 6).

Figure 4: Single-Turnover reaction of active site variant Y175S under aerobic conditions. Representative spectra at time points: 0.2, 1.3, 3, 4.3, 8.3, 11, 13.6, 17.6, 19, 21.6, 27, 31, 35, 39, 43, 47, 51, 55, 57.6 and 59 minutes.

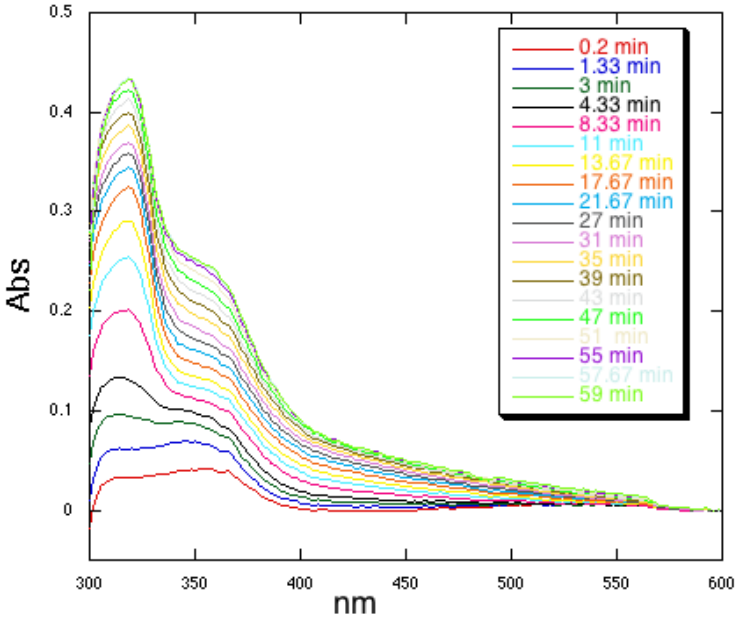

Figure 5: Single-Turnover reaction of active site variant H154N under aerobic conditions. Representative spectra at time points: 0, 0.6, 1.2, 1.8, 3, 4.2, 5.4, 6.6, 7.8, 9, 10.8, 12.6, 14.4, 18, 22.5, 28.5, 34.5, 39, 45 minutes.

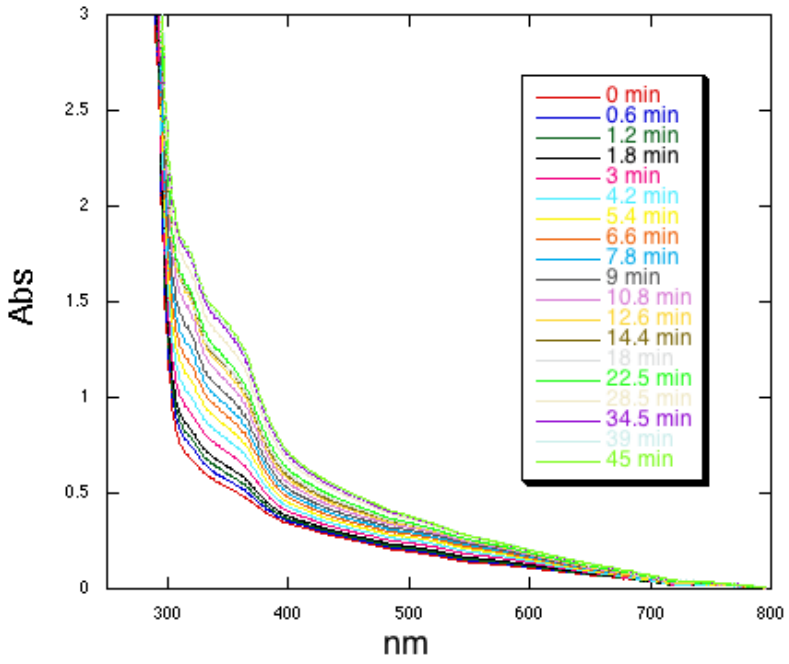

Figure 6: Single-Turnover reaction of active site variant R179S with aerobic conditions. Representative spectra at time points: 0.2, 0.6, 1, 1.4, 2.6, 3.4, 4, 6, 8, 10, 12.2, 14.2, 19, 22.5, 27, 32, 37, and 42.5 minutes.

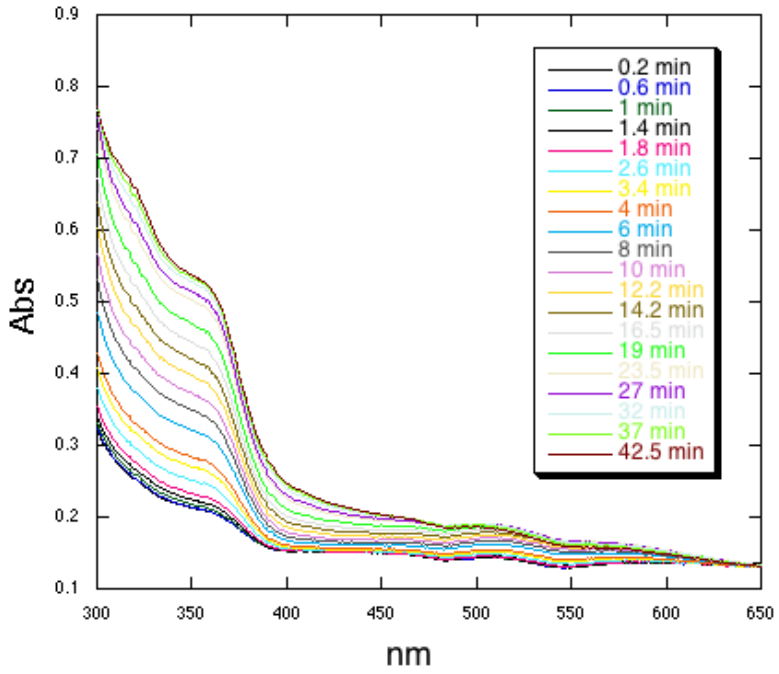

Table 1: Y175F Aerobic Data

Species	λmax (nm)	ε (mM^{-1} cm^{-1})	Rate of formation (min^{-1})
Y175F-AHQQ	532	2.1	
Y175F-I_{A1}	318	12.4	14.4e-2 (±0. 2)
Y175F-I_{A2}	356	10.7	6.6e-2 (±0.2)
PQQ	331, 475	10, 0.7	

Table 2: Y175S Aerobic Data

Species	λmax (nm)	ε (mM^{-1} cm^{-1})	Rate of formation (min^{-1})
Y175S-AHQQ	532	2.1	
Y175S-I_A	344	2.3	27 e-2 (±0.2)
Y175S-I_B	318	10.1	7.6 e-2 (±0.3)
Y175S-I_{C1}	356	17.5	2.3 e-2 (±0.2)
PQQ	331, 475	10, 0.7	

Table 3: H154N Aerobic Data

Species	λmax (nm)	ε (mM^{-1} cm^{-1})	Rate of formation (min^{-1})
H154N-AHQQ	532	2.1	
H154N-I_{A1}	318	12.1	10.1e-2 (±0.6)
H154N-I_{A2}	356	9.8	10.2e-2 (±0.5)
PQQ	331, 475	10, 0.7	

Table 4: R179S Aerobic Data

Species	λmax (nm)	ε (mM^{-1} cm^{-1})	Rate of formation (min^{-1})
R179S-AHQQ	532	2.1	
R179S-I_{A1}	318	11.3	5.67e-2 (±0.08)
R179S-I_{A2}	356	8.9	6.5 e-2 (±0.1)
PQQ	331, 475	10, 0.7	

H154N forms similar species, but with slightly shifted λmax at 315nm and 360nm (Figure 5). The differences in λmax are possibly due to difference in charge stabilization of electronically excited states among the active sites of the various PqqC variants. The two spectral species from Y175S are distinct from intermediates seen with the other three active site variants discussed here (Figure 4). First, a quinoid intermediate is seen in the Y175S reaction, which is not the case for H154N, Y175F and R179S. This indicates that the tautomerization step from quinoid to quinol is inhibited in the Y175S reaction (Figure 2). We speculate that size, rather than hydrogen bonding is involved in the positioning of O_2. Removal of steric bulk from that position and probable repositioning of the hydrogen bonds, which is what occurs in Y175S, slows the tautomerization so that the quinoid intermediate can be seen, though it seems that in the presence of a hydrogen donator in the tautomerization step stops the step from being dependent on the presence of molecular oxygen. Previous work with the PqqC variant of H84 show similar results anaerobically, with varying degrees of inhibition of the quinoid to quinol seen. Following formation of the quinoid, the Y175S reaction proceeds to a quinol intermediate.

Anaerobic results:

When reacted anaerobically the first step of the PQQ reaction can be probed. The results of the aerobic PqqC assay indicate that the ability to reoxidize a quinol to a quinone has been lost in the O_2 core mutants. Interestingly, the intermediates formed by Y175F, H154N and R179S anaerobically are not the same as seen aerobically (Figures 7, 9 and 10). Anaerobically these mutants form a quinoid with a λmax at 338nm. Previously, in other active site mutants H84A and H84N, this quinoid has been described as having a λmax of 344nm. In the Y175S variant, the quinoid forms with a λmax at 344nm and then goes on to form a quinol species that absorbs at 318nm (Figure 8).

Figure 7: Single-Turnover reaction of active site variant Y175F under anaerobic conditions. Representative spectra at time points: 0.2, 0.8, 1.6, 2.4, 4, 5.6, 7.2, 8.8, 10.4, 12, 14.4, 19.5, 25.5, 31.5, 37.5, 43.5, 49.5, 55.5, and 59.5 minutes.

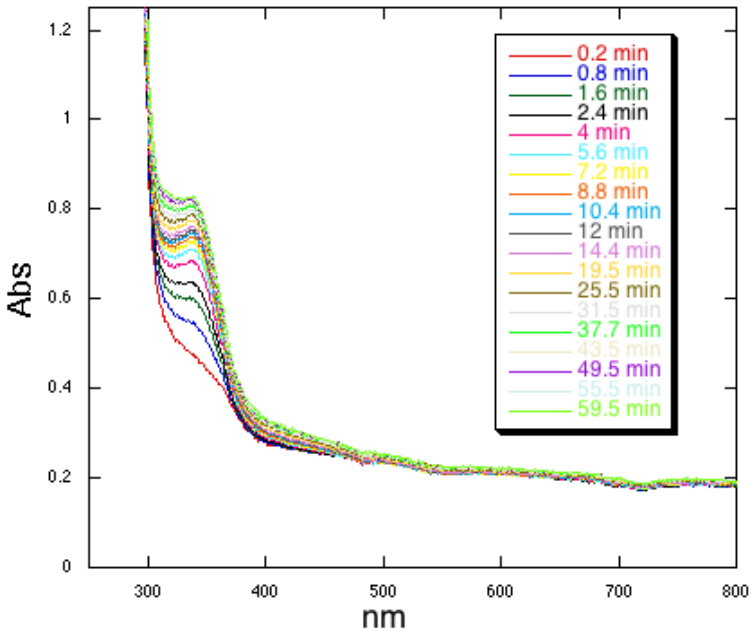

Figure 8: Single-Turnover reaction of active site variant Y175S under anaerobic conditions. Representative spectra at time points: 0.2, 1.3, 3, 4.3, 8.3, 11, 13.6, 19, 21.6, 27, 31, 35, 39, 43, 47, 51, 55, 59 minutes.

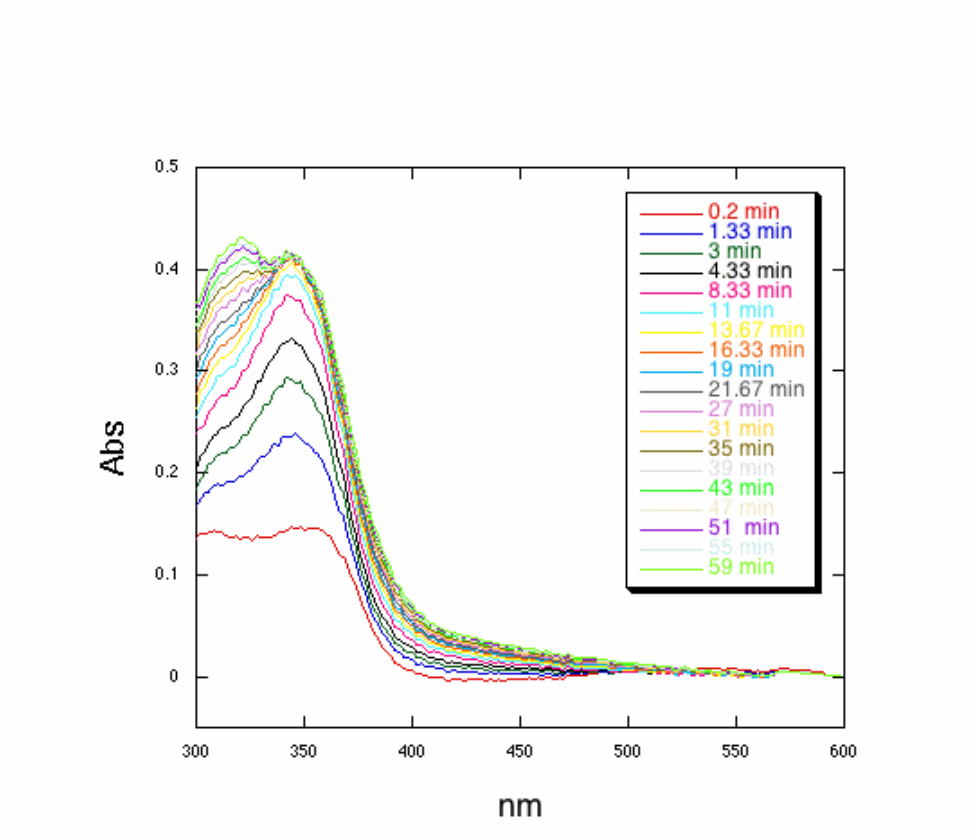

Figure 9: Single-Turnover reaction of active site variant H154N under anaerobic conditions. Representative spectra at time points: 0.2, 0.6, 1, 1.0, 1.6, 3.2, 4.8, 6, 7, 9, 10.2, 11.6, 13, 15, 17.5, 20, 22.5, 26, 31.5, 37, and 42.5 minutes.

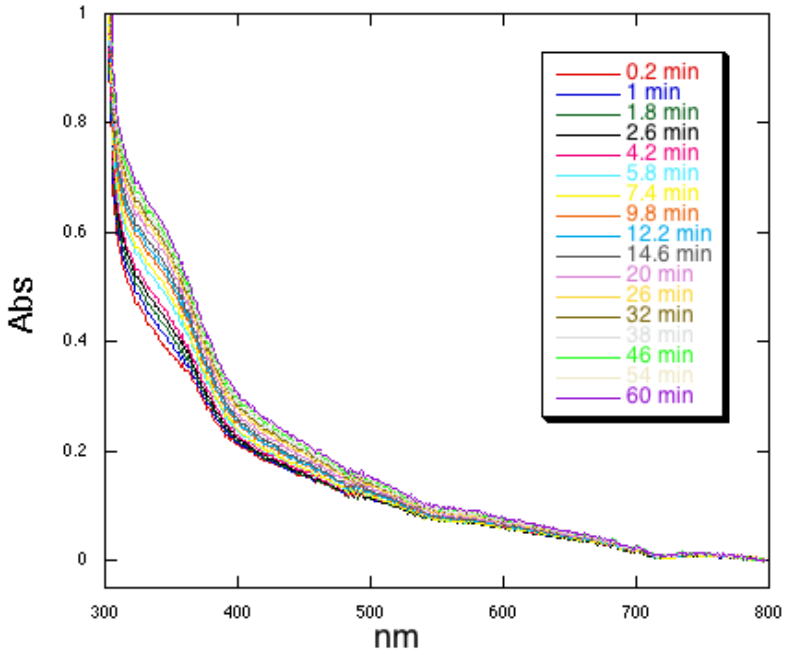

Figure 10: Single Turnover reaction of active site variant R179S under anaerobic conditions. Representative spectra at time points: 0.2, 1, 1.8, 2.6, 4.2, 5.8, 7.4, 9.8, 12.2, 14.6, 20, 26, 32, 38, 46, 54, and 60 minutes.

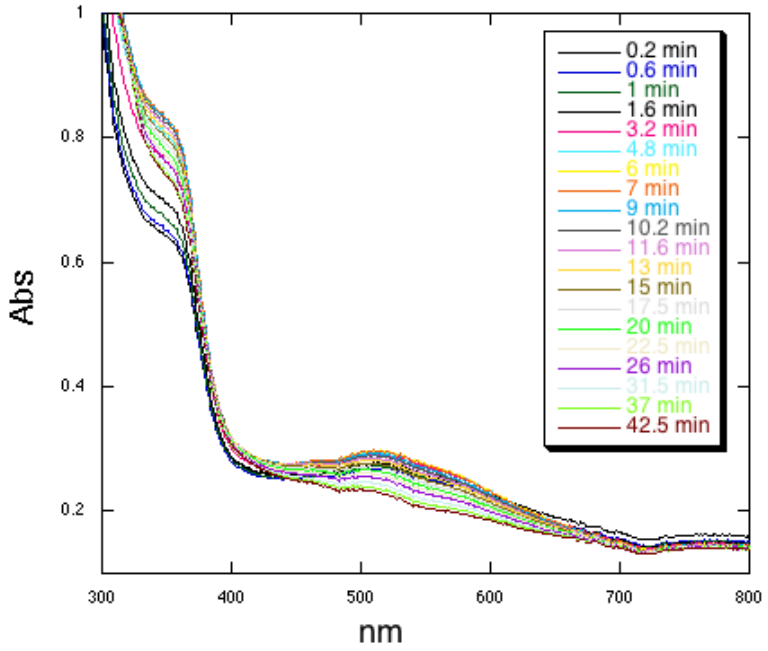

Table 5: Y175F Anaerobic Data

Species	λmax (nm)	ε (mM^{-1} cm^{-1})	Rate of formation (min^{-1})
Y175F-AHQQ	532	2.1	
Y175F-I_A	338	7.6	6.94e-2 (±0.40)
PQQ	331, 475	10, 0.7	

Table 6: Y175S Anaerobic Data

Species	λmax (nm)	ε (mM^{-1} cm^{-1})	Rate of formation (min^{-1})
Y175S-AHQQ	532	2.1	
Y175S-I_{A1}	344	6.2	7.7 e-2 (±0.3)
Y175S-I_{A2}	318	8.5	2.3 e-2 (±0.2)
PQQ	331, 475	10, 0.7	

Table 7: H154N Anaerobic Data

Species	λmax (nm)	ε (mM^{-1} cm^{-1})	Rate of formation (min^{-1})
H154N-AHQQ	532	2.1	

H154N-I_A	338	6.6	2.22e-2 (±0.62)
PQQ	331, 475	10, 0.7	

Table 8: R179S Anaerobic Data

Species	λmax (nm)	ε (mM^{-1} cm^{-1})	Rate of formation (min^{-1})
R179S-AHQQ	532	2.2	
R179S-I_A	338	7.9	3.34e-2 (±0.79)
PQQ	331, 475	10, 0.7	

Anaerobic to aerobic experiments:

Anaerobic reactions were exposed to air and the resulting spectra recorded. A new intermediate forms at 318nm, which is proposed to be a quinol species, showing that oxygen does bind (Figure 11, 12). Since these mutants are not forming PQQ it has been proposed that they are incapable of activating oxygen. Without the presence of oxygen the reaction stops at an earlier intermediate than it does aerobically indicating that the presence of oxygen, even if it isn't activated, plays a role in the quinoid to quinol transition.

Figure 11: Y175F anaerobic to aerobic transition. The 338nm peak decreases as the 318nm peak increases. This indicates that molecular oxygen must be bound in Y175F for the quinoid to tautomerize to the quinol in the first step of the reaction. Representative spectra at time points: 0.2, 0.6, 1.2, 1.8, 3, 4.2, 5.4, 6.6, 7.8, 9, 10.2, 11.4, 12.6, 13.8, 15, 18, 21, 24, 27, and 30 minutes

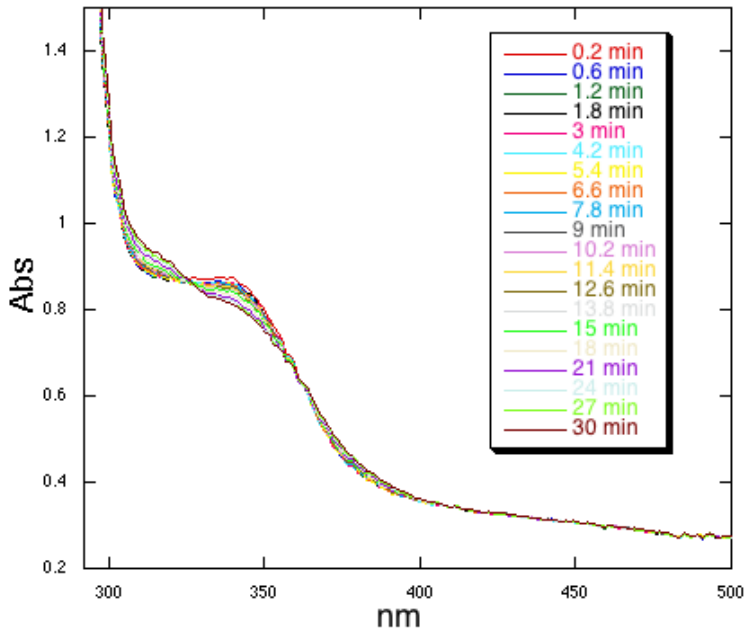

Figure 12: H154N anaerobic to aerobic transition. Representative spectra at time points: 0.2, 0.6, 1.2, 1.8, 3, 4.2, 5.4, 6.6, 7.8, 9, 10.2, 11.4, 12.6, 13.8, 15, 18, 21, 24, 27, and 30 minutes

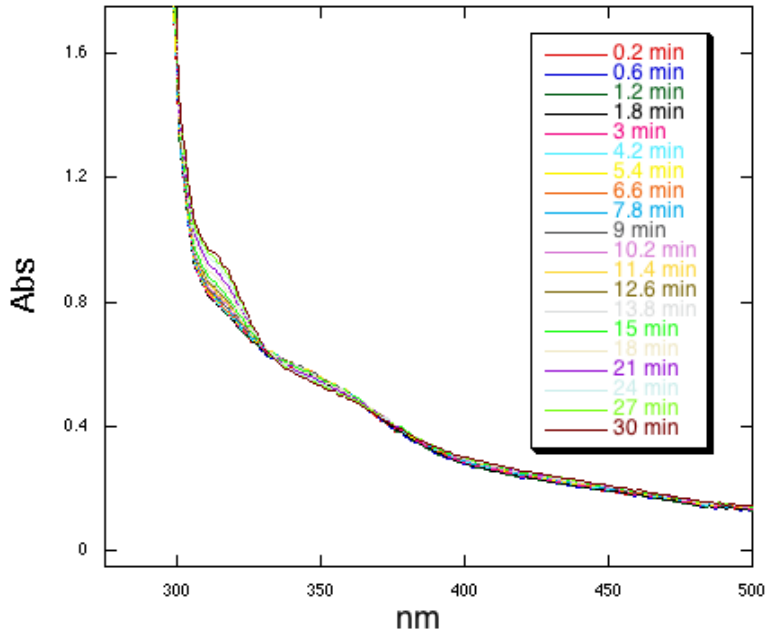

PQQ binding:

Spectroscopic studies with PQQ show that that Y175 and H154 mutants do not form the same spectral signals from reaction with AHQQ as they do when combined with authentic PQQ (Table 9). This means that these mutants are not completing the reaction and that Y175 and H154 are necessary for PQQ formation. The K_Ds for H154N and Y175S are close to that of WT, with H154N (K_D= 0.66nM, Figure 13) binding slightly tighter than WT (K_D= 2.0nM) and Y175S (K_D=12.3nM, Figure 14) binding weaker.

Table 9:

Enzyme	Enzyme-PQQ Absorbance (nm)
Wild Type	346, 498
H84A	366, 329
H84N	366, 329
Y175S	344
Y175F	342
H154N	344

Figure 13: H154N K_D. Binding curve of PQQ (20 nM) to H154N form of PqqC as determined by fluorescence spectroscopy. Data yielded a K_D of 0.66 nM

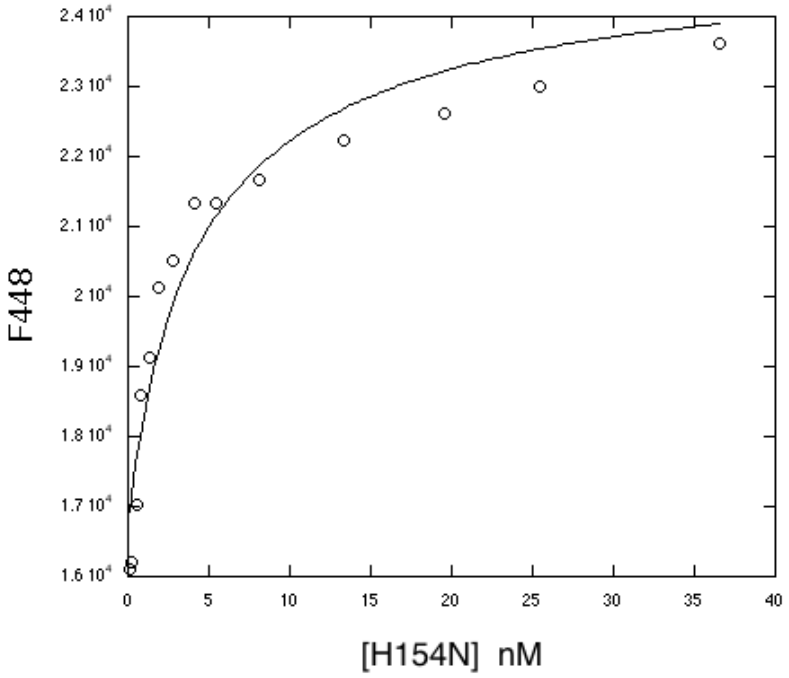

Figure 14: Y175S K_D. Binding curve of PQQ (20 nM) to Y175S form of PqqC as determined by fluorescence spectroscopy. Data yielded a K_D of 12.23 nM

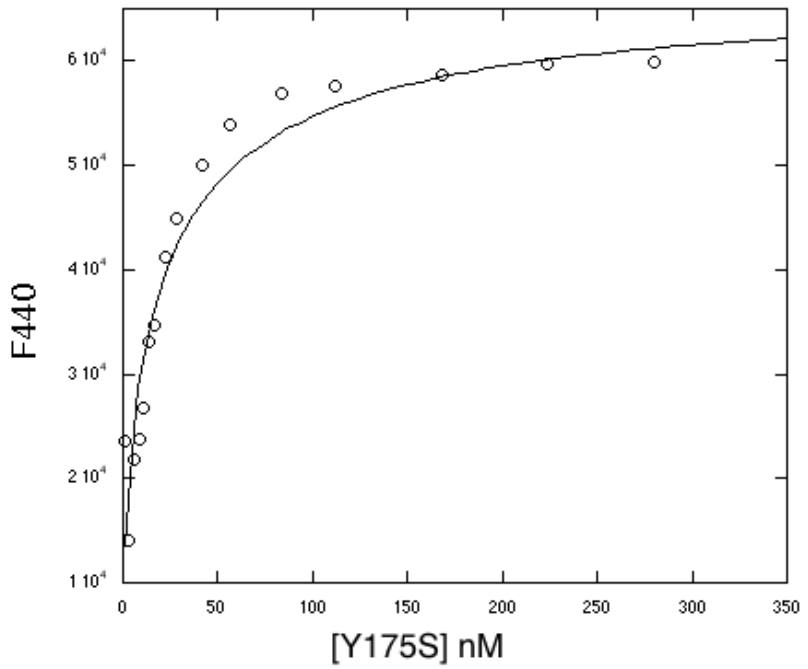

Discussion:

Under single turnover conditions, the PqqC reaction consumes three equivalents of O_2 and produces two equivalents of H_2O_2, with the remaining two electrons needed to complete the oxidation cycle presumably obtained from an intermediary H_2O_2 molecule produced in the enzyme active site ultimately forming water. The proposed mechanism of PqqC (Figure 2) shows how the enzyme may facilitate this reaction, utilizing the inherent chemical reactivity of the quinone substrate to bring about the oxidative chemistry. The first step is illustrated as the ring closure process, followed by O_2-mediated oxidation of the resulting quinol. Although not explicitly shown in Figure 2, oxidation presumably occurs in two steps in which an outer sphere electron transfer forms a transient superoxide:semiquinone intermediate. The subsequent steps are proposed to involve three successive tautomerization reactions (I-III), which are driven by aromatization and activate each of the intermediates for oxidation in the absence of a cofactor. The specifics of how PqqC activates molecular oxygen for turnover have not been well studied. There are few examples of oxygen turnover in enzyme without the presence of a metal or cofactor. It is thought the PqqC takes advantage of the inherent reactivity of the quinone/quinol moiety of the substrate to activate oxygen. This study identifies three residues in the active site of PqqC that appear to have a role in the activation of oxygen for reactivity with substrate (Figure 15).

Figure 15A: Distances in the PqqC active site for core residues (Y175, H154, R179). PQQ is shown in gold with the putative oxygen molecule in red over the quinone ring. Active site residues H84, H154, Y175 and R179 are shown in green. PQQ is shown in gold and the putative oxygen density is shown in red.

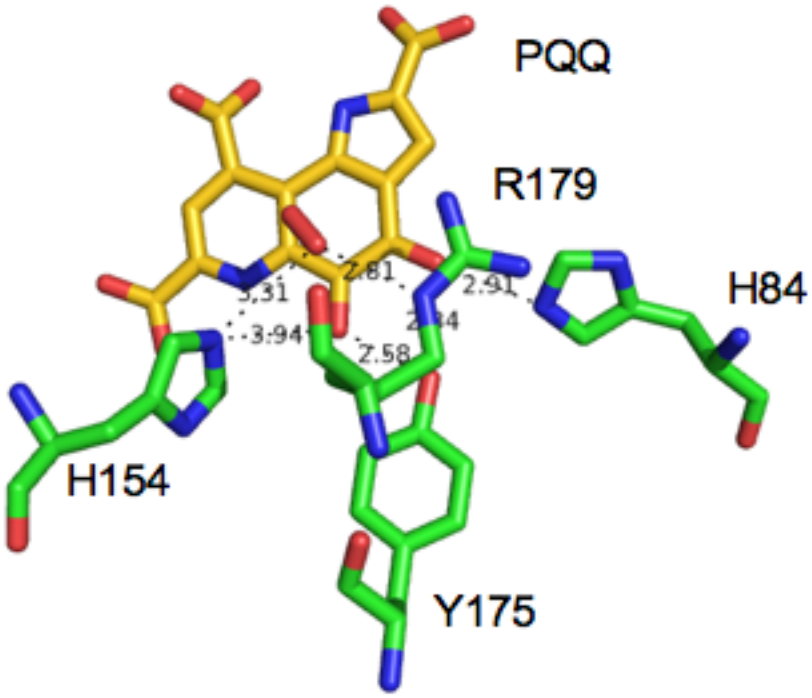

Figure 15B: The densities of the O2 core. The densities of H154, Y175 and R179 are shown to illustrate the pocket formed. O_2 is shown in purple and PQQ is shown in gold.

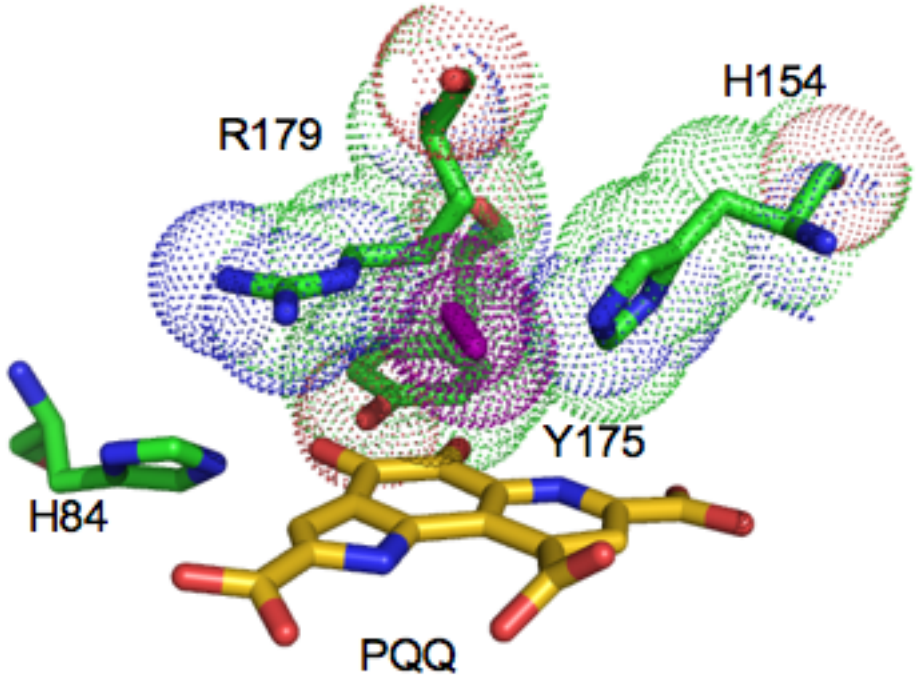

This study looks at the behavior of the H154N, Y175F, Y175S and R179S active site variants. Enzymes with mutations at these positions do not form spectral intermediates from AHQQ indicative of PQQ. Previously described mutations in the PqqC active site at the H84 position do form PQQ in the presence of oxygen. The intermediates that we see spectroscopically in the O_2 core mutant reactions have previously been described as quinoids and quinols, indicating that these enzymes are capable of the first steps of reaction (possible ring closure and quinoid/quinol tautomerization: Figure 2) but incapable of proceeding to form PQQ. In PQQ sensing GDH assays we did not even see the reaction seen with substrate, AHQQ. This also lends support to the idea that these mutations are not forming PQQ, but are capable of reaction with substrate. With the anaerobic denaturation of the PqqC reactions before incubation with GDH, we can stop any quinol intermediates from reoxidizing to a quinone, which would react in a GDH Assay.

It has been proposed that the quinol species in the wild type PqqC reaction react with molecular oxygen or hydrogen peroxide to re-oxidize to a quinone species and then the reaction continues (Figure 2). In the O_2 core mutants the quinol species persists in an aerobic environment. This is very different from what was observed with the wild type enzyme of the H84 mutants where the quinol species was seen anaerobically in wild type and H84A. The H84N variant stops at the quinoid anaerobically due to its inability to protonate the quinoid at the C4 oxygen, but is capable of forming PQQ. There are now four examples of PqqC variants that cannot proceed from the quinoid to quinol intermediate anaerobically- H84N, H154N, Y175F and R179S. To explain this behavior, either these PqqC variants are incapable of binding molecular oxygen in a productive manner or are incapable of activating the bound molecular oxygen.

The crystal structure of Y175F/PQQ indicates a chlorine ion density in the crystal structure in a position attributed to O_2 or H_2O_2 in the WT structure. Chlorine has been shown before to be an oxygen mimic in a cofactorless oxidase. Evidence for binding of O_2 in Y175F and the other O_2 core mutants is also seen in the spectroscopic reactions. Spectroscopic changes seen upon the addition of oxygen to an anaerobic reaction indicate that oxygen is binding to the enzyme.

That the quinoid to quinol tautomerization is only seen in the presence of oxygen in H84N, Y175F, H154N and R179S again shows a non-oxidative role for O_2 in the PqqC mechanism. This again indicates that the O_2 core residues must have a role in the activation of oxygen in the PqqC reaction. Oxygen binding also plays a role in the quinoid to quinol tautomerization. Anaerobic experiments of H154N, Y175F, R179S show the persistence of what is proposed to be a quinoid intermediate at 338nm[11] (Figure 7-10). If O_2 is added, a quinol peak builds in giving an isosbestic point (Figure 11 and 12). This indicates that the intermediate assigned as a quinoid is capable of tautomerizing to a quinol, and that the binding of oxygen is necessary for this process. These two pieces of evidence, the Y175F structure and further reaction of a number of mutants in the presence of O_2, indicate that O_2 is binding in the O_2 core mutants. The inability of these mutant to proceed to product indicates that the most direct effect of mutation is the subsequent activation of the bound O_2.

In a single turnover of AHQQ to PQQ four equivalents of oxygen are used. With the reduction of oxygen to hydrogen peroxide and hydrogen peroxide to water two protons are necessary for each of the four reductions. This means that for every PQQ molecule formed there are eight protons transferred to O2 and H_2O_2. Such a large number of protons could not be taken from the active site in a nonspecific manner. We propose that there is a proton pathway involving the residues R157, H30 and H34 leading from the solvent into the active site of PqqC and that H154 and Y175 are the residues responsible for distributing these protons to the quinoid intermediate and the reactive oxygen species during reaction. During reaction the oxygen in assumed to form a superoxide:semiquinone intermediate initially. If the superoxide does not proceed forward along the reaction path it is reactive enough to re-reduce the semiquinone back to a quinol and no reaction would be observable. R179 is within 3Å of the putative O_2 density, and is concluded to have a definitive role in stabilization of any reactive oxygen species formed during reaction.

The different behaviors between Y175F and Y175S are intriguing and suggest, in accordance with the structural information, that the hydroxyl group and the phenyl group of Y175 play separate roles in the quinoid to quinol conversion. This is manifested in the presence or absence of the quinoid and quinol intermediates in the spectroscopic assays. In the aerobic reactions the quinoid intermediate is seen with Y175S, but not with Y175F. This indicated that the quinoid to quinol tautomerization is faster in Y175F than Y175S. But Y175S can proceed to the quinol anaerobically, which Y175F cannot. The hydroxyl group, which can hydrogen bond or donate a proton, must therefore be playing a role in the quinoid/quinol tautomerization. We have two enzymes that have vary by one active site residues and have different sensitivities to O_2. In previous studies on H84, it was found that the ability to protonate a quinoid allowed tautomerization to a quinol. Anaerobically, we see that when a residue capable of donating a proton is in the 175 position, such as Y175S and WT (Tyr), the reaction can proceed to a quinol. But if there is bulk in the aerobic reaction, such as a Phe or Tyr at 175 position the quinoid/quinol tautomerization is so fast that the quinoid intermediate is not seen spectroscopically. This bulk possibly plays a role in forcing the C4 oxygen of PQQ near to H84,

the proton donor which protonates the C4 oxygen allowing the quinoid to tautomerize to a quinol and avoiding formation of a dianion. This explanation would explain the presence of the quinoid in the Y175S aerobic reaction and not in the Y175F aerobic reaction. Once again, we see behavior which seems to indicate that oxygen can force a reaction through the quinoid/quinol tautomerization when the enzyme is incapacitated and here we have found two variants at the Y175 position that have different sensitivities to O_2 in the quinoid/quinol tautomerization.

In conclusion, we have characterized four mutations that indicate the vital role that the polar residues H154, Y175 and R179 play in formation of PQQ. These residues have a role in the oxidative chemistry carried out by PqqC. This not only adds precedence to the previous proposal of a proteinaceous oxygen binding site, but also shows how small structural changes can destroy the ability of the enzyme to do oxidative chemistry. These mutants do catalyze an incomplete reaction but the presence of quinol intermediates that persist aerobically indicates that the ability of the enzyme to do oxidative chemistry is what has been lost with the mutant enzymes. The O_2 binding core mutants in PqqC show that not only is the oxygen site polar, which is novel, but also, that the H154, Y175 and R179 residues are directly involved in oxygen activation. This supports the idea that polar residues are necessary for activation of oxygen because they can stabilize, via hydrogen bonds, proton donation or electrostatic stabilizationthe various reactive oxygen species that are formed during turnover.

Chapter 5

PQQ Bioinformatics: The Prevalence of PQQ Biosynthetic Machinery in Bacteria

Introduction:

PQQ has long been thought of as a bacterial vitamin[1] because it confers growth adavantage and has important roles in nature[2]. It is a cofactor for numerous bacterial dehydrogenases, the most well studied being glucose and methanol dehydrogenase[3, 4]. PQQ is synthesized by many bacteria, but not all- with *E. coli* being an example of an organism that does not have the genes necessary for PQQ production but uses PQQ and, thus, must pick up PQQ from its environment[5]. There have been claims that PQQ can act as an enzymatic cofactor in mammals[6], but these claims have been refuted and there is no known role for PQQ in mammals[7, 8]. PQQ biogenesis has been studied best in pathogenic systems, such as *Klebsiella pneumoniae*[9]. PQQ biogenesis is based on specific genes that form the *pqq* operon. These operons consist of 6 genes, *pqqABCDEF* in *K. pneumoniae*[10]. We have used bioinformatics to try and investigate the prevalence of PQQ biosynthesis in bacteria and to determine if there are any ties between pathogenicity in bacteria and PQQ synthesis.

Of the genes in the *pqq* operon, we used three in our studies. PqqA, the gene encoded peptide precursor of PQQ, was not suitable for homology searches due to its short length. In *K. pneumoniae* PqqA is a 23 amino acid peptide[11]. The next gene in the operon, PqqB, forms a protein with unknown function[12]. This would be a possible gene to use for homology searches to the PQQ operon, but PqqB has sequence similarity to hydrolases and β-lactamases, which could introduce organisms that do not, in fact, have the genes relating to PQQ biogenesis. PqqF has high sequence similarity to zinc dependent proteases, making it, like PqqB, a less than optimal target.

PqqC is the best studied enzyme in the PQQ pathway[13, 14]. It catalyzes the final step of PQQ formation and is one of two known cofactorless oxidases, the other being urate oxidase[15]. PqqD is a small protein that has no known function, but has been shown recently in this laboratory to associate with PqqE (S. Wecksler, in preparation). PqqE is a radical SAM enzyme with 2 Fe-S clusters[16]. All of these proteins, PqqC, D and E, have no known homology with any other non-Pqq proteins and therefore represent optimal targets to do homology searches to find PQQ forming bacteria without the introduction of possible false positives.

To try and develop a list of PQQ forming bacteria, we first looked at bacteria with experimental evidence for PQQ production. Five bacteria were found; *Klebsiella pneumoniae*[9, 10], *Methylobacterium extorquens* AM1[17], *Gluconobacter oxydans 621H*[18, 19], *Rahnella aquatilis*[20] and *Streptomyces rochei*[21, 22]. PQQ operons from these five bacteria are shown in Table 1. These operons vary, with two of the five organisms (*K. pneumoniae* and *R. aquatilis*) having the same PQQ genes, *pqqA-F*. *M. extorquens* has an extra gene in its operon, *pqqG*. The role of the protein product of this gene is unknown and it, like PqqF, has sequence similarity to zinc dependent proteases. The *G. oxydans* and *S. rochei* operons have no *pqqF* gene. This is possibly because the gene was not annotated as part of the PQQ pathway or that endogenous peptidases in these organisms are capable of acting in the PQQ pathway. There have been indications that PqqF is not an absolute necessity for PQQ formation[23]. The PqqC, D and E protein sequences from these five seed organisms (Table 1) were submitted separately to the Phylobuilder web server, developed by the Sjölander lab at UC Berkeley[24]. PhyloBuilder was used in the global-global mode (the program default) where retrieved sequences are aligned along the entire length of the protein. PhyloBuilder gathers homologs for a user-supplied query sequence using the program FlowerPower[24, 25], constructs a multiple sequence alignment using MUSCLE[24], applies

alignment masking, constructs a phylogenetic tree using a Neighbor-Joining method and identifies functional subfamilies using SCI-PHY[24, 25]. Phylobuilder was run with 7 iterations of Specialized Hidden Markov Models (SHMM), 3 Psi Blasts iterations and a 15% identity cutoff.

The sequences and alignments given by Phylobuilder were modified with the program belvu, and organized by identity to the original sequence. All sequences with less that 30% identity were eliminated in agreement with Sander-Schneider rule[26]. For a particular organism, the sequences homologous to PqqC, D and E (Alignments 1, 2 and 3) were compared and any organism that did not have homologs at the 30% cutoff for PqqC, D and E was discarded. For *M. extorquens*, PqqC and PqqD are fused, forming PqqC/D[27]. Together they gave no homologous sequences. PqqC/D was divided and submitted to Phylobuilder separately to find homologs. Apart, the PqqC portion of PqqC/D had homologous sequences, but the PqqD part of PqqC/D did not. Because of this the *M. extorquens* sequence analysis did not involve PqqD but only looked at homologs found in both PqqC and PqqE. The number of homologs before and after analysis are given in Table 2.

Following completion of the list of Uniprot numbers, which are the output of Phylobuilder and belvu, the uniprot website was used to develop a list of homologous organisms for each of our starting organisms (Lists 1-5). These lists were used to construct a list of all the bacteria found to have proteins homologous to PqqC, D and E as described above (List 6).

The PqqC, D and E protein sequences from the five organisms that have been shown to form PQQ autonomously were subjected to this method to find organisms that contain homologs to the PQQ biosynthetic genes. This group of organisms is a diverse group and contains both pathogenic, meaning invasive and toxic, and non-pathogenic bacteria as well as Gram positive and Gram negative bacteria. Pathogenicity was identified from the literature and from annotations in the HAMAP database. *Klebsiella pneumoniae* has long been studied, and PQQ biogenesis is often studied with genes from *K. pneumoniae*[14]. *K. pneumoniae* is a Gram negative γ-proteobacteria. *K. pneumoniae* is a rod shaped soil bacteria that is pathogenic and found mainly in hospital acquired wound and urinary tract infections. In 1998, *K. pneumoniae* and *K. oxytoca* accounted for 8% of nosocomial bacterial infections in the United States and in Europe[28]. It is a facultative anaerobe. As stated before, PQQ biosynthesis in *K. pneumoniae* is based on six genes, *pqqABCDEF*[9].

PQQ biogenesis has also been studied in *Methylobacterium extorquens* AM1[11]. *M. extorquens* is a methylotrophic bacteria that can survive on numerous one carbon sources such as methanol or methylamine. Methanotrophes are key to the global cycling of one carbon compounds, such as methane[29] and halogenated methanes[30]. *M. extorquens* is a nonpathogenic, Gram negative α-proteobacteria[17]. In *M. extorquens*, PqqC and PqqD are fused together, though it has been shown that this fusion is not necessary for normal function of PqqC[27].

Streptomyces rochei is one of the recently discovered organisms that are Gram positive but still contains the *pqq* operon[22]. *S. rochei* is a filamentous soil bacteria in the Actinobacteria phylum and is pathogenic in mammals[22]. This is one of the first examples of a Gram positive bacteria that contains the genes for PQQ biogenesis[21]. Since PQQ is used by periplasmic dehydrogenases in Gram negative bacteria it is unclear what role PQQ plays in Gram positive bacteria.

Gluconobacter oxydans 621H is a Gram negative plant pathogen, previously known as *Acetobacter suboxydans*[19]. It is a α-proteobacteria and is capable of growing in concentrated sugar solutions and at low pH values. It is found in flowers, fruits, garden soil, alcoholic beverages, cider, and soft drinks. *G. oxydans* can cause fruits, such as apples and

pears, to rot[31]. *G. oxydans* tends to have a small genome size due and limited metabolic abilities[32], which makes its ability to form PQQ a subject of interest.

Rahnella aquatilis is an opportunistic human pathogen. It is a rod shaped bacterium that is Gram negative and an enteric γ-proteo-bacteria and is the only marine bacteria of the original five PQQ forming organisms. *R. aquatilis* was also found to form PQQ[20]. It has been found in a burn wound and in the bronchial washings of an immune deficient patient[33].

The least number of homologs were seen with PqqD of the three PQQ biosynthetic proteins. When treated with the method described above, PqqC and PqqE give very similar numbers of homologs (Table 2) no matter which organism was searched, with the total number of homologous sequences for these enzymes varying by only a few numbers. PqqD consistently has the lowest numbers of homologs. This is possibly due to its smaller size (10 KDa) but also possible due to it being more specific in its sequence. The number of sequences that are common to all three PQQ proteins vary, but can often be attributed to homology with PqqD being limiting for incorporation as a possible PQQ forming organism via this method. This is seen with *G. oxydans*, where all the PqqD homologs are found in the PqqC and PqqE homolog list. Elimination of PqqD from the process, so that only presence of PqqC and PqqE are necessary for being considered as a PQQ forming bacteria, results in the incorporation of two more species, *Enterobacter itermedius* and γ-proteobacterium HTCC2207. *Enterobacter intermedius* is the second Enterobacter species to be found to be PQQ forming, the first being *Enterobacter sakazaii*.

A total of 144 distinct species were found to contain PqqC, PqqD and PqqE genes and 144 species were found to contain both PqqC and PqqE (List 6). The vast majority of these sequences are proteobacteria. Only organisms in the α, β and γ classes of proteobacteria phylum were found. No δ or ε proteobacteria were found. Two Verrumicrobia phylum organisms were found and five Actinobacteria phylum organisms were found. Verrucomicrbioa are a recently discovered phylum that is a sister phylumnot Chylamidae. Of the Actinobacteria, incuding *S. rochei*, four Gram positive bacteria were found to be PQQ forming. These are Saccharopolyspora, Stackebrandtia, Streptomyces and Mycobacterium genera. These were found in numerous different homology lists, not just the *S. rochi* sequence which is interesting since we expected *S. rochei*, being a PQQ forming Gram positive organism, to have more identity to *pqq* genes in other Gram positive organisms. From this we conclude that PQQ biogenesis, while not unheard of in Gram positive organisms, is much less widespread that it is in Gram negative organisms.

The High-quality Automated and Manual Annotation of microbial Proteomes (HAMAP)[34] database is a curated database that consists of annotated proteome sets. HAMAP profiles are created manually when proteins are identified as part of well-conserved bacterial, archaeal and plastid-encoded proteins families or subfamilies. Since it is impossible to know the total number of bacteria species, the HAMAP database is a reasonable place to try and elucidate how prevalent PQQ formation is. There are 933 bacterial organisms in the HAMAP database as of March 2010. Of these organisms, 95 were selected by our method as being PQQ forming bacteria. This indicates that at least 10% of the known bacterial kingdom is capable of forming PQQ, giving a very rough idea of how prevalent PQQ biosynthesis is in nature. Considering how stringent the method used here is, this is a lower limit of the percentage of PQQ formation in bacteria.

PQQ has been long been associated with pathogenicity in bacteria. One of the most studied PQQ forming enzymes, *Klebsiella pneumoniae*, is pathogenic. When looking at the

pathogenic bacteria in the lists developed, we found numerous types of invasive bacteria that are thought to contain PQQ by our method. We found that there are animal pathogens, plant pathogens and plant symbiotes, as well as nonpathogenic and noninvasive bacteria. This leads us to need to define "pathogenicity" for our purposes. Traditionally, pathogenicity has certain requirements. To be pathogenic a bacteria must be able to invade a host and also be toxic to that host. While the traditionally pathogenic bacteria in our list fit this idea, the numerous plant symbiotes do not. They are not toxic to their hosts, but actually the opposite, they are beneficial. Because of this we have divided the traditionally pathogenic bacteria and the plant symbiotes into two separate lists. A high percentage (~50%) of bacteria seen in the PQQ forming are capable of invasiveness. This could be significant for numerous reasons. First, PQQ confers a growth advantage to bacteria. Not competing for the available PQQ, or being able to form more than other bacteria can scavenge, would give an organism a competitive edge. Also, if the organism is invading an environment where there should be no other bacteria, PQQ may not be available. The only way to survive would be to form PQQ autonomously.

The presence and assumed importance of PQQ biosynthesis in bacteria that are symbiotic with plants is interesting. PQQ added to soil conferred a significant increase in growth of the plants. Bacteria are symbiotic with plans have been show to solubilize soil phosphorus and iron, increasing uptake in plants[35]. It is possible that PQQ dependent dehydrogenases cause the surrounding environment to become more acidic by forming gluconic acid from glucose (catalyze with GDH) and therefore make more soil nutrients accessible to plants, thereby giving them a growth advantage. There are studies that indicate that PQQ is used in roles other than simply as a cofactor for bacterial dehydrogenases. Other known roles are as an O_2 scavenger, nerve growth factor activity and signaling[2] and mitochondrial biogenesis[36]. It is unknown whether these roles have anything importance to plant or animal growth. Again, PQQ could be important for achieving a growth factor over other bacteria. If a bacteria that is not toxic to plants is out-competing a bacteria that is pathogenic to plants, it is beneficial to the plant.

When looking at pathogenicity instead of just invasiveness, we see different behavior. About 25% of the bacteria are pathogenic. Comparing this to three surveys of 30 random organisms from the HAMAP database, an enrichment of pathogenicity was not seen in the PQQ forming bacteria. These surveys showed invasiveness between 46% and 57% (average 53%). This indicates that the pathogenicity and invasiveness seen in the PQQ forming bacteria is by no means out of the ordinary. Pathogenicity in humans also has similar levels, with 20% of the PQQ forming bacteria being human pathogens and the HAMAP surveys being an average of 26% human pathogens. While we consider PQQ to still be a viable target for antibiotic development due to its role as a bacterial vitamin, it does not seem to be unique to pathogenic or invasive bacteria.

What these results show is that a high percentage of PQQ forming bacteria are invasive (~50%) and pathogenic (~25%), comparison to an existing database shows similar percentages, indicating that there are no associations between PQQ biosynthetic capabilities and pathogenicity. We have developed a list of PQQ forming bacteria, giving an idea of how prevalent the *pqq* operon is and what types of bacteria are capable of forming PQQ autonomously. PQQ formation is not seen in δ and ε proteobacteria, but is seen in α-, β- and γ-proteobacteria. It is seen in both Gram negative and Gram positive bacteria, though overwhelmingly more prevalent in Gram negative bacteria. How PQQ is being used in Gram positive bacteria is unknown, but 4 new Gram positive PQQ forming bacteria have been identified.

Table 1: The genes for demonstrated PQQ forming organism. NCBI Loci are given in parenthesis after the organism name. The PQQ operon encoded biosynthetic proteins in these organisms are shown below. The old and new *M. extorquens* columns are the original and current names, respectively, for the gene products.

K.pneumoniae (X58778)	*M.extorquens* (old)	*M.extorquens* (new) (NC_012808)	*S. rochei* (AB088224)	*G.oxydans* (CP000009)	*R.aquatilis* (FJ868974)
PqqA	PqqD	PqqA	lkcK	PqqA	PqqA
PqqB	PqqG	PqqB	lkcO	PqqB	PqqB
PqqC	PqqC	PqqC/D	lkcL	PqqC	PqqC
PqqD	PqqB	PqqC/D	lkcM	PqqD	PqqD
PqqE	PqqA	PqqE	lkcN	PqqE	PqqE
PqqF	PqqE	PqqF			PqqF
	PqqF	PqqG			

Table 2: Phylobuilder and analysis results. The numbers given are the numbers of discreet sequences seen after elimination of any protein with less than 30% identity to the original protein sequence. The number of sequences in PqqCDE are the number of sequences that are found in the PqqC, PqqD and PqqE sequence lists. In the case of *M. extorquens*, PqqD was not found to have any homology as searched so only the PqqC and PqqD lists were combined.

Organism	Seq. PqqC	Seq. PqqD	Seq. PqqE	Seq. PqqCDE	Seq. PqqCE
K. pneumoniae	149	125	157	82	97
M. extorquens	150	1	157	131*	131
R. aquatilis	151	123	158	102	143
G. oxydans	151	56	158	56	143
S. rochei	150	117	158	94	143

*Sequences for PqqCE, with PqqD not taken into account

Table 3: In this table, percentage are shown for each of the organisms in Table 2 (PqqCDE) belonging to the sub-phylums, α-, β- and γ-proteobacteria as well as the percentage that function either as pathogens or plant symbiotes

Organism	%α	%β	%γ	%pathogenic	%plant symbiotic
K. pneumoniae	11	32	52	26	22
M. extorquens	33	20	41	28	20
R. aquatilis	14	29	54	37	20
G. oxydans	57	9	32	18	29
S. rochei	30	26	37	39	15
Overall	31	22	42	24	21

List 1: Klebsiella pneumoniae as the seed organism. Pathogens are marked with a 'Y' and plant and animal symbiots are marked Ps and As, respectively.

Genus	Species	Pathogenic
Acintobacter	baumanii (strain AYE)	Y
	baumanii (strain SDF)	Y
	baumanii (strain ACICU)	Y
	baumanii (strain AB307-0294)	Y
	baumanii (strain AB0057)	Y
	sp. (strain ADP1)	
	sp. ATCC27244	
Azoarcus	sp. (BH72)	
Azotobacter	vinelandii ATCC BAA-1303	
B proteobacter	KB13	
Bradyrhizobium	sp. ATCC BAA-1182	Ps
Burkholderia	ambifara (strain MCO40-6)	
	ambifara (strain ATCC BAA-244)	
	cenocepacia (strain AU 1054)	Y
	cenocepacia (strain H12424)	Y
	cenocepacia (strain MCO-3)	Y
	cenocepacia (strain PC184)	Y
	cepacia (strain J2315)	Y
	dolosa AU0158	
	graminis C4DIM	Y
	glumae (strain BGK1)	Ps
	multivorans (strain ATCC 17616)	Y
	phymatum (strain DSM17167)	Ps
	vietnamiensis (strain CMG22486)	Ps
	xenovorans (strain LB400)	
Colwellia	psychrerythraea ATCC BAA-681	
Chthoniobacter	flavus Ellin428	
Cupravidius	taiwanensis (strain R1)	Ps
Dechloromonas	aromatica (strain RCB)	
γ proteobacter	NOR51-B	
Geodermatophilus	obscurus DMS43160	
Gluconoacetobacter	diazotrophicus (strain ATCC 49037)	Ps
Klebsiella	pneumoniae	Y
	pneumoniae NTUH-K2044	Y
	pneumoniae (strain 342)	Y
Leptothrix	cholodnii (strain ATCC 51168)	
Marine γ proteobacteria	HTCC2080	
	HTCC2143	
Marinobacter	sp. ELB17	
	algicola DG893	Ps Methylacidiphilium
infernorum		
Methylobacillus	flagellatus (strain ATCC 51484)	

Methylococcus	capsulatus	
Methylophaga	thiooxidans DMS010	
Neptuniibacter	caesariensis	
Nitrobacter	winogradskyi (ATCC 25391)	
Nitrococcus	mobilis Nb-231	
Nitrosococcus	oceani (strain ATCC 19707)	
Polarmonas	napthalenivorans (strain CJ2)	
Pseudomonas	aeruginosa (strain LESB58)	Y
	aeruginosa	Y
	aeruginosa C3719	
	aeruginosa 2192	
	entomophilia (strain L48)	
	syringae pv. phaseolicola (strain 1448A)	Ps
	syringae pv. tomato	Ps
	putida (strain KT2440)	
	stutzeri (strain A1501)	
	fluorenscens BW25	Y
	putida (strain W619)	
Ralstonia	eutropha (strain ATCC 17699)	Y
	eutropha (strain JMP134)	
	picketii (strain 12J)	
Rhodopseudomonas	palustris	
	palustris (strain BISA53)	
	palustris (strain TIE-1)	Y
Rickettsiella	grylli	Y
Roseovarious	sp. 217	
	sp.TM1035	Ps
Serratia	marcescens	
Shewanella	woodyi (strain ATCC 51908)	
Stackebrandtia	nassauensis DSM44728	
Variovorax	paradoxus (strain S110)	
Verminephrobacter	eiseniae (strain EF01-2)	
Xanthomonas	autotrophicus (strain ATCC BAA-1158)	Ps
	axonopodis pv. citri	Ps
	campestris	Ps
	campetris pv. vesicatoria	Ps
	campetris pv. campestris (strain 8004)	Ps
	campetris pv. campestris 85-10	Ps
	oryzae pv. oryzae (strain PX099A)	Ps
	oryzae pv. oryzae (strain MAFF 311018)	Ps

List 2: Methylobacterium extorquens AM1 as the seed organism. Pathogens are marked with a 'Y' and plant and animal symbiots are marked Ps and As, respectively.

Genus	Species	Pathogenic
Acidiphilium	cryptum (strain JF-5)	
Acinetobacter	baumannii (strain AB0057)	Y
	baumannii (strain AB307-0294)	Y
	baumannii (strain ACICU)	Y
	baumannii (strain AYE)	Y
	baumannii (strain SDF)	Y
	calcoaceticus	
	sp. (strain ADP1)	
	sp. ATCC 27244	
Agrobacterium	radiobacter	Y
Azoarcus	sp. (strain BH72)	Ps
Azotobacter	vinelandii	
Beijerinckia	indica subsp. Indica	Ps
Bradyrhizobium	japonicum	Ps
	sp. (strain BTAi1 / ATCC BAA-1182)	Ps
	sp. (strain ORS278)	Ps
Burkholderia	ambifaria (strain ATCC BAA-244)	Y
	ambifaria (strain MC40-6)	Y
	cenocepacia (strain AU 1054)	Y
	cenocepacia (strain HI2424)	Y
	cenocepacia (strain MC0-3)	Y
	cenocepacia PC184	Y
	cepacia (strain J2315 / LMG 16656)	Y
	dolosa AUO158	
	glumae (strain BGR1)	Ps
	graminis C4D1M	Y
	phymatum (strain DSM 17167)	Ps
	sp. H160	Y
	vietnamiensis (strain G4)	Ps
Chromohalobacter	salexigens (strain DSM 3043)	
Chthoniobacter	flavus Ellin428	
Colwellia	psychrerythraea (strain 34H)	
Cupriavidus	taiwanensis (strain R1 / LMG 19424)	Ps
Dechloromonas	aromatica (strain RCB)	
Dinoroseobacter	shibae (strain DFL 12)	As
Enterobacter	sakazakii (strain ATCC BAA-894)	Y
Erwinia	tasmaniensis (strain DSM 17950)	Ps
Fulvimarina	pelagi HTCC2506	
γ proteobacterium NOR51-B		
Gluconacetobacter	diazotrophicus (strain ATCC 49037)	Y
Gluconobacter	oxydans	Y
	sp. H24	

Granulibacter	bethesdensis (strain ATCC BAA-1260)	Y
Klebsiella	pneumoniae	Y
	pneumoniae (strain 342)	Y
	pneumoniae NTUH-K2044	Y
	pneumoniae subsp. pneumoniae	Y
Leptothrix	cholodnii (strain ATCC 51168)	
Lutiella	nitroferrum 2002	
Manganese-oxidizing bacterium (strain SI85-9A1)		
marine γ proteobacterium HTCC2080		
marine γ proteobacterium HTCC2143		
Marinobacter	algicola DG893	Ps
	sp. ELB17	
Methylacidiphilum	infernorum (isolate V4)	Y
Methylobacillus	flagellatus (strain KT)	
Methylobacterium	extorquens (strain ATCC 14718)	
	nodulans (strain ORS2060)	Ps
	radiotolerans (strain ATCC 27329)	Ps
Methylocella	silvestris (strain BL2)	
Methylococcus	capsulatus	
Methylophaga	thiooxidans DMS010	
Mycobacterium	smegmatis (strain ATCC 700084)	Y
Neptuniibacter	caesariensis	
Nitrobacter	winogradskyi (strain Nb-255)	
Nitrosococcus	oceani (strain ATCC 19707)	
	oceani AFC27	
Paracoccus	denitrificans (strain Pd 1222)	
Physcomitrella patens	subsp. patens (plant)	
Polaromonas	naphthalenivorans (strain CJ2)	
Pseudomonas	aeruginosa	Y
	aeruginosa (strain LESB58)	Y
	aeruginosa (strain PA7)	Y
	aeruginosa (strain UCBPP-PA14)	Y
	aeruginosa 2192	Y
	aeruginosa C3719	Y
	entomophila (strain L48)	
	fluorescens (strain Pf0-1)	
	fluorescens (strain Pf-5 / ATCC BAA-477)	
	fluorescens (strain SBW25)	
	mendocina (strain ymp)	
	putida (strain F1 / ATCC 700007)	
	putida (strain GB-1)	
	putida (strain KT2440)	Ps
	syringae pv. phaseolicola (strain 1448A)	Ps
	syringae pv. syringae (strain B728a)	Ps
	syringae pv. tomato	Ps
Rahnella	aquatilis	Y

Ralstonia	eutropha (strain ATCC 17699)	
	eutropha (strain JMP134)	
	pickettii (strain 12J)	Y
Rhizobium	meliloti	
Rhodobacter	sphaeroides (strain ATCC 17023)	
	sphaeroides (strain ATCC 17025)	
	sphaeroides (strain ATCC 17029)	
	sphaeroides (strain KD131)	
Rhodobacterales	bacterium HTCC2654	
	bacterium Y4I	
Rhodopseudomonas	palustris	
	palustris (strain BisA53)	
	palustris (strain BisB18)	
	palustris (strain BisB5)	
	palustris (strain HaA2)	
	palustris (strain TIE-1)	
Rickettsiella	grylli	Y
Roseobacter	denitrificans (strain ATCC 33942)	
	litoralis Och 149	
	sp. AzwK-3b	
	sp. GAI101	
Roseovarius	sp. 217	
	sp. HTCC2601	
	sp. TM1035	Ps
Saccharopolyspora	erythraea (strain NRRL 23338)	
Sagittula	stellata E-37	
Serratia	marcescens	Y
Shewanella	woodyi (strain ATCC 51908)	
Silicibacter	pomeroyi	
Sinorhizobium	medicae (strain WSM419)	
Stackebrandtia	nassauensis DSM 44728	
Streptomyces	rochei	Y
Variovorax	paradoxus (strain S110)	
Verminephrobacter	eiseniae (strain EF01-2)	As
Xanthobacter	autotrophicus (strain ATCC BAA-1158)	
	axonopodis pv. citri	Ps
	campestris pv. campestris	Ps
	campestris pv. campestris (strain 8004)	Ps
	campestris pv. campestris (strain B100)	Ps
	campestris pv. vesicatoria (strain 85-10)	Ps
	oryzae pv. oryzae	Ps
	oryzae pv. oryzae (strain MAFF 311018)	Ps
	oryzae pv. oryzae (strain PXO99A)	Ps

List 3: Rahnella aquatilis as the seed organism. Pathogens are marked with a 'Y' and plant and animal symbiots are marked Ps and As, respectively.

Genus	Species	Pathogenic
Acidiphilium	cryptum	
Acinetobacter	baumannii (strain AB0057)	Y
	baumannii (strain AB307-0294)	Y
	baumannii (strain ACICU)	Y
	baumannii (strain AYE)	Y
	baumannii (strain SDF)	Y
	calcoaceticus	
	sp (ADP1)	
	sp. ATCC 27244	
Azoarcus	sp (BH72)	Ps
	sp. (strain BH72)	
Azotobacter	vinelandii	
β proteobacterium KB13		
Burkholderia	ambifaria (strain ATCC BAA-244)	Y
	ambifaria (strain MC40-6)	Y
	ambifaria IOP40-10	Y
	cenocepacia (strain AU 1054)	Y
	cenocepacia (strain HI2424)	Y
	cenocepacia (strain MC0-3)	Y
	cenocepacia PC184	Y
	cepacia	Y
	dolosa	
	glumae	Ps
	graminis	Y
	phymatum	Ps
	sp. H160	Y
	vietnamiensis	Ps
	xenovorans	Y
	xenovorans (strain LB400)	Y
Chthoniobacter	flavus Ellin428	
Colwellia	psychrerythraea	
Cupriavidus	taiwanensis	Ps
Dechloromonas	aromatica	
Enterobacter	sakazakii	
Erwinia	tasmaniensis	Y
γ proteobacterium NOR51-B		
Gluconacetobacter	diazotrophicus	Ps
Gluconobacter	sp. H24	
Granulibacter	bethesdensis	Y
Klebsiella	pneumoniae	Y
	pneumoniae (strain 342)	Y
	pneumoniae NTUH-K2044	Y

Limnobacter	sp. MED105	
Lutiella	nitroferrum 2002	
marine γ proteobacterium HTCC2143		
Marinobacter	algicola DG893	Ps
	sp. ELB17	
Methylobacillus	flagellatus	
Methylobacterium	extorquens	
	nodulans	Ps
Methylocella	silvestris	Y
Methylococcus	capsulatus	
Methylophaga	thiooxidans	
	thiooxidans DMS010	
Mycobacterium	smegmatis	Y
Neptuniibacter	caesariensis	
Nitrococcus	mobilis Nb-231	
Nitrosococcus	oceani AFC27	
	oceani (strain ATCC 19707)	
Polaromonas	naphthalenivorans	
Pseudomonas	aeruginosa	Y
	aeruginosa (strain LESB58)	Y
	aeruginosa (strain PA7)	Y
	aeruginosa (strain UCBPP-PA14)	Y
	aeruginosa 2192	Y
	aeruginosa C3719	Y
	fluorescens	Y
	fluorescens (strain Pf0-1)	Y
	fluorescens (strain SBW25)	Y
	putida (strain F1 / ATCC 700007)	
	putida (strain W619)	Ps
	stutzeri	Ps
	entomophila	
	fluorescens (pf-5)	
	putida (strain GB-1)	
	putida (strain KT2440)	Ps
	syringae pr. phaseolicola	Ps
	syringae pr. syringae	Ps
	syringae pr. tomato	Ps
Rahnella	aquatilis	Y
Ralstonia	eutropha	
	eutropha (strain JMP134)	
	pickettii	Y
Rhizobium	sp. (strain NGR234)	
Rhodobacterales	bacterium Y4I	
Rhodopseudomonas	palustris	
	palustris (strain HaA2)	
	palustris (strain TIE-1)	

Rickettsiella	grylli	Y
Roseobacter	sp. GAI101	
Serratia	marcescens	Y
Shewanella	woodyi	
Variovorax	paradoxus	
Verminephrobacter	eiseniae	Y
Xanthobacter	autotrophicus	
Xanthomonas	axonopodis pv. citri	Ps
	campestris pv. campestris	Ps
	campestris pv. campestris (strain 8004)	Ps
	campestris pv. vesicatoria	Ps
	oryzae pv. oryzae (strain MAFF 311018)	Ps
	oryzae pv. oryzae (strain PXO99A)	Ps

List 4: Gluconobacter oxydans as the seed organism. Pathogens are marked with a 'Y' and plant and animal symbiots are marked Ps and As, respectively.

Genus	Species	Pathogenic
Agrobacterium	radiobacter	
Beijerinckia	indica subsp. indica	Ps
Bradyrhizobium	japonicum	Ps
	sp. (strain BTAi1)	Ps
	sp. (strain ORS278)	Ps
Burkholderia	ambifaria IOP40-10	Y
	cenocepacia PC184	Y
Chromohalobacter	salexigens	
Chthoniobacter	flavus	
Cupriavidus	taiwanensis	Y
Dinoroseobacter	shibae	As
Fulvimarina	pelagi	
Gluconacetobacter	diazotrophicus	Y
Gluconobacter	oxydans	Y
	sp. H24	Y
Granulibacter	bethesdensis	
Klebsiella	pneumoniae	Y
Lutiella	nitroferrum	
Marinobacter	sp. ELB17	
Methylacidiphilum	infernorum	Y
Methylobacterium	extorquens	
	nodulans	Y
Methylocella	silvestris	Y
Nitrobacter	winogradskyi	
Paracoccus	denitrificans	Y
Pseudomonas	aeruginosa	Y
	aeruginosa C3719	Y
Rahnella	aquatilis	Y
Ralstonia	pickettii	Y
Rhizobium	meliloti	
	sp. (strain NGR234)	
Rhodobacter	sphaeroides	
Rhodobacterales	bacterium HTCC2654	
	bacterium Y4I	
Rhodopseudomonas	palustris	
	palustris (strain BisA53)	
	palustris (strain BisB18)	
	palustris (strain BisB5)	
	palustris (strain HaA2)	
Roseobacter	denitrificans	
	litoralis Och 149	
	sp. AzwK-3b	

Roseovarius	sp. 217	
	sp. HTCC2601	
	sp. TM1035	
Sagittula	stellata E-37	
Silicibacter	pomeroyi	
Sinorhizobium	medicae	
Stackebrandtia	nassauensis	
Xanthobacter	autotrophicus	
Xanthomonas	axonopodis pv. citri	Ps
	campestris pv. campestris	Ps
	campestris pv. campestris (strain 8004)	Ps
	campestris pv. vesicatoria	Ps
	oryzae pv. oryzae	Ps
	oryzae pv. oryzae (strain MAFF 311018)	Ps

List 5: Streptomyces rochei as the seed organism. Pathogens are marked with a 'Y' and plant and animal symbiots are marked Ps and As, respectively.

Genus	Species	Pathogenic
Acidiphilium	cryptum (strain JF-5)	Y
Acinetobacter	baumannii (strain AB0057)	Y
	baumannii (strain AB307-0294)	Y
	baumannii (strain ACICU)	Y
	baumannii (strain AYE)	Y
	baumannii (strain SDF)	Y
	calcoaceticus	Y
Agrobacterium	radiobacter	Y
Azotobacter	vinelandii	
Beijerinckia	indica subsp. indica)	Y
Bradyrhizobium	sp. (strain BTAi1)	
Burkholderia	ambifaria (strain ATCC BAA-244)	Y
	ambifaria (strain MC40-6)	Y
	ambifaria IOP40-10	Y
	cenocepacia (strain AU 1054)	Y
	cenocepacia (strain HI2424)	Y
	cenocepacia (strain MC0-3)	Y
	cenocepacia PC184	Y
	cepacia (strain J2315 / LMG 16656)	Y
	dolosa AUO158	
	glumae (strain BGR1)	Ps
	multivorans (strain ATCC 17616 / 249)	Y
	phymatum (strain DSM 17167 / STM815)	Ps
	sp. H160	Y
	vietnamiensis (strain G4 / LMG 22486)	Ps
	xenovorans (strain LB400)	Y
Chromohalobacter	salexigens	
Chthoniobacter	flavus Ellin428	
Cupriavidus	taiwanensis (strain R1 / LMG 19424)	Y
Dechloromonas	aromatica (strain RCB)	
Dinoroseobacter	shibae (strain DFL 12)	As
Fulvimarina	pelagi HTCC2506	
Klebsiella	pneumoniae	Y
	pneumoniae (strain 342)	Y
	pneumoniae NTUH-K2044	Y
Leptothrix	cholodnii	
Limnobacter	sp. MED105	
Marinobacter	algicola DG893	Ps
	sp. ELB17	
Methylacidiphilum	infernorum	Y
Methylobacterium	nodulans	Ps
Methylocella	silvestris	Y

Methylococcus	capsulatus	
Mycobacterium	smegmatis	Y
Nitrobacter	winogradskyi	
Nitrococcus	mobilis Nb-231	
Paracoccus	denitrificans (strain Pd 1222)	
Polaromonas	naphthalenivorans (strain CJ2)	
Pseudomonas	aeruginosa	Y
	aeruginosa (strain LESB58)	Y
	aeruginosa (strain PA7)	Y
	aeruginosa (strain UCBPP-PA14)	Y
	aeruginosa 2192	Y
	aeruginosa C3719	Y
	entomophila (strain L48)	
	entomophila (strain L48)	
	putida (strain GB-1)	
	putida (strain KT2440)	Ps
Ralstonia	eutropha (strain JMP134)	
	pickettii (strain 12J)	Y
Rhizobium	meliloti	
	sp. (strain NGR234)	
Rhodobacter	sphaeroides (strain ATCC 17023)	
	sphaeroides (strain KD131)	
Rhodobacterales	bacterium HTCC2654	
	bacterium Y4I	
Rhodopseudomonas	palustris	
	palustris (strain BisA53)	
	palustris (strain HaA2)	
Roseobacter	denitrificans	
	litoralis Och 149	
	sp. AzwK-3b	
	sp. GAI101	
Roseovarius	sp. 217	
	sp. HTCC2601	
	sp. TM1035	
Saccharopolyspora	erythraea (strain NRRL 23338)	
Sagittula	stellata E-37	
Serratia	marcescens	Y
Shewanella	woodyi (strain ATCC 51908 / MS32	
Silicibacter	pomeroyi	
Sinorhizobium	medicae (strain WSM419)	
Streptomyces	rochei (Streptomyces parvullus)	Y
Variovorax	paradoxus (strain S110)	
Verminephrobacter	eiseniae (strain EF01-2)	Y
Xanthobacter	autotrophicus	
Xanthomonas	axonopodis pv. citri	Ps
	campestris pv. campestris	Ps

campestris pv. campestris (strain 8004)	Ps
campestris pv. campestris (strain B100)	Ps
campestris pv. vesicatoria (strain 85-10)	Ps
oryzae pv. oryzae	Ps
oryzae pv. oryzae (strain MAFF 311018)	Ps
oryzae pv. oryzae (strain PXO99A)	Ps

List 6: Combined list of all PQQ forming organisms. Pathogens are marked with a 'Y' and plant and animal symbiots are marked Ps and As, respectively.

Genus	Species	Pathogenic	
Acidiphilium	cryptum (strain JF-5)		Copeland et al. 2007
Acinetobacter	baumannii (strain AB0057)	Y	Adams et al. 2008
	baumannii (strain AB307-0294)	Y	Adams et al. 2008
	baumannii (strain ACICU)	Y	Iacono et al. 2008
	baumannii (strain AYE)	Y	Vallenent et al. 2008
	baumannii (strain SDF)	Y	Vallenent et al. 2008
	calcoaceticus		Goosen et al. 1989
	sp. (strain ADP1)		Barbe et al. 2004
	sp. ATCC 27244		Qin et al. 2008
Agrobacterium	radiobacter	Y	Slater et al. 2009
Azoarcus	sp. (strain BH72)	Ps	Krause et al. 2006
Azotobacter	vinelandii		Setubal et al. 2009
Beijerinckia	indica subsp. Indica	Ps	Copeland et al. 2008
β proteobacterium KB13			Rappe et al. 2008
Bradyrhizobium japonicum		Ps	Kaneko et al. 2002
	sp. (strain BTAi1 / ATCC BAA-1182)	Ps	Giraud et al. 2007
	sp. (strain ORS278)	Ps	Giraud et al. 2007
Burkholderia	ambifaria (strain ATCC BAA-244)	Y	Copeland et al. 2006
	ambifaria (strain MC40-6)	Y	Copeland et al. 2008
	ambifaria IOP40-10		Copeland et al. 2008
	cenocepacia (strain AU 1054)	Y	Copeland et al. 2006
	cenocepacia (strain HI2424)	Y	Copeland et al. 2006
	cenocepacia (strain MC0-3)	Y	Copeland et al. 2008
	cenocepacia PC184	Y	Birren et al. 2005
	cepacia (strain J2315 / LMG 16656)	Y	Holden et al. 2007
	dolosa AUO158		Birren et al. 2005
	glumae (strain BGR1)	Y	Lim et al. 2009
	graminis C4D1M	Y	Copeland et al. 2008
	multivorans (strain ATCC 17616 / 249)		Copeland et al. 2007
	phymatum (strain DSM 17167)	Ps	Copeland et al. 2008
	sp. H160	Y	Lucas et al. 2008
	vietnamiensis (strain G4)	Y	Copeland et al. 2007
	xenovorans		Chain et al. 2006
	xenovorans (strain LB400)		Chain et al. 2006
Chromohalobacter	salexigens (strain DSM 3043)		Copeland et al. 2006
Chthoniobacter	flavus Ellin428		Lucas et al. 2008
Colwellia	psychrerythraea (strain 34H)		Methe et al. 2005
Cupriavidus	taiwanensis (strain R1 / LMG 19424)	Y	Amadou et al. 2008
Dechloromonas	aromatica (strain RCB)		Copeland et al. 2005
Dinoroseobacter	shibae (strain DFL 12)	As	Copeland et al. 2007
Enterobacter	sakazakii (strain ATCC BAA-894)	Y	McClelland et al. 2007
Erwinia	tasmaniensis (strain DSM 17950)	Ps	Kube et al. 2008
Fulvimarina	pelagi HTCC2506		Giovanni et al. 2006
γ proteobacterium NOR51-B			Amann et al. 2008
Geodermatophilus	obscurus (DMS43160)		Lucas et al. 2010
Gluconacetobacter	diazotrophicus (strain ATCC 49037)	Y	Bertalan et al. 2007
Gluconobacter	oxydans	Y	Prust et al. 2005
	sp. H24		Gao et al. 2009
Granulibacter	bethesdensis (strain ATCC BAA-1260)	Y	Greenberg et al. 2007
Klebsiella	pneumoniae	Y	Meulenberg et al. 1992
	pneumoniae (strain 342)	Y	Fouts et al. 2008

	pneumoniae NTUH-K2044	Y	Wu et al. 2009
	pneumoniae subsp. pneumoniae	Y	McClelland et al. 2006
Leptothrix	cholodnii (strain ATCC 51168)		Copeland et al. 2008
Limnobacter	sp. MED105		Pihassi et al. 2007
Lutiella	nitroferrum 2002		Lucas et al. 2009
Manganese-oxidizing bacterium (strain SI85-9A1)			Dick et al. 2008
marine γ proteobacterium HTCC2080			Giovannoni et al. 2006
marine γ proteobacterium HTCC2143			Giovannoni et al. 2006
Marinobacter	algicola DG893	Ps	Green et al. 2007
	sp. ELB17		Ward et al. 2006
Methylacidiphilum	infernorum (isolate V4)	Y	Hou et al. 2008
Methylobacillus	flagellatus (strain KT)		Copeland et al. 2006
Methylobacterium	extorquens (strain ATCC 14718)		Vuilleumier et al. 2009
	nodulans (strain ORS2060)	Y	Lucas et al. 2009
	radiotolerans (strain ATCC 27329)	Ps	Copeland et al. 2008
Methylocella	silvestris (strain BL2)		Lucas et al. 2008
Methylococcus	capsulatus		Ward et al. 2004
Methylophaga	thiooxidans DMS010		Schaefer et al. 2008
Mycobacterium	smegmatis (strain ATCC 700084)	Y	Fleischmann et al. 2006
Neptuniibacter	caesariensis		Pinhassi et al. 2006
Nitrobacter	winogradskyi (strain Nb-255)		Starkenburg et al. 2006
Nitrococcus	mobilis Nb-231		Waterbury et al. 2006
Nitrosococcus	oceani (strain ATCC 19707)		Klotz et al. 2006
	oceani AFC27		Klotz et al. 2008
Paracoccus	denitrificans (strain Pd 1222)		Copeland et al. 2006
Polaromonas	naphthalenivorans (strain CJ2)		Copeland et al. 2006
Pseudomonas	aeruginosa	Y	Stover et al. 2000
	aeruginosa (strain LESB58)	Y	Winstanley et al. 2009
	aeruginosa (strain PA7)	Y	Dodson et al. 2007
	aeruginosa (strain UCBPP-PA14)	Y	Lee et al. 2006
	aeruginosa 2192	Y	Mathee et al. 2008
	aeruginosa C3719	Y	Mathee et al. 2008
	entomophila (strain L48)		Vodovar et al. 2006
	fluorescens		Schnider et al. 1995
	fluorescens (strain Pf0-1)		Silby et al. 2009
	fluorescens (strain Pf-5 / ATCC BAA-477)		Paulsen et al. 2005
	fluorescens (strain SBW25)		Tett et al. 2007
	mendocina (strain ymp)		Copeland et al. 2007
	putida (strain F1 / ATCC 700007)		Copeland et al. 2007
	putida (strain GB-1)		Copeland et al. 2008
	putida (strain KT2440)	Ps	Nelson et al. 2002
	putida (W619)	Ps	Copeland et al. 2008
	sturtzi (A1501)	Ps	Yan et al. 2006
	syringae pv. phaseolicola (strain 1448A)	Ps	Joardar et al. 2005
	syringae pv. syringae (strain B728a)	Ps	Feil et al. 2005
	syringae pv. tomato	Ps	Buell et al. 2003
Rahnella	aquatilis	Ps	Guo et al. 2009
Ralstonia	eutropha (strain ATCC 17699)		Pohlmann et al. 2006
	eutropha (strain JMP134)		Copeland et al. 2005
	pickettii (strain 12J)	Y	Lucas et al. 2008
Rhizobium	meliloti		Capela et al. 2001
	sp. (strain NGR234)		Schmeisser et al. 2009
Rhodobacter	sphaeroides (strain ATCC 17023)		Copeland et al. 2007
	sphaeroides (strain ATCC 17025)		Copeland et al. 2007
	sphaeroides (strain ATCC 17029)		Copeland et al. 2009
	sphaeroides (strain KD131)		Lim et al. 2009

Rhodobacterales	bacterium HTCC2654		Giovannoni et al. 2006
	bacterium Y4I		Moran et al. 2008
Rhodopseudomonas	palustris		Larimer et al. 2004
	palustris (strain BisA53)		Copeland et al. 2006
	palustris (strain BisB18)		Copeland et al. 2006
	palustris (strain BisB5)		Copeland et al. 2006
	palustris (strain HaA2)		Copeland et al. 2006
	palustris (strain TIE-1)		Lucas et al. 2008
Rickettsiella	grylli	Y	Seshadri et al. 2006
Roseobacter	denitrificans (strain ATCC 33942)		Swingley et al. 2007
	litoralis Och 149		Brinkhoff et al. 2007
	sp. AzwK-3b		Francis et al. 2007
	sp. GAI101		Edwards et al. 2008
Roseovarius	sp. 217		Murrell et al. 2006
	sp. HTCC2601		Giovannoni et al. 2006
	sp. TM1035	Ps	Belas et al. 2007
Saccharopolyspora	erythraea (strain NRRL 23338)		Oliynyk et al. 2007
Sagittula	stellata E-37		Moran et al. 2006
Serratia	marcescens	Y	Kim et al. 2006
Shewanella	woodyi (strain ATCC 51908)		Copeland et al. 2008
Silicibacter	pomeroyi		Moran et al. 2004
Sinorhizobium	medicae (strain WSM419)		Copeland et al. 2007
Stackebrandtia	nassauensis DSM 44728		Lucas et al. 2009
Streptomyces	rochei	Y	Guo et al. 2009
Variovorax	paradoxus (strain S110)		Lucas et al. 2009
Verminephrobacter	eiseniae (strain EF01-2)	Y	Copeland et al. 2006
Xanthobacter	autotrophicus (strain ATCC BAA-1158)		Copeland et al. 2007
Xanthomonas	axonopodis pv. citri	Ps	daSilvia et al. 2002
	campestris pv. campestris	Ps	daSilvia et al. 2002
	campestris pv. campestris (strain B100)	Ps	Qian et al. 2005
	campestris pv. campestris (strain 8004)	Ps	Vorhoelter et al. 2008
	campestris pv. vesicatoria	Ps	Thieme et al. 2005
	oryzae pv. oryzae	Ps	Lee et al. 2005
	oryzae pv. oryzae (strain MAFF 311018)	Ps	Ochini et al. 2005
	oryzae pv. oryzae (strain PXO99A)	Ps	Salzberg et al. 2008

Alignment 1: Alignment of PqqC from *K. pneumoniae*, *M. extorquens*, *G. oxydans*, *R. aquatilis* and *S. rochei*. The sequence from M. extorquens is PqqC/D. The symbol * indicates that this residue is absolutely conserved between these five organisms. Residues that cluster into strongly related groups (STA, NEQK, NHQK, NDEQ, QHRK, MILV, MILF, HY, and FYW) are marked with a :, while a . symbol marks residues in more weakly related group (CSA, ATV, SAG, STNK, STPA, SGND, SNDEQK, NDEQHK, NEQHRK, FVLIM, and HFY).

```
----------MLITDTLSPQAFEEALRAKGAF-YHIHHPYHIAMHNGDAT
MTAQFPPPVPDTEQRLLSHEELEAALRDIGARRYHNLHPFHRLLHDGKLS
----MSMSVTREVAAPWSEAEFRQRLHALESS-YWDRHPFHRRMHEGLLD
------------MTLLTPDQLEAQLRQIGAERYHNRHPFHRKLHDGKLD
------MTTSSNRTSPMTPEAFEQALRAKGAF-YHIHHPYHIAMHNGQAT
                 :   :.  *:   :  *   **:*  :*:*

RKQIQGWVANRFYYQTTIPLKDAAIMANCPDAQTRRKWVQRILDHDGSHG
KDQVRAWALNRYYYQAMIPVKDAALLARLPDAQLRRIWRQRIVDHDGDHE
EGELRLWAANRWYYQRCLPQKDAAIVANCPLPEVRRQWLSRIVYHDGADA
KAQVQAWALNRYYYQARIPAKDATLLARLPTAELRREWRRRIEDHDGTEP
REQIQGWVANRFYYQTSIPLKDAAIMANCPDAQTRRKWVQRILDHDGYGG
. ::: *. **:***  :* ***:::*. * .: ** *  **  ***

EDGGIEAWLRLGEAVGLSRDDLLSERHVLPGVRFAVDAYLNFARRACWQE
GDGGIERWLKLAEGVGFTRDYVLSTKGILSATRFSVDAYVHFVSERSLLE
CAGGAEKWLRLAEAVGLRRDEVHDERLVLAGTRFAVDAYVDFARRRPWLE
GTGGVARWLMLTDGLGLDRDYVESLDGLLPATRFSVDAYVNFVRDQSILA
SEGGIEAWLRLGEAVGLDRDVLLSEERVLPGVRFAVDAYVNFARRAVWQE
  **   ** * :.:*: ** : .   :*...**:****:.*.

AACSSLTELFAPQIHQSRLDSWPQHYPWIKEEGYFYFRSRLSQANRDVEH
AIASSLTEMFSPTIISERVAGMLKNYDFITKDTLAYFDKRLTQAPRDADF
AAASGLTELFSPGLLAHRLGRLREHYPWIAEEGFEYFTARIEVVGPEGRS
AIASSLTELFSPTIISERVSGMLRHYDFVSEKTLAYFTPRLTQAPRDSDF
AACSSLTELFAPQIHQARLDTWPQHYKWIEEEGYGYFRSRLSQANRDVEH
* .*.***:*:* :   *:    .:* :: :.   **  *:  .  :

GLALAKAYCDSAEKQNRMLEILQFKLDILWSMLDAMTMAYALQRPPYHTV
ALDYVKRHATTPEMQRAAIDALTFKCNVLWTQLDALYFAYVAPGMVPPDA
LLDLVARHAVSREQQEACVRALAFKCRVLNAVLDSLDYHTGNGATRS---
ALAYVREKARTPEQQKEVLGALEFKCSVLWTMLDALDYAYVEG-HIPPGA
GLQLALEYCDTVEKQQRMLEILQFKLDILWSMLDAMSMAYELNRPPYHSV
 *  .   . : * *.  :  * **  :* : **::

TDKAAWHTTRLV-----------------------------------
WQPGEGLVAETNSAEDSPAAAASPAATTAEPTAFSGSDVPRLPRGVRLRF
-----------------------------------------------
FVP-------------------------------------------
TQQAVWHKGRLL-----------------------------------
```

```
--------------------------------------------------
DEVRNKHVLLAPERTFDLDDNAVAVLKLVDGRNTVSQIAQILGQTYDADP
--------------------------------------------------
--------------------------------------------------
--------------------------------------------------

----------------------
AIIEADILPMLAGLAQKRVLER
----------------------
----------------------
----------------------
```

Alignment 2: Alignment of PqqD from *K. pneumoniae*, *M. extorquens*, *G. oxydans*, *R. aquatilis* and *S. rochei*. The sequence from *M. extorquens* is PqqC/D. The symbol * indicates that this residue is absolutely conserved between these five organisms. Residues that cluster into strongly related groups (STA, NEQK, NHQK, NDEQ, QHRK, MILV, MILF, HY, and FYW) are marked with a :, while a . symbol marks residues in more weakly related group (CSA, ATV, SAG, STNK, STPA, SGND, SNDEQK, NDEQHK, NEQHRK, FVLIM, and HFY).

```
--------------------------------------------------
MTAQFPPPVPDTEQRLLSHEELEAALRDIGARRYHNLHPFHRLLHDGKLS
--------------------------------------------------
--------------------------------------------------
--------------------------------------------------

--------------------------------------------------
KDQVRAWALNRYYYQAMIPVKDAALLARLPDAQLRRIWRQRIVDHDGDHE
--------------------------------------------------
--------------------------------------------------
--------------------------------------------------

--------------------------------------------------
GDGGIERWLKLAEGVGFTRDYVLSTKGILSATRFSVDAYVHFVSERSLLE
--------------------------------------------------
--------------------------------------------------
--------------------------------------------------

--------------------------------------------------
AIASSLTEMFSPTIISERVAGMLKNYDFITKDTLAYFDKRLTQAPRDADF
--------------------------------------------------
--------------------------------------------------
--------------------------------------------------

--------------------------------------------------
ALDYVKRHATTPEMQRAAIDALTFKCNVLWTQLDALYFAYVAPGMVPPDA
--------------------------------------------------
--------------------------------------------------
```

```
-------------------------------------------------

--------------------------------MQKTSIVAFRRGYRLQW
WQPGEGLVAETNSAEDSPAAAASPAATTAEPTAFSGSDVPRLPRGVRLRF
-------------------------MTEAPHVVAEGTVLSFARGHRLQH
-----------------------------------------MFRRGYRMQF
-----------------------------MTGLPEPTVPRLRPGVRLTR
                                                :  * *:
EAAQESHVILYPEGMAKLNETAAAILELVDGRRDVAAIIAMLNERFPEAG
DEVRNKHVLLAPERTFDLDDNAVAVLKLVDGRNTVSQIAQILGQTYDADP
DRVRDVWIVQAPEKAFVVEGAAPHILRLLDGKRSVGEIIQQLAIEFSAPR
EKTQDCHVILYPEGMAKLNDSATFILQLVDGERTIANIIDELNARFPEAG
DPAR-GELALLPERVVVLNDTAAAVLAHCDGTTSLAGIVERLAEEYEG--
: .:   :   **    ::  *  :*   **   :. *   *   :

GVDDDVIEFLQIACQQKWITCREPE
AIIEADILPMLAGLAQKRVLER---
EVIAKDVLALLSELTEKNVLHT---
GVNDDVKDFFAQAHAQKWITFREPA
-VSAEDVRELLLRLAQRRVVDLHG-
 :       :     :: :
```

Alignment 3: PqqE sequences from *K. pneumoniae*, *M. extorquens*, *G. oxydans*, *R. aquatilis* and *S. rochei*. The symbol * indicates that this residue is absolutely conserved between these five organisms. Residues that cluster into strongly related groups (STA, NEQK, NHQK, NDEQ, QHRK, MILV, MILF, HY, and FYW) are marked with a :, while a . marks residues in more weakly related group (CSA, ATV, SAG, STNK, STPA, SGND, SNDEQK, NDEQHK, NEQHRK, FVLIM, and HFY).

```
----------------------MTLPSPPMSLLAELTHRCPLSCPYCSN
----------------------MDVIPAPVGLLAELTHRCPLRCPYCSN
------------------MSQSKPTVNPPLWLLAELTYRCPLQCPYCSN
MMTSKISSLRPMLKSGLPSVNLLKPAVKPPLWLLAELTYRCPLQCPYCSN
--------------------MADPAVGAPAGMLIELTHRCPLHCPYCSN
                             .*  :* ***:**** ******

PLELERKAAELDTATWTAVLEQAAELGVLQVHFSGGEPMARPDLVELVSV
PLELDRRSAELDTQTWLRVLTEAAGLGVLHVHLSGGEPTARPDIVEITAK
PLDFARQDKELTTEQWIEVFRQARAMGSVQLGFSGGEPLTRKDLPELIRA
PLDFAKQDKELTTAQWIKVFEEAREMGAVQIGFSGGEPLVRKDLPELIRA
PLELVRREAELTCEQWTDILTQARELGVVQMHFSGGEPLARPDLPDLVGH
**:: ::  **    *  :: :*  :* ::: :***** .* *: ::

ARRLNLYSNLITSGVLLDEPKLEALDRAGLDHIQLSFQDVTEAGAERIGG
CAELGLYSNLITSGVGGALAKLDALYDVGLDHVQLSVQGVDAANAEKIGG
ARDLGFYTNLITSGIGLTESKLDAFSEAGLDHIQISFQASDEVLNAALAG
ARDLGFYTNLITSGIGLTEKKIDAFAEAGLDHIQISFQASDETLNAALAG
ARRLGAYVNLVTSGVGLTAERAHDLARRGVDHVQLSLQDADPAAGQAIAG
```

```
.  *. * **:***:     : . :   *:**:*:*.*    .    :.*

LKGAQARKVAAARLIRASGIPMTLNFVVHRENVARIPEMFALARELGAGR
LKNAQPQKMQFAARVTELGLPLTLNSVIHRGNIHEVPGFIDLAVKLGAKR
NKKAFQQKLAMAKAVKARDYPMVLNFVLHRHNIDQLDKIIELCIELEADD
NAKAFRQKLEMAKAVKAHGYPMVLNFVLHRHNIDQIDKIIDLSIELEADD
AR-VHTAKLEAARAVTAAGLPLTVNIVLHRGNIDRTGRMVDLAVDLGADR
   .   *:  *  :   . *:.:* *:** *: .   :. *. .* *

VEIAHTQYYGWGLKNREALLPSRDQLEESTRAVEAERAKGG-----LSVD
LEVAHTQYYGWAYVNRAALMPDKSQVDESIRIVEAARERLKGQ---LVID
VELATCQFYGWAFLNREGLLPTREQIARAEQVVADYRQKMAASGNLTNLL
VELATCQFYGWAQLNREGLLPTREQIARAENVVHQYREKMAGTGNLANLL
IELANTQYYGWGLRNRAALMPTAAQLAAAREAVRHARTRYAGG---PELV
:*:*  *:***.  ** .*:*   *:  : . *   * :         :

YVTPDYHADRPKPCMGGWGQRFVNVTPSGRVLPCHAAEIIPDVAFPNVQD
LVVPDYYAKYPKACAGGWGRKLMNVTPQGKVLPCHAAETIPGLEFWYVTD
FVTPDYYEERPKGCMGGWGSIFLSVTPEGTALPCHSARQLP-VAFPSVLE
FVTPDYYEERPKGCMGGWGAIFLSVTPEGMALPCHSARQLP-VEFPSVLE
YVAADYYDDRPKPCMDGWGSTQLTVTPAGDVLPCPAAYAITTLPVENALR
 *..**: . ** * .***   :.*** * .*** :*  :. : .  .

VTLSEIWNISPLFNMFRGTDWMPEPCRSCERKERDWGGCRCQAMALTGNA
HALGEIWTKSPAFAAYRGTSWMKEPCRSCDRREKDWGGCRCQALALTGDA
QSLESIWYDSFGFNRYRGYDWMPEPCRSCDEKEKDFGGCRCQAFMLTGSA
NTLQEIWYDSFGFNKYRGFDWMPEPCRSCSEKEKDFGGCRCQAFMLTGNA
RPLSEIWYASRSFNAYRGTGWMREPCRTCPERHADHGGCRCQAFQLTGDA
 .* .**  *  *  :** .** ****:* .:. * *******: ***.*

ANTDPVCSLSPYHDRVEQAVENNMQPESTLFYRRYT--------------
ANTDPACSLSPLHAKMRDLAKEEAAETPPDYIYRSIGTNVQNPLSEKAPL
DNADPVCSKSPHHHKILEARREAACSDIKVSQLQFRNRTRSQLIYQTRDL
DNADPVCSKSEHHGKIVAAREQANCTNIQINQLQFRNRANSQLIFKG---
AATDPACGLSPHRSLVDAALAEVTDGPVPAFVPRGPVPA-----------
  :**.*. *  :  :     :           :
```

References

Chapter 1

1. Hauge, J. G. Glucose dehydrogenase from Bacterium antiratum: An enzyme with a novel prosthetic group. J. Biol. Chem. 239, 3630 (1964).
2. Salisbury, S. A., Forrest, H.A., Cruse, W.B.T., and Kennard, O. A novel coenzyme from bacterial primary alcohol dehydrogenases. Nature 280, 843 (1979).
3. Kawai, F., Yamanaka, H., Ameyama, M., Shinagawa, E., Matsushita, K., and Adachi, O. Identification of the prosthetic group and further characterization of a novel enzyme, polyethylene glycol dehydrogenase. Agri. Biol. Chem. 49, 1071 (1985).
4. Shimoa, M., Ninomiya, K., Kuno, O., Kato, N., and Sakazawa, C. Pyrroloquinoline quinone as an essential growth factor for a polyvinyl alcohol-degrading symbiont, Pseudomonas sp. VM15C. Appl. Environ. Microbiol. 51, 268 (1986).
5. Ameyama, M., Shinagawa, E., Matsishita, K., and Adachi, O. Solubilization, purification, and properties of a membrande-bound glycerol dehydrogenase from Gluconobacter industrius. Agri. Biol. Chem. 49, 1001 (1985).
6. van Kleef, M. A. G., and Duine, J.A. Bacterial NAD(P)-independent quinate dehydrogenase is a quinoprotein. Arch. Microbiol. 150, 132 (1988).
7. Duine, J. A., and Frank, J. Quinoproteins: A novel class of dehydrogenases. Trends Biochem. Sci. 6, 278 (1981).
8. Nagasawa, T., and Yamada, H. Nitrile hydratase is a quinoprotein. Biochim. Biophys. Res. Commun. 147, 701 (1987).
9. Houck, D. R., Hanners, J. L., Unkefer, C. J., Vankleef, M. A. G. & Duine, J. A. PQQ – biosynthetic-studies in Methylobacterium-AM1 and Hyphomicrobium-X using specific C-13 labeling and NMR. Antonie Van Leeuwenhoek Journal of Microbiology 56, 93-101 (1989).
10. James, S. M., Mu, D., Wemmer, D., Smith, A.J., Kaur, S., Burlingfame, A.L., and Klinman J.P. A new redox cofactor in eukaryotic enzymes: 6-Hydroxydopa at the active site of bovine serum amine oxidase. Science 248, 981 (1990).
11. DuBois, J. L. & Klinman, J. P. Mechanism of post-translational quinone formation in copper amine oxidases and its relationship to the catalytic turnover. Archives of Biochemistry and Biophysics 433, 255-265 (2005).
12. Klinman, J. P. & Mu, D. Quinoenzymes in Biology. Annual Review of Biochemistry 63, 299-344 (1994).
13. Cai, D. Y. & Klinman, J. P. Evidence for a self catalytic mechanism of 2,4,5-trihydroxyphenylalanine quinone biogenesis in yeast amine oxidase. Journal of Biological Chemistry 269, 32039-32042 (1994).
14. Mu, D. et al. Tyrosine codon corresponds to topa quinone at the active-site of copper amine oxidases. Journal of Biological Chemistry 267, 7979-7982 (1992).
15. Mu, D. et al. Primary structure for a mammalian cellular and serum copper amine oxidase. Journal of Biological Chemistry 269, 9926-9932 (1994).
16. McIntire, W. S., Wemmer, D.E., Christoserdov, A.Y., Lidstrom, M.E. A new cofactor in the prokaryotic enzyme: Tryptophan tryptophylquinone as the redox prosthetic group in methylamine dehydrogenase. Science 252, 817 (1991).

17. de Beer, R., Duine, J.A., Frank, J., Large, P.J. The Prosthetic Group of Methylamine Dehydrogenase EC-1.4.99 from Pseudomonas AM-1: Evidence for a Quinone Structure. Biochima et Biophysica Acta 622, 370-374 (1980).
18. Pearson, A. R. et al. Further insights into quinone cofactor biogenesis: Probing the role of mauG in methylamine dehydrogenase tryptophan tryptophylquinone formation. Biochemistry 43, 5494-5502 (2004).
19. Pearson, A. R. et al. Understanding quinone cofactor biogenesis in methylamine dehydrogenase through novel cofactor generation. Biochemistry 42, 3224-3230 (2003).
20. Jensen, L. M. R., Sanishvili, R., Davidson, V. L. & Wilmot, C. M. In Crystallo Posttranslational Modification Within a MauG/Pre-Methylamine Dehydrogenase Complex. Science 327, 1392-1394.
21. Oubrie, A. Structure and mechanism of soluble glucose dehydrogenase and other PQQ-dependent enzymes. Biochimica Et Biophysica Acta-Proteins and Proteomics 1647, 143-151 (2003).
22. Kissel, J., Krueger, F. R., Silen, J. & Clark, B. C. The Cometary and Interstellar Dust Analyzer at Comet 81P/Wild 2. Science 304, 1774-1776 (2004).
23. Krueger, F. R., Werther, W., Kissel, J. & Schmid, E. R. Assignment of quinone derivatives as the main compound class composing 'interstellar' grains based on both polarity ions detected by the "Cometary and Interstellar Dust Analyser' WIDA) onboard the spacecraft STARDUST. Rapid Communications in Mass Spectrometry 18, 103-111 (2004).
24. Arakawa, K., Sugino, F., Kodama, K., Ishii, T. & Kinashi, H. Cyclization mechanism for the synthesis of macrocyclic antibiotic lankacidin in Streptomyces rochei. Chemistry & Biology 12, 249-256 (2005).
25. Anthony, C. The quinoprotein dehydrogenases for methanol and glucose. Archives of Biochemistry and Biophysics 428, 2-9 (2004).
26. Kasahara, T. & Kato, T. A new redox-cofactor vitamin for mammals. Nature 422, 832-832 (2003).
27. Rucker, R., Storms, D., Sheets, A., Tchaparian, E. & Fascetti, A. Is pyrroloquinoline quinone a vitamin? Nature 433, E10-E11 (2005).
28. Felton, L. M. & Anthony, C. Role of PQQ as a mammalian enzyme cofactor? Nature 433, E10-E10 (2005).
29. Chen, Z. W. et al. Structure at 1.9 angstrom resolution of a quinohemoprotein alcohol dehydrogenase from Pseudomonas putida HK5. Structure 10, 837-849 (2002).
30. Oubrie, A. et al. Structure and mechanism of soluble quinoprotein glucose dehydrogenase. Embo Journal 18, 5187-5194 (1999).
31. Stites, T. E., Mitchell, A.E, Rucker, R.B. Physiological importance of quinoenzymes and the O-quinone family of cofactors. J. Nutr. 130, 719-727 (2000).
32. Choi, O., Kim, J., Kim, J.G. et al. . Pyrroloquinoline quinone is a plant growth promotion factor produced by Pseudomonas fluorescens B16. Plant Physiol. 146, 657-668 (2008).
33. Kumazawa, T., Sato, K., Seno, H., et al. Levels of pyrroloquinoline quinone in various foods. Biochem. J. 307, 331-333 (1995).
34. Steinberg, F. M., Gershwin, M.E., Rucker, R.B. Dietary pyrroloquinoline quinone: growth and immune response in BALB/c mice. J. Nutr. 124, 744-753 (1994).
35. Urakami, T. (USA, 1994).
36. Tsuji, T., Yamaguchi, K., Kondo, K., Urakami, T., . (USA, 1998).

37. Watanabe, A., Hobara, N., Ohsawa, T., et al. Nephrotoxicity of pyrroloquinoline quinone in rats. Hiroshima J. Med. Sci. 38, 49-51 (1989).
38. Kumazawa, T., Sato, K., Seno, H., Ishii, A. & Suzuki, O. Levels of Pyrroloquinoline quinone in various foods. Biochemical Journal 307, 331-333 (1995).
39. Choi, O. et al. Pyrroloquinoline quinone is a plant growth promotion factor produced by Pseudomonas fluorescens B16. Plant Physiology 146, 657-668 (2008).
40. Babukhan, S. et al. Cloning of a mineral phosphate-solubilizing gene from Pseudomonas cepacia. Applied and Environmental Microbiology 61, 972-978 (1995).
41. Meulenberg, J. J. M. et al. Cloning of Klebsiella pneumoniae PQQ genes and PQQ biosynthesis in Eschericia coli. Fems Microbiology Letters 71, 337-344 (1990).
42. Meulenberg, J. J. M., Sellink, E., Riegman, N. H. & Postma, P. W. Nucleotide sequence and structure of the Klebsiella pneumoniae PQQ operon. Molecular & General Genetics 232, 284-294 (1992).
43. Velterop, J. S., Sellink, E., Meulenberg, J.J., David, S., Bulder, I., and Postma, P.W. Synthesis of pyrroloquinoline quinone in vivo and in vitro and detection of an intermediate in the biosynthetic pathway. J. Bacteriol. 177, 5088-5098 (1995).
44. Vuilleumier, S. et al. Methylobacterium Genome Sequences: A Reference Blueprint to Investigate Microbial Metabolism of C1 Compounds from Natural and Industrial Sources. Plos One 4 (2009).
45. Magnusson, O. T., RoseFigura, J. M., Toyama, H., Schwarzenbacher, R. & Klinman, J. P. Pyrroloquinoline quinone biogenesis: Characterization of PqqC and its H84N and H84A active site variants. Biochemistry 46, 7174-7186 (2007).
46. Magnusson, O. T. et al. Quinone biogenesis: Structure and mechanism of PqqC, the final catalyst in the production of pyrroloquinoline quinone. Proceedings of the National Academy of Sciences of the United States of America 101, 7913-7918 (2004).
47. Magnusson, O. T., Toyama, H., Saeki, M., Schwarzenbacher, R. & Klinman, J. P. The structure of a biosynthetic intermediate of pyrroloquinoline quinone (PQQ) and elucidation of the final step of PQQ biosynthesis. Journal of the American Chemical Society 126, 5342-5343 (2004).
48. Schwarzenbacher, R., Stenner-Liewen, F., Liewen, H., Reed, J. C. & Liddington, R. C. Crystal structure of PqqC from Klebsiella pneumoniae at 2.1 A resolution. Proteins-Structure Function and Bioinformatics 56, 401-403 (2004).
49. Colloc'h, N. et al. Oxygen pressurized X-ray crystallography: Probing the dioxygen binding site in cofactorless urate oxidase and implications for its catalytic mechanism. Biophysical Journal 95, 2415-2422 (2008).
50. Fetzner, S. & Steiner, R. A. Cofactor-independent oxidases and oxygenases. Applied Microbiology and Biotechnology 86, 791-804.
51. Phillips, J. D. et al. Crystal structure of the oxygen-dependant coproporphyrinogen oxidase (Hem13p) of Saccharomyces cerevisiae. Journal of Biological Chemistry 279, 38960-38968 (2004).
52. Lee, D. S. et al. Structural basis of hereditary coproporphyria. Proceedings of the National Academy of Sciences of the United States of America 102, 14232-14237 (2005).
53. Kahn, K. & Tipton, P. A. Spectroscopic characterization of intermediates in the urate oxidase reaction. Biochemistry 37, 11651-11659 (1998).

54. Gabison, L. et al. Structural analysis of urate oxidase in complex with its natural substrate inhibited by cyanide: Mechanistic implications. Bmc Structural Biology 8, 8 (2008).
55. Fetzner, S. Oxygenases without requirement for cofactors or metal ions. Applied Microbiology and Biotechnology 60, 243-257 (2002).
56. Shen, B. & Hutchinson, C. R. Tetracenomycin F1 monooxygenase oxidation of a napthacenone to a napthacenequinone in the biosynthesis of tetracenomycin-C in Streptomyces-glaucensens. Biochemistry 32, 6656-6663 (1993).
57. Rafanan, E. R., Le, L., Zhao, L. L., Decker, H. & Shen, B. Cloning, sequencing, and heterologous expression of the elmGHIJ genes involved in the biosynthesis of the polyketide antibiotic elloramycin from Streptomyces olivaceus Tu2353. Journal of Natural Products 64, 444-449 (2001).
58. Qi, R., Fetzner, S. & Oakley, A. J. Crystallization and diffraction data of 1H-3-hydroxy-4-oxoquinoline 2,4-dioxygenase: a cofactor-free oxygenase of the alpha/beta-hydrolase family. Acta Crystallographica Section F-Structural Biology and Crystallization Communications 63, 378-381 (2007).
59. Steiner, R. A., Frerichs-Deeken, U. & Fetzner, S. Crystallization and preliminary X-ray analysis of 1H-3-hydroxy-4-oxoquinaldine 2,4-dioxygenase from Arthrobacter nitroguajacolicus Ru61a: a cofactor-devoid dioxygenase of the alpha/beta-hydrolase-fold superfamily. Acta Crystallographica Section F-Structural Biology and Crystallization Communications 63, 382-385 (2007).

Chapter 2

1. Schwarzenbacher, R., Stenner-Liewen, F., Liewen, H., Reed, J. C. & Liddington, R. C. Crystal structure of PqqC from Klebsiella pneumoniae at 2.1 A resolution. Proteins-Structure Function and Bioinformatics 56, 401-403 (2004).
2. Toyama, H., Chistoserdova, L. & Lidstrom, M. E. Sequence analysis of pqq genes required for biosynthesis of pyrroloquinoline quinone in Methylobacterium extorquens AM1 and the purification of a biosynthetic intermediate. Microbiology-Uk 143, 595-602 (1997).
3. Velterop, J. S., Sellink, E., Meulenberg, J.J., David, S., Bulder, I., and Postma, P.W. Synthesis of pyrroloquinoline quinone in vivo and in vitro and detection of an intermediate in the biosynthetic pathway. J. Bacteriol. 177, 5088-5098 (1995).
4. Magnusson, O. T. et al. Quinone biogenesis: Structure and mechanism of PqqC, the final catalyst in the production of pyrroloquinoline quinone. Proceedings of the National Academy of Sciences of the United States of America 101, 7913-7918 (2004).
5. Magnusson, O. T., Toyama, H., Saeki, M., Schwarzenbacher, R. & Klinman, J. P. The structure of a biosynthetic intermediate of pyrroloquinoline quinone (PQQ) and elucidation of the final step of PQQ biosynthesis. Journal of the American Chemical Society 126, 5342-5343 (2004).
6. Duine, J. A., Frank, J., and Jongejan, J.A. Enzymology of quinoproteins. Adv. Enzymology 59, 170-212 (1987).
7. Meulenberg, J. J. M., Sellink, E., Riegman, N. H. & Postma, P. W. Nucleotide sequence and structure of the Klebsiella pneumoniae PQQ operon. Molecular & General Genetics 232, 284-294 (1992).
8. Fetzner, S. Oxygenases without requirement for cofactors or metal ions. Applied Microbiology and Biotechnology 60, 243-257 (2002).

9. Colloc'h, N. et al. Oxygen pressurized X-ray crystallography: Probing the dioxygen binding site in cofactorless urate oxidase and implications for its catalytic mechanism. Biophysical Journal 95, 2415-2422 (2008).
10. Fischer, F. & Fetzner, S. Site-directed mutagenesis of potential catalytic residues in 1H-3-hydroxy-4-oxoquinoline 2,4-dioxygenase, and hypothesis on the catalytic mechanism of 2,4-dioxygenolytic ring cleavage. Fems Microbiology Letters 190, 21-27 (2000).
11. Qi, R., Fetzner, S. & Oakley, A. J. Crystallization and diffraction data of 1H-3-hydroxy-4-oxoquinoline 2,4-dioxygenase: a cofactor-free oxygenase of the alpha/beta-hydrolase family. Acta Crystallographica Section F-Structural Biology and Crystallization Communications 63, 378-381 (2007).
12. Steiner, R. A., Frerichs-Deeken, U. & Fetzner, S. Crystallization and preliminary X-ray analysis of 1H-3-hydroxy-4-oxoquinaldine 2,4-dioxygenase from Arthrobacter nitroguajacolicus Ru61a: a cofactor-devoid dioxygenase of the alpha/beta-hydrolase-fold superfamily. Acta Crystallographica Section F-Structural Biology and Crystallization Communications 63, 382-385 (2007).
13. Sciara, G. et al. The structure of ActVA-Orf6, a novel type of monooxygenase involved in actinorhodin biosynthesis. Embo Journal 22, 205-215 (2003).
14. Nabiullin, A. A., Fedoreev, S.A., and Deshko, T.N. Circular dichroism of quinoid pigments from Far Eastern representatives of the family Boraginaceae. Chemistry of Natural Compounds 19, 532-537 (1984).
15. DuBois, J. L. & Klinman, J. P. Role of a strictly conserved active site tyrosine in cofactor genesis in the copper amine oxidase from Hansenula polymorpha. Biochemistry 45, 3178-3188 (2006).
16. Dekker, R. H. et al. Covalent addition of H2O, enzyme substrates and activator to Pyrroloquinoline quinone, the coenzyme of quinoproteins. European Journal of Biochemistry 125, 69-73 (1982).
17. Magnusson, O. T., RoseFigura, J. M., Toyama, H., Schwarzenbacher, R. & Klinman, J. P. Pyrroloquinoline quinone biogenesis: Characterization of PqqC and its H84N and H84A active site variants. Biochemistry 46, 7174-7186 (2007).

Chapter 3

1. Anthony, C. Pyrroloquinoline quinone (PQQ) and quinoprotein enzymes. Antioxidants & Redox Signaling 3, 757-774 (2001).
2. Goodwin, P. M. & Anthony, C. in Advances in Microbial Physiology, Vol 40 1-80 (1998).
3. He, K., Nukada, H., Urakami, T. & Murphy, M. P. Antioxidant and pro-oxidant properties of pyrroloquinoline quinone (PQQ): implications for its function in biological systems. Biochemical Pharmacology 65, 67-74 (2003).
4. Magnusson, O. T., Toyama, H., Saeki, M., Schwarzenbacher, R. & Klinman, J. P. The structure of a biosynthetic intermediate of pyrroloquinoline quinone (PQQ) and elucidation of the final step of PQQ biosynthesis. Journal of the American Chemical Society 126, 5342-5343 (2004).
5. Magnusson, O. T. et al. Quinone biogenesis: Structure and mechanism of PqqC, the final catalyst in the production of pyrroloquinoline quinone. Proceedings of the National Academy of Sciences of the United States of America 101, 7913-7918 (2004).

6. Magnusson, O. T., RoseFigura, J. M., Toyama, H., Schwarzenbacher, R. & Klinman, J. P. Pyrroloquinoline quinone biogenesis: Characterization of PqqC and its H84N and H84A active site variants. Biochemistry 46, 7174-7186 (2007).
7. Colloc'h, N. et al. Oxygen pressurized X-ray crystallography: Probing the dioxygen binding site in cofactorless urate oxidase and implications for its catalytic mechanism. Biophysical Journal 95, 2415-2422 (2008).
8. Gabison, L. et al. Structural analysis of urate oxidase in complex with its natural substrate inhibited by cyanide: Mechanistic implications. Bmc Structural Biology 8, 8 (2008).
9. Schwarzenbacher, R., Stenner-Liewen, F., Liewen, H., Reed, J. C. & Liddington, R. C. Crystal structure of PqqC from Klebsiella pneumoniae at 2.1 A resolution. Proteins-Structure Function and Bioinformatics 56, 401-403 (2004).
10. Olsthoorn, A. J. J. & Duine, J. A. Production, characterization, and reconstitution of recombinant quinoprotein glucose dehydrogenase (soluble type; EC 1.1.99.17) apoenzyme of Acinetobacter calcoaceticus. Archives of Biochemistry and Biophysics 336, 42-48 (1996).

Chapter 4

1. Anthony, C. Pyrroloquinoline quinone (PQQ) and quinoprotein enzymes. Antioxidants & Redox Signaling 3, 757-774 (2001).
2. Goodwin, P. M. & Anthony, C. in Advances in Microbial Physiology, Vol 40 1-80 (1998).
3. He, K., Nukada, H., Urakami, T. & Murphy, M. P. Antioxidant and pro-oxidant properties of pyrroloquinoline quinone (PQQ): implications for its function in biological systems. Biochemical Pharmacology 65, 67-74 (2003).
4. Duine, J. A. The PQQ story. Journal of Bioscience and Bioengineering 88, 231-236 (1999).
5. Houck, D. R., Hanners, J. L. & Unkefer, C. J. Biosynthesis of Pyrroloquinoline quinone .2. Biosynthetic assembly from glutamate and tyrosine. Journal of the American Chemical Society 113, 3162-3166 (1991).
6. Houck, D. R., Hanners, J. L., Unkefer, C. J., Vankleef, M. A. G. & Duine, J. A. PQQ – biosynthetic-studies in Methylobacterium-AM1 and Hyphomicrobium-X using specific C-13 labeling and NMR. Antonie Van Leeuwenhoek Journal of Microbiology 56, 93-101 (1989).
7. Magnusson, O. T., Toyama, H., Saeki, M., Schwarzenbacher, R. & Klinman, J. P. The structure of a biosynthetic intermediate of pyrroloquinoline quinone (PQQ) and elucidation of the final step of PQQ biosynthesis. Journal of the American Chemical Society 126, 5342-5343 (2004).
8. Magnusson, O. T. et al. Quinone biogenesis: Structure and mechanism of PqqC, the final catalyst in the production of pyrroloquinoline quinone. Proceedings of the National Academy of Sciences of the United States of America 101, 7913-7918 (2004).
9. Magnusson, O. T., RoseFigura, J. M., Toyama, H., Schwarzenbacher, R. & Klinman, J. P. Pyrroloquinoline quinone biogenesis: Characterization of PqqC and its H84N and H84A active site variants. Biochemistry 46, 7174-7186 (2007).

10. Schwarzenbacher, R., Stenner-Liewen, F., Liewen, H., Reed, J. C. & Liddington, R. C. Crystal structure of PqqC from Klebsiella pneumoniae at 2.1 A resolution. Proteins-Structure Function and Bioinformatics 56, 401-403 (2004).
11. Nabiullin, A. A., Fedoreev, S.A., and Deshko, T.N. Circular dichroism of quinoid pigments from Far Eastern representatives of the family Boraginaceae. Chemistry of Natural Compounds 19, 532-537 (1984).

Chapter 5

1. Anthony, C. Pyrroloquinoline quinone (PQQ) and quinoprotein enzymes. Antioxidants & Redox Signaling 3, 757-774 (2001).
2. Rucker, R., Chowanadisai, W. & Nakano, M. Potential Physiological Importance of Pyrroloquinoline Quinone. Alternative Medicine Review 14, 268-277 (2009).
3. Anthony, C. The quinoprotein dehydrogenases for methanol and glucose. Archives of Biochemistry and Biophysics 428, 2-9 (2004).
4. Goodwin, P. M. & Anthony, C. in Advances in Microbial Physiology, Vol 40 1-80 (1998).
5. Matsushita, K., Arents, J.C., Bader, R., et al. Escherichia coli is unable to produce pyrroloquinoline quinone (PQQ). Microbiology 143, 3149-3156 (1997).
6. Kasahara, T. & Kato, T. A new redox-cofactor vitamin for mammals. Nature 422, 832-832 (2003).
7. Rucker, R., Storms, D., Sheets, A., Tchaparian, E. & Fascetti, A. Is pyrroloquinoline quinone a vitamin? Nature 433, E10-E11 (2005).
8. Felton, L. M. & Anthony, C. Role of PQQ as a mammalian enzyme cofactor? Nature 433, E10-E10 (2005).
9. Meulenberg, J. J. M. et al. Cloning of Klebsiella pneumoniae PQQ genes and PQQ biosynthesis in Eschericia coli. Fems Microbiology Letters 71, 337-344 (1990).
10. Meulenberg, J. J. M., Sellink, E., Riegman, N. H. & Postma, P. W. Nucleotide sequence and structure of the Klebsiella pneumoniae PQQ operon. Molecular & General Genetics 232, 284-294 (1992).
11. Toyama, H., Chistoserdova, L. & Lidstrom, M. E. Sequence analysis of pqq genes required for biosynthesis of pyrroloquinoline quinone in Methylobacterium extorquens AM1 and the purification of a biosynthetic intermediate. Microbiology-Uk 143, 595-602 (1997).
12. Velterop, J. S. et al. Synthesis of Pyrroloquinoline quinone in vivo and in vitro and detection of an intermediate in the biosynthetic pathway. Journal of Bacteriology 177, 5088-5098 (1995).
13. Magnusson, O. T., RoseFigura, J. M., Toyama, H., Schwarzenbacher, R. & Klinman, J. P. Pyrroloquinoline quinone biogenesis: Characterization of PqqC and its H84N and H84A active site variants. Biochemistry 46, 7174-7186 (2007).
14. Magnusson, O. T. et al. Quinone biogenesis: Structure and mechanism of PqqC, the final catalyst in the production of pyrroloquinoline quinone. Proceedings of the National Academy of Sciences of the United States of America 101, 7913-7918 (2004).
15. Gabison, L. et al. Structural analysis of urate oxidase in complex with its natural substrate inhibited by cyanide: Mechanistic implications. Bmc Structural Biology 8, 8 (2008).

16. Wecksler, S. R. et al. Pyrroloquinoline Quinone Biogenesis: Demonstration That PqqE from Klebsiella pneumoniae Is a Radical S-Adenosyl-L-methionine Enzyme. Biochemistry 48, 10151-10161 (2009).
17. Vuilleumier, S. et al. Methylobacterium Genome Sequences: A Reference Blueprint to Investigate Microbial Metabolism of C1 Compounds from Natural and Industrial Sources. Plos One 4 (2009).
18. Holscher, T. & Gorisch, H. Knockout and overexpression of pyrroloquinoline quinone biosynthetic genes in Gluconobacter oxydans 621H. Journal of Bacteriology 188, 7668-7676 (2006).
19. Prust, C. et al. Complete genome sequence of the acetic acid bacterium Gluconobacter oxydans. Nature Biotechnology 23, 195-200 (2005).
20. Guo, Y. B. et al. Mutations That Disrupt Either the pqq or the gdh Gene of Rahnella aquatilis Abolish the Production of an Antibacterial Substance and Result in Reduced Biological Control of Grapevine Crown Gall. Applied and Environmental Microbiology 75, 6792-6803 (2009).
21. Arakawa, K., Sugino, F., Kodama, K., Ishii, T. & Kinashi, H. Cyclization mechanism for the synthesis of macrocyclic antibiotic lankacidin in Streptomyces rochei. Chemistry & Biology 12, 249-256 (2005).
22. Kinashi, H., Fujii, S., Hatani, A., Kurokawa, T. & Shinkawa, H. Physical mapping of the linear plasmid pSLA2-L and localization of the eryAI and actI homologs. Bioscience Biotechnology and Biochemistry 62, 1892-1897 (1998).
23. Velterop, J. S., Sellink, E., Meulenberg, J.J., David, S., Bulder, I., and Postma, P.W. Synthesis of pyrroloquinoline quinone in vivo and in vitro and detection of an intermediate in the biosynthetic pathway. J. Bacteriol. 177, 5088-5098 (1995).
24. Glanville, J. G., Kirshner, D., Krishnamurthy, N. & Sjolander, K. Berkeley Phylogenomics Group web servers: resources for structural phylogenomic analysis. Nucleic Acids Research 35, W27-W32 (2007).
25. Krishnamurthy, N., Brown, D. & Sjolander, K. FlowerPower: clustering proteins into domain architecture classes for phylogenomic inference of protein function. Bmc Evolutionary Biology 7 (2007).
26. Sander, C., Schneider, R. Database of homology-derived protein structures and the structural meaning of sequence alignment. Proteins-Structure Function and Bioinformatics 9, 56-68 (1991).
27. Toyama, H. et al. PqqC/D, which converts a biosynthetic intermediate to pyrroloquinoline quinone. Biochemical and Biophysical Research Communications 299, 268-272 (2002).
28. Podschun, R. & Ullmann, U. Klebsiella spp. as nosocomial pathogens: Epidemiology, taxonomy, typing methods, and pathogenicity factors. Clinical Microbiology Reviews 11, 589-+ (1998).
29. King, G. M. Ecological aspects of methane oxidation, a key determination of global methane dynamics. Advances in Microbial Ecology 12, 431-468 (1992).
30. McDonald, I. R. et al. A review of bacterial methyl halide degradation: biochemistry, genetics and molecular ecology. Environmental Microbiology 4, 193-203 (2002).
31. Gupta, A., Singh, V. K., Qazi, G. N. & Kumar, A. Gluconobacter oxydans: Its biotechnological applications. Journal of Molecular Microbiology and Biotechnology 3, 445-456 (2001).

32. Verma, V., Qazi, P., Cullum, J. & Qazi, G. N. Genetic heterogeneity among keto-acid-producing strains of Gluconobacter oxydans. World Journal of Microbiology & Biotechnology 13, 289-294 (1997).
33. Harrell, L. J., Cameron, M. L. & Ohara, C. M. Rahnella aquitilis, an unusual Gram negative rod isolated from the bronchial washings of a patient with acquired immunodeficiency syndrome. Journal of Clinical Microbiology 27, 1671-1672 (1989).
34. Lima, T. et al. HAMAP: a database of completely sequenced microbial proteome sets and manually curated microbial protein families in UniProtKB/Swiss-Prot. Nucleic Acids Research 37, D471-D478 (2009).
35. Choi, O. et al. Pyrroloquinoline quinone is a plant growth promotion factor produced by Pseudomonas fluorescens B16. Plant Physiology 146, 657-668 (2008).
36. Chowanadisai, W., Bauerly, K., Tchaparian, E. & Rucker, R. B. A1104-A1104 (2007).

Appendix: Modeling of PqqC reaction.

Since PqqC mutants were seen to be capable of stopping reaction at the first oxidation or forming PQQ, the order of the steps of the mechanism are still unclear. X-ray crystallography has indicated that attack of the primary amine of AHQQ to form the five-membered ring is the first step of the PqqC reaction. The remaining three steps were modeled to try and indicate the order of the reactions. This was done Kun Zhang for her senior thesis. The project was started by building the all the possible intermediates of the PqqC reaction in the program Maestro (Fig. 1). All possible intermediates mechanistically occur after the product of the first step, which is a unoxidized tricycle intermediate. These intermediates were fit into the active site of PqqC, using the crystal structure (1OTW) with PQQ removed from the structure. Structures were docked into the PqqC active site using the program Glide and docking scores were determined (Table 1). These show that all the intermediates are viable binders. In agreement with the X-ray crystal structure, the binding data indicates that the C9 position of these molecules is in the S configuration, rather than the R configuration. The distances between the active site side chains and the various intermediates (Table 2). Next the program Gaussian was used to do frequency calculations to measure the energy values of the various intermediates (Figure 2).

Figure 1: The 12 possible intermediates in the last three steps of the PqqC reaction.

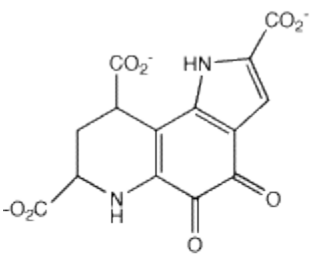

Intermediate 1

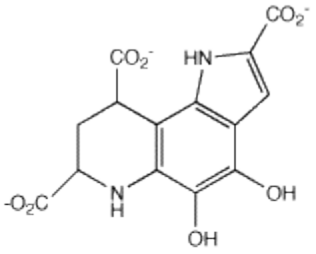

Intermediate 2

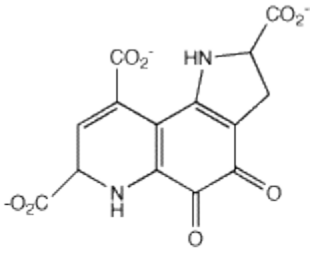

Intermediate 3

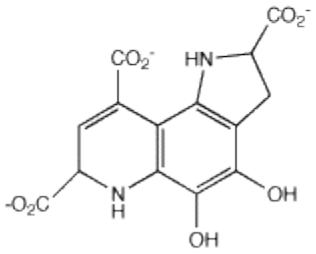

Intermediate 4

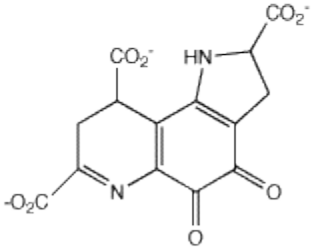

Intermediate 5

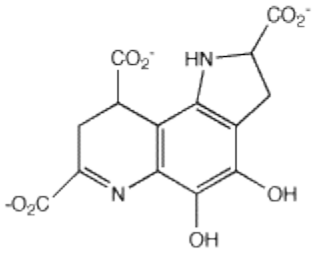

Intermediate 6

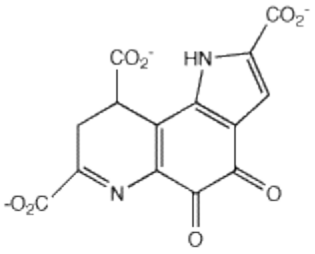

Intermediate 7

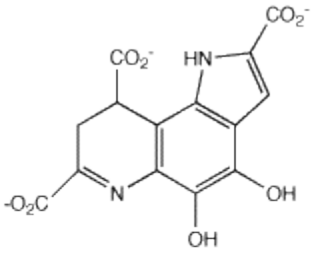

Intermediate 8

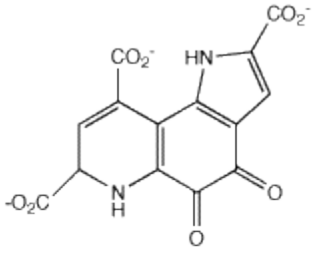

Intermediate 9

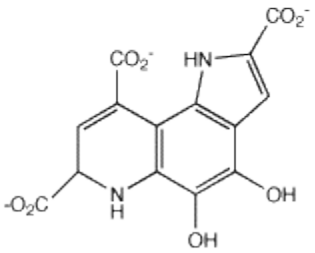

Intermediate 10

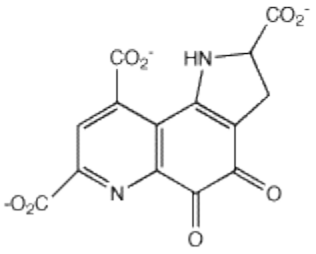

Intermediate 11

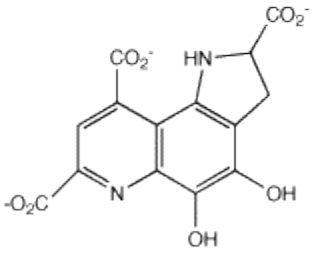

Intermediate 12

Table 1: Docking scores in kcal/mol for all 14 structures.

	Docking Score (kcal/mol)		Docking Score (kcal/mol)
Intermediate 1	-14.098	Intermediate 7	-12.802
Intermediate 2	-12.741	Intermediate 8	-11.384
Intermediate 3	-12.768	Intermediate 9	-12.953
Intermediate 4	-11.795	Intermediate 10	-11.815
Intermediate 5	-11.415	Intermediate 11	-13.646
Intermediate 6	-10.169	Intermediate 12	-11.971
Tri-cyclic intermediate (C9S)	-14.116	Tri-cyclic intermediate (C9R)	-13.051

PQQ	-13.000		

Table 2: The distance in Angstroms between active site residues side chain atoms and C3, N6 or C9 of bound ligand (PQQ). The top row is the ligand, either PQQ, the tricyclic compound (TC) or intermediates 1-12.

	PQQ	1	2	3	4	5	6	7	8	9	10	11	12	TC
Y23 O-C9	3.800	3.503	3.543	3.825	3.771	3.878	3.908	3.614	3.501	3.708	3.764	3.845	3.777	3.255
H24 N-C9	5.058	5.166	5.197	5.242	5.216	5.685	5.722	5.343	5.030	5.035	5.205	5.051	5.067	5.217
H24 N-	5.777	5.826	5.826	5.742	5.784	5.550	5.674	5.695	5.662	5.640	5.830	5.672	5.590	5.664
R50 N-N6	3.311	3.608	3.647	3.206	3.179	3.119	3.103	3.061	3.095	3.115	3.251	3.118	3.066	3.121
Y53 O-C3	4.766	4.394	4.435	4.820	4.732	4.842	4.820	4.636	4.491	4.479	4.568	4.811	4.647	4.658
Q54 N-C3	6.138	5.852	5.862	6.067	5.789	6.031	5.925	5.962	5.867	5.666	5.733	5.907	5.830	5.5791
Q54 N-N6	5.597	5.849	5.852	5.478	5.513	5.481	5.421	5.477	5.579	5.611	5.543	5.562	5.518	5.576
R157 N-N6	5.549	5.436	5.505	5.714	5.510	5.903	5.894	5.538	5.387	5.374	5.495	5.453	5.450	5.405
K60 N-C3	5.613	5.638	5.609	5.409	5.645	5.347	5.410	5.586	5.698	5.743	5.667	5.690	5.659	5.710
D61 C-C3	6.978	6.987	6.943	6.648	6.843	6.550	6.588	6.883	7.027	7.005	6.910	6.911	6.910	7.052
R80 N-C3	5.686	6.099	6.061	5.655	5.940	5.660	5.758	5.867	6.042	6.195	6.079	5.927	5.963	6.010
H84 N-C3	5,236	5.188	5.166	5.091	4.933	5.030	4.955	5.138	5.161	4.998	4.986	5.010	5.026	4.881
Y128 O-C3	5.868	5.781	5.780	5.794	5.975	5.782	5.841	5.823	5.861	5.944	5.922	6.006	5.927	6.028
T146 O-C9	4.586	4.656	4.571	4.568	4.672	4.499	4.569	4.652	4.710	4.728	4.682	4.724	4.730	4.945
H154 N-N6	3.337	2.974	3.026	3.636	3.381	4.106	3.883	3.569	3.400	3.390	3.278	3.448	3.470	3.247
Y175 O-N6	4.940	5.001	5.009	4.959	4.904	5.186	4.973	4.973	5.008	5.034	4.876	5.001	4.940	4.897
R179	3.84	4.24	4.23	4.00	4.00	4.06	4.08	4.03	4.11	4.19	4.14	3.84	4.03	3.99

N-C3	9	8	2	5	1	7	1	8	0	2	3	4	1	2
K214 N-C9	5.367	5.369	5.551	5.364	5.498	5.373	5.431	5.617	5.679	5.584	5.511	5.475	5.526	5.929
L218 C-C9	5.124	5.342	5.282	5.295	5.334	5.283	5.372	5.309	5.272	5.246	5314	5.160	5.283	5.230

Figure 2: The energetic results and the six possible pathways.

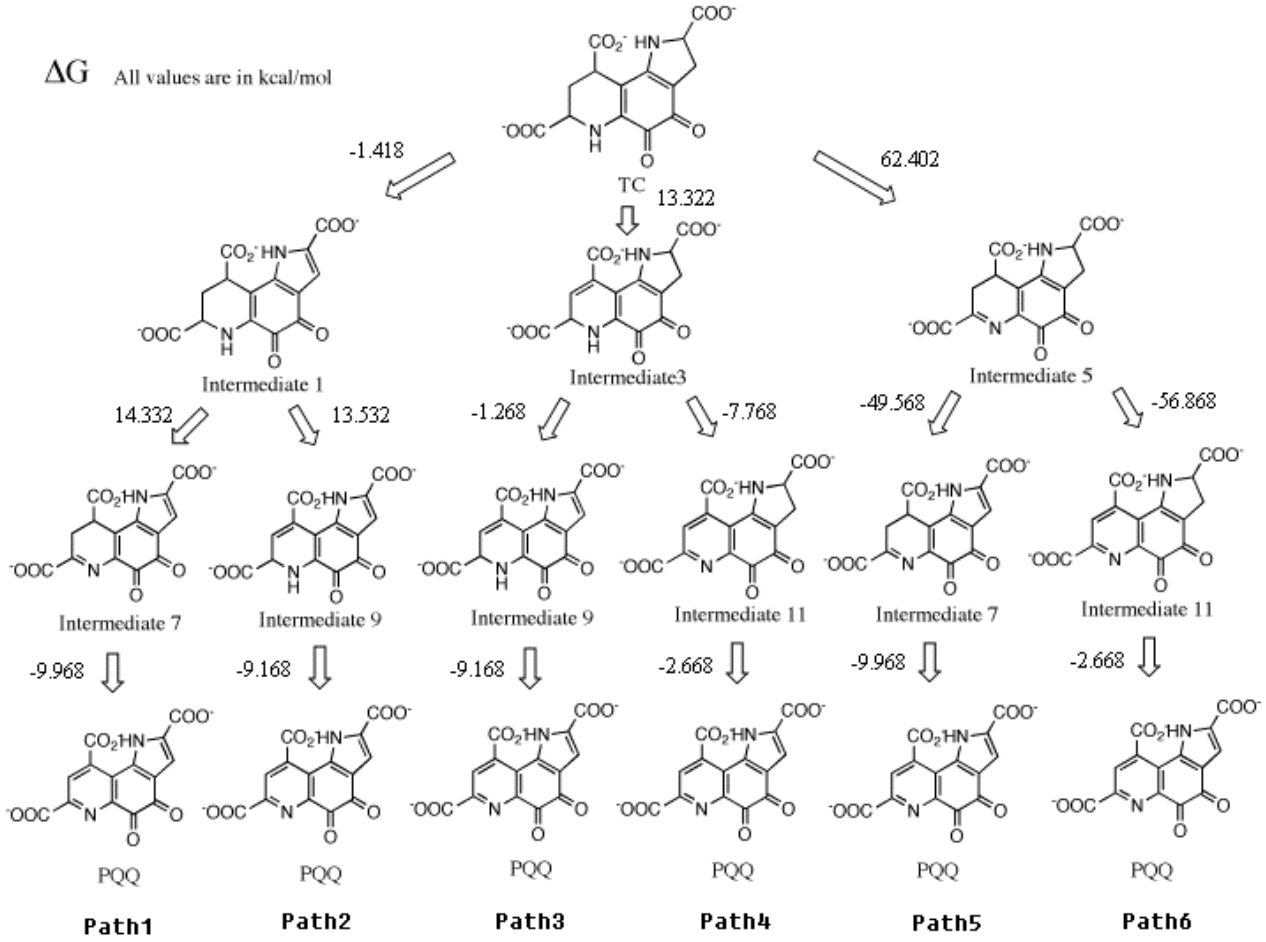

What was found was that all intermediates were reasonable binders to the PqqC active site. This is not surprising given that the active site of PqqC is very positively charged and all intermediates contain three carboxyl groups. What is interesting is that intermediate 1 was found to be the best binder, with a score very similar to that of the tricyclic intermediate (TC) that was the mechanism starting point of this study.

To analyse the distance between active site residues and bound intermediates, the distances between the active site residues and PQQ were compared to the distances with the bound intermediates. Any changes in distance more than 0.3 Angstroms were considered significant. As shown in Table 2, changes in distance were the distance get smaller are highlighted in yellow. When distances get larger, they are highlighted in green and changes that are discussed here are highlighted in red. These significant changes are the changes seen in Y53,

H84 and H154. What is seen is that with intermediate 8 and TC, Y53 gets closer to C9. With H84, TC and intermediate 4 are closer than PQQ. H154 shows interesting behavior, with intermediates 1 and 2 getting closer to this residue and intermediate 5 and 6 getting farther, relative to PQQ.

Energetically, the free energy of formations were found for the 14 structures. One the free energy was found the change in Gibbs free energy of each reaction was determined. Due to computing needs these energies are for the computed in solution rather than on the enzyme. These are shown in Figure 2 along with the possible pathways in this reaction.

Taking these three sources of information, binding, distance and energetics, into acoount an attempt at painting a mechanistic picture of the last three steps of the PqqC reaction. With the docking scores and the distances, we propose that path 1 is mechanism that PqqC follows. This is supported by the binding data, where intermediate 1 is the strongest binder, ie. the lowest docking score, of any of the possible intermediates. Looking at the changes in active site distances, Y23 is seen to move into a abstraction to generate 3. The tricyclic intermediate is also gets closer to H84, suggesting that proton abstraction at C3 is a possible first step, generating intermediate 1. Since the binding score and the energetic computations support formation intermediate 1 more than formation of intermediate 3 or 5, we can assume that this is the first step. This makes sense chemically, because this step forms an aromatic system, which no other single step does. This means that aromaticity could help drive this reaction. For the second step, the distance data plays the most important role in discerning this step. Since no residue was seen to grown closer to the C9 position and the binding and energetic data don't support a pathway, breaking of the nitrogen-hydrogen bond is thought to be the next step because of the movements of H154. H154 grows closer to the N6 position in intermediate 1. This leads is to believe that the second step in formation of intermediate 7 from intermediate 1. This leaves abstraction of a proton from C9 as the last remaining step of PQQ formation. Y23 gets slightly closer to the C9 position of intermediate 8, which is the quinol form of intermediate 7), indicating that Y23 could be the base in this step.

Taken into account, all this data indicate that the mechanism of PqqC follows path1 (Figure 2, 3). While this is not experimentally proven, future mutagenic experiments could be directed by this work. Mutations at Y23 could prove very clarifying to the PqqC mechanism.

Figure 3: The most probable PqqC mechanism. Step A has experimental evidence to support it and the work presented here indicates that this is the most likely order of the steps in B.